Environmental contamination of potentially toxic elements (PTE) and its effect on soil microbial communities in former industrial cities of Northern Hungary (Salgótarján and Ózd)

by

Gorkhmaz Abbaszade

Lithosphere Fluid Research Lab, Department of Petrology and Geochemistry,
Institute of Geography and Earth Sciences,
and
Department of Microbiology, Institute of Biology,
Eötvös Loránd University, Budapest

Ph.D. thesis

submitted to the

Ph.D. Program of Environmental Biology and Environmental Earth sciences, Doctoral School of Environmental Sciences at the Eötvös Loránd University, Budapest.
Director: Turányi Tamás, DSc
Program leaders: Erika Tóth, DSc and Zoltán Szalai, PhD

Supervisors:

Erika Tóth, DSc
Department of Microbiology, Institute of Biology, Eötvös Loránd University, Budapest

Csaba Szabó, PhD
Lithosphere Fluid Research Lab, Department of Petrology and Geochemistry, Institute of Geography and Earth Sciences, Eötvös Loránd University, Budapest

Budapest, August 2022

DOI: 10.15476/ELTE.2022.179

List of Abbreviations

As – Arsenic

ADI – Average Daily Intake

ATP – adenosine triphosphate

BLAST – Basic Local Alignment Search Tool

bp – base pairs

Cd – Cadmium

CDC – Centres for Disease Control and Prevention

CDF – Cation Diffusion Facilitator

CFU – Colony Forming Units

COG – Clusters of Orthologous Groups

CSF – Cancer Slope Factor

DNA – Desoxyribonucleic Acid

DSMZ – Deutsche Sammlung von Mikroorganismen und Zellkulturen

EC – Enzyme Commission

EF – Enrichment Factor

EPS – Exopolysaccharides

GO – Gene Ontology

Hg – Mercury

HI – Hazard Index

HQ – Hazard Quotient

IARC – International Agency for Research on Cancer

KEGG – Kyoto Encyclopedia of Genes and Genomes

LGB – Local Geochemical Background

m.a.s.l. – Meters Above Sea Level

MIC – Minimum Inhibitory Concentration

NCBI – National Centre for Biotechnology Information

NMDS – Non-metric Multidimensional Scaling

OTU – Operational Taxonomic Units

Pb – Lead

PCA – Principal Component Analysis

PCR – Polymerase Chain Reaction

PTE – Potentially Toxic Elements (considered four heavy metal(loid)s-As, Pb, Hg, Cd)

RfD – Reference Dose

RSD – Relative Standard Deviation

SOC – Soil Organic Carbon

SOM – Soil Organic Matter

SRA – Sequence Read Archive

TN – Total Nitrogen

TOC – Total Organic Carbon

RAST – Rapid Annotation System Technology

V% – Volume percent

WGS – Whole Genome Sequence

Table of Contents

List of Tables

List of Figures

Chapter 1. INTRODUCTION

Over centuries, anthropogenic activities (mining, manufacturing, industrial activities, etc.) have resulted in widespread metal(loid) contamination in urban areas that threatens the well-being of residents and the environment (Alloway, 2013; Hooda, 2010). The principal increase of potentially toxic elements (PTE[1])occurred after their usage in various industrial products (e.g., pipes, steel, glass, paint, battery, ammunition, etc.) due to their chemical and physical characteristics. Continuous accumulation of heavy metal/metalloid contaminants changes the physical, chemical, and biological properties of soils. The behaviour of PTE in the soil is controlled by various environmental parameters, mainly pH and redox potential, presence of Fe and Mn oxy-hydroxides, organic content, etc. (Wu, et al., 2017). Soil contamination is a primary environmental concern because of its interactions with the hydrosphere, atmosphere, and biosphere. Due to their high affinity for specific soil components (e.g., clay minerals, iron and manganese oxides, organic matter), PTE can be retained by the soil matrix, or with high solubility under oxidative conditions, they can be mobilized by particle and colloids to different environments (Ibanez et al., 2007; Löv et al., 2018; Hooda, 2010). Hence, in the biogeochemical cycle, numerous PTE contaminants have remained within the biosphere and continue to be an exposure source for organisms. Human exposure occurs mainly through the food chain, drinking water, inhalation, and direct or indirect contact with contaminants (Zacháry et al. 2015; Zhang et al. 2010). Once PTEs enter the organism, they can cause a wide range of physical and mental issues. At high levels of human exposure to one of the PTEs, there is damage to nearly all organs and organ systems, most notably the central nervous system and kidneys, that might result in death (Jaishankar et al., 2014; Park & Zheng, 2012).

Excess amount of metal(loid)s in soils also affect the soil microbial community which long-term exposure can alter soil microbial community structure by restraining or killing the sensitive members (Sheik et al., 2012; Yao et al., 2016). Even in small amounts, PTEs can accumulate in microorganisms that damage cell structure, disrupt metabolism, denatures proteins, DNA, and other functional groups. However, the toxicity mainly depends on soil inorganic ion content, the chemical forms of metal(loid)s and their solubility, soil fractions, pH, temperature, soil organic matter composition, etc. (Caporale & Violante, 2016; Friedlová, 2010). Moreover, various species may respond to metal(loid)s in different ways, as the metal(loid)concentrations may have a regulatory effect on microbes, such as high Hg

[1] In the current study As, Pb, Hg, and Cd were referred as PTE and metal(loid)s. Among them, As is metalloid, Pb, Hg, and Cd are metals.

concentration was reported to cause severe alpha diversity loss and increase of betta diversity that shifts the community structure, whereas low Hg concentration increased microbial diversity (Hall et al., 2020; Mahbub et al., 2017). Thus, understanding the changes in the diversity and structure of soil microbial communities is essential to clarify their ecological roles.

Soils with permanent metal(loid) contamination push communities to develop various resistance mechanisms to cope with pollution and adapt to the environment (Gomathy & Sabarinathan, 2015). Microorganisms can neutralize or transfer contaminants to a less harmful state through adsorption, precipitation, or transformation processes. The process of using metal(loid) resistance mechanisms of microorganisms to clean contaminated environments is called bioremediation. The method is defined as a process of treating polluted environments to regain a healthy state (Abbas et al., 2018). It is more efficient and environmentally friendly than current physicochemical remediation methods, which are rather expensive and have various drawbacks; Gaur et al., 2014).

Aims of the research

Our study aims to explore the spatial distribution and enrichment of As, Pb, Hg, and Cd in urban soils from two former industrial cities of Hungary, Salgótarján and Ózd. The overall objectives of this research were the following:

1- Determine the concentration of As, Pb, Hg, and Cd (PTE) in the urban soils of Salgótarján and Ózd and identify the role of soil physicochemical parameters in their distribution.
2- Identify the enrichment and contamination of As, Pb, Hg, and Cd in urban soils and determine their possible local sources.
3- Characterization of microbial community structure in Salgótarján and Ózd soils samples, and to reveal the influence of soil physicochemical parameters, as well as selected toxic compounds on the composition of prokaryotic communities.
4- Isolate and characterize PTE resistant/tolerant bacteria from selected contaminated urban soil samples.
5- Health risk assessment of selected PTE to reveal exposure pathways and risky areas and evaluate the possible impact of PTEs on residents in both cities.

Chapter 2: LITERATURE REVIEW

2.1. Potentially Toxic Elements contamination in industrial cities

Potentially toxic elements (PTE) are natural constituents of the soil environment, however, their concentration dramatically increased after industrialization, which resulted in an alteration of the soil quality (Alloway, 2013; Dragović et al., 2008; Liao et al., 2018). Soil acts as an interface between lithosphere, hydrosphere, atmosphere and biosphere, and plays a crucial role in regulating natural biogeochemical cycles (Ibanez et al., 2007). Whereas the further addition of the PTEs to the environment by anthropogenic activities, such as mining, smelting, burning of fossil fuels, disturb the natural cycle and processes (Figure 1) (Ettler, 2015; Kelepertzis et al., 2016; Wei et al., 2011). Due to strong and direct-indirect anthropogenic influence, urban soils differ from natural, "undisturbed" soils: considered as an environmental sink of chemical emissions and therefore generally rich in metal(loid)s (Argyraki et al., 2018).

Assessment of soil potentially toxic element concentration has been generally focused to reveal the specific sources in the environment, but the accumulation and persistence nature of the PTEs make them potentially good indicators of polluted environments (Ali et al., 2019; Mohammad Ali et al., 2021; Okoro & Fatoki, 2012). According to the United States Environmental Protection Agency (USEPA) and European Environmental Agencies (EEA), soil metal(loid) pollution is a major global problem that threatens environmental health and exceeds the environmental quality standards for PTE (EEA, 2007; US EPA, 2014)

Metallurgical and smelting processes are highly polluting anthropogenic activities and emit high quantities of various pollutants, including PTE (Ettler, 2015; McIlwaine et al., 2017; Šajn, 2002). In the late 1980s, mining and smelting activities emitted 356 - 857 tonnes lead (Pb) into the environment each year. Furthermore, Pirrone et al., (2010) reported that ore mining and processing accounts for 13% of global mercury (Hg) emissions. The global average yearly production of cadmium climbed from 20 tonnes in the 1920s to almost 24 000 tonnes in 2021 (Statista, 2022). Smelting and refining of nonferrous metals, as well as fossil fuel combustion, account for roughly 85–90% of total airborne cadmium (Cd) emissions in the European Union and worldwide. Even though Hg, Pb, and Cd emissions from the nonferrous metals industry have declined in Europe during the last 50 years, as a result of the installation of efficient flue gas cleaning systems (Pacyna et al., 2007). According to Kierczak et al., 2013, soils around ancient smelters that operated during the 14th and 16th centuries are still extensively polluted

with metal(loids), owing to the centuries-long breakdown of smelter wastes into the soils. They concluded that the legacy of historic smelting sites, even those that have been inactive for centuries, should still be considered a severe environmental issue today (Kierczak et al., 2013). Another significant PTE contamination source in the environment is coal mining and combustion. U.S. Energy Information Administration (EIA) reported that in 2016 the global coal consumption reaches 8.5 bln tonnes (EIA, 2016). Coal is a heterogeneous material that contains a variety of trace elements in its organic and mineral fractions. The geological processes that create the coal beds and the depositional environment have an impact on the presence of trace elements in coal. According to Noll (2003), the concentration of trace elements in coal residues (such as ash) is extremely variable and depends on the composition of the coal source, conditions during coal combustion, the effectiveness of emission control devices, storage and treatment of the by-product. Potentially toxic elements which associate with organic compounds and sulfides of coal, have a tendency to evaporate and subsequently adsorb on the fine particles, when the flue gas temperature drops (Bhanarkar et al., 2008).

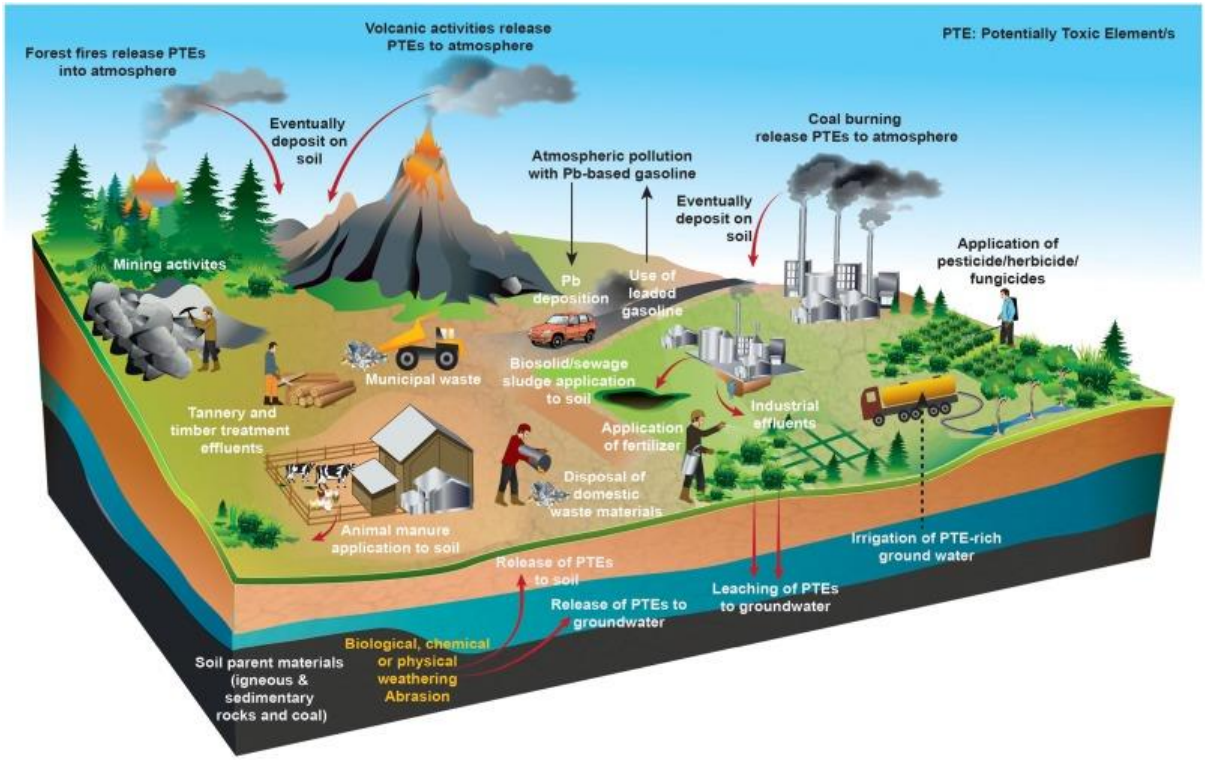

Figure 1. Various sources of potentially toxic elements in the environment (Palansooriya et al., 2020). The main natural sources are soil parent material and volcanic activities, whereas, anthropogenic activities are quite diverse, such as mining activities, coal combustion, industrial byproducts (e.g., slag), leaded gasoline, etc.

Additionally, vehicle exhaust and fuel combustion are other main factors that play a significant role in PTE contamination. The usage of lead in gasoline as an antiknock agent was introduced to the market in the 1920s as leaded-gasoline. Until recently, lead from vehicle exhausts, in the form of tetraethyllead, was a significant source of contamination. During the 1980s in Europe and North America, engine Pb emissions rapidly dropped after the average Pb content of petrol was decreased to 0.15 g/l (Bollhöfer et al., 2001; Löfgren & Hammar, 2000), resulting in a robust decline in Pb concentration in the atmosphere and hydrosphere (Zhu et al. 2010). Spatial variability of PTE levels in soils is associated with greater atmospheric PTE emissions. Because the PTEs are concentrated mostly in submicrometric particles, when released into the atmosphere they could be transported long distances and deposited over large areas of the Earth (Ilacqua et al., 2003; J. Wang et al., 2019).

Hungary is no exception where mining, ore processing, smelting, use of leaded gasoline and other industrial activities, as well as coal-fired power plants affected the environment for around 150 years. Salgótarján and Ózd cities are two examples of mining and iron-steel industries in Hungary. The ecological wounds of mining infrastructure (inclined shafts, mine cars, loading platforms, ropeways, and railways with cuttings, embankments, and tunnels), metallurgy, and their dumps drastically altered the landscape, exposed/contaminated both cities with PTE for many decades and thus affected the urban residents, soil microorganisms, etc.

2.2. Behaviour of selected metal(loid)s in the environment (characterization of PTE)

2.2.1. Arsenic (As)

Arsenic (the atomic number is 33) is the twentieth most abundant element in the earth's crust. The main ores include arsenic sulfide - orpiment (As_2S_3), realgar (AsS/As_4S_4), and arsenopyrite (FeAsS), occurring primarily in hydrothermal and magmatic ore deposits (Alloway, 2013). Arsenic dominantly exists in the form of arsenite (AsO_3^{3-}) and arsenate (AsO_4^{3-}) in reducing and oxidizing environments, respectively. In aerobic conditions As^{5+} forms insoluble precipitations (e.g., with Fe oxy/hydroxides) and has low mobility. However, soil redox changes, for example, from oxic to anoxic circumstance As^{5+} reduces to As^{3+}, to the soluble form of arsenic. In anoxic conditions, it bounds to sulfides and manganese-oxy-hydroxides in the form of As^{3+}, which plays a significant role in the mobility of toxic arsenic compounds. The global arsenic production is 50 000 t/year and has a broad spectrum of applications, including pesticides, herbicides, insecticides, fungicides (Cu-arsenates), etc. (White, 2018).

The semiconductor industry, fossil fuels, mining, and smelting activities are the primary anthropogenic contributors to As in the environment (Alloway, 2013; White, 2018).

2.2.2. Lead (Pb)

Lead (the atomic number is 82) is one of the most prevalent heavy metals in the Earth's crust and is widely distributed and mobilized in the environment. Lead forms many useful compounds, and due to its ductile and malleable nature, low melting temperature, and easy smelting, it was widely used in industrial production (White, 2018). However, that resulted in severe environmental contamination, evidenced by the increased lead concentration in all spheres. It forms insoluble metal sulfides and oxides, whereas in high pH conditions soluble Pb complexes. In the environment, Pb deposits/ores are found mainly in the form of galena (PbS-generally together with Zn-sulfide), cerussite ($PbCO_3$) and anglesite ($PbSO_4$) (Alloway, 2013; White, 2018). Lead is known for its immobile feature as it strongly binds to soil fractions (humus/organic matter), metal oxides, etc., and does not migrate much to groundwater. Pb is one of the oldest known metals that has been used since ancient times in various products, such as pipes, toys, jewelry, glass, paints, etc. (White, 2018). The main anthropogenic Pb pollution sources involve industries (steelworks), mines, and leaded gasoline, which was used from 1920 until the 2000s.

2.2.3. Mercury (Hg)

Mercury (the atomic number is 80) is a non-essential metal that is liquid at room temperature (White, 2018). The most common minerals in the environment are cinnabar (HgS) and livingstonite ($HgSb_4S_6$) (Alloway, 2013). The atmospheric depositions, volcanos, mining, and other industrial productions increase Hg concentration in the soil environment. Where in oxic conditions, Hg is tented to bind to organic matter, whereas in anoxic conditions, it forms HgS. Due to its low melting and evaporation temperature, inorganic mercury is considered highly volatile (it can easily evaporate). Inorganic mercury compounds can be converted to methyl-Hg, one of the most toxic compounds, by soil microorganisms and bio-accumulate in soil/ aquatic environments (Petrus et al., 2015; Cheng et al., 2020). In the industry, mercury is widely used for electrical equipment, such as batteries and semi-conductors, medical tools, paints, etc. Mercury pollution is regulated by European Union based on the Minamata UN convention, (2017), a universal environmental agreement to control mercury pollution sources

(Horvart et al, 2019). The agreement intends to ban all mercury-containing products, export, and imports, since 2017 (Minamata UN convention, 2017).

2.2.4. Cadmium (Cd)

Cadmium (the atomic number is 48) is relatively rare in most soils. Its concentration is 0.1 mg/kg on the earth's crust and do not have an own ore mineral, except greenockite (CdS) which is found together with ZnS (sphalerite). Additionally, it can be found rarely as $CdCO_3$ (otavite). In oxic environments, Cd is present as Cd^{2+} and bound to Fe and Mn oxides, clays, sulfur, or organic matter. Whereas in anoxic environments, it mainly exists as CdS. The pH changes affect its mobility in the environment, as increases in low pH and saline conditions (forms $CdCl_2$ in the saline environment). Cadmium production increased substantially in recent decades, from 11000 t in 1960 to 25000 t in 2019 (USGS, 2020). It was mainly used in semiconductors, nickel-cadmium batteries, different alloys, anti-corrosion in the steel industry, pigments, and nuclear reactors (Alloway, 2013). Contamination of soil and water is caused mainly by the mining and smelting industries, sewage sludge application, and fossil fuel combustion (Alloway, 2013; Evangelou, 2008).

2.3. Toxicity and health effects of the selected metal(loid)s

Heavy metals and metalloids are essential environmental contaminants that significantly affect to all ecosystems (Dash et al., 2013; Kamunda et al. 2016; Gbogbo et al., 2018; Huseen and Mohammed, 2019). The hazard is determined by their persistence, toxicity, and capacity to bioaccumulate in the environment or organisms. Human exposure mainly occurs through food and drinking water, ultimately reaching the human body and causing health threats. Additionally, humans are exposed to soil pollution inadvertently through dermal contact and intake of inhalable soil particles (Jaishankar et al., 2014; Pandey, 2014). Children were shown to be the most susceptible group, and it is noteworthy that children suffer more from severe poisoning than adults due to the characteristic “hand-mouth-contact”. This results in intellectual disability, learning difficulties, and brain damage due to faster metabolism, growth, and developing nervous system (Matta & Gjyli, 2016; CDC, 2021). Exposure of people to PTE results in thousands of deaths and millions of mental disabilities every year (Tchounwou et al., 2013).

In 2019, Agency for Toxic Substances and Disease Registry ranked As, Pb, Cd, and Hg as the most toxic[2] chemicals and ranked them 1st, 2nd, 3rd, and 7th among the chemicals with great public health concern (CDC, 2019). The list prioritizes the substances based on a combination of their frequency, toxicity, and potential for human exposure. Arsenic, cadmium, lead and mercury are highly toxic to most biological systems at any concentration however can result in death above critical levels. Table 1 shows the maximum permitted PTE levels for humans in various environments.

The toxicity of **arsenic** is determined by its valence, which arsenic III compounds are mobile and therefore more poisonous than arsenic V compounds. The toxicity of arsenic is based on the interaction with different proteins (sulfhydryl groups) as well as reactive oxygen radicals can be formed. In the 1980s, arsenic and its compounds are classified as group 1 carcinogens by the International Agency for Research on Cancer (IARC) (Hong et al. 2014), and arsenic pentoxide, arsenic trioxide, and arsenate salts are classified as category 1 carcinogens by the European Union (EU). Long-term exposure to inorganic arsenic can result in serious illnesses such as skin and lung cancer, hypertension-related vascular diseases, stroke, respiratory diseases, diabetes, liver, and kidney damage (Naujokas et al., 2013; Hong et al. 2014). Due to its similar chemical characteristics to phosphorus, arsenic can replace phosphorus (P) in tissues (e.g., teeth, bones) (Tawfik & Viola, 2012).

Lead can cause severe damage to the kidney, brain, and liver and accumulate in bones and teeth. Exposure to the central nervous system is observed with lower IQ, development disturbance, and mental retardation; however, chronic high exposure can cause anemia, autism, coma, and even death (Goyer, 1993; Flora et al. 2012). Lead is a biogeochemical analog to calcium and zinc, the essential elements (Smith & Flegal, 1995). As a result, it integrates into trophic and metabolic networks easily. Thus, most of the lead released into the environment has persisted in the biosphere, which continues to be a source of exposure for organisms, including people (Shotyk & Le Roux, 2005).

[2] "Most toxic" substances are rather a prioritization of substances based on a combination of their frequency, toxicity, and potential for human exposure

Table 1. The maximum permitted PTE concentrations in drinking water, air, soil, and blood. The limit for workplace air is considered for 8-hour shifts and 40 hours/week of work. The elements were ordered based on the substance priority list introduced by Agency for Toxic Substances and Disease Registry (CDC, 2019).

PTE	**EPA regulatory limit for drinking water (mg/L)**	**OSHA limit for workplace air ($\mu g/m^3$)**	**Soil (mg/kg)**	**Blood (mg/L)**
Arsenic (As)	0.01	10.0	15	0.05
Lead (Pb)	0.015	50	100 Hungarian regulation, 300 European Union regulation	0.1
Mercury (Hg)	0.002	100 for organic and 50 for inorganic Hg	0.5	0.01-0.03
Cadmium (Cd)	0.005	5.0	1.0	0.005
References	(US EPA, 2016)	(OSHA, 1991)	(CSTEE, 2000; HUGD, 2009)	(CDC, 2021)

Mercury toxicity occurs from inorganic and organic mercury contaminants. Metallic mercury exposures most commonly occur when metallic mercury is spilled, exposing mercury to the air or food chain (Park & Zheng, 2012). Long-term and/or acute exposures can cause the following symptoms: insomnia, neuromuscular changes, headaches, etc. Mercury exposure can harm the neurological system, kidneys, liver, and immune system, depending on the level of exposure. Mercury fumes easily travel through the lungs and get into blood circulation, affecting the neurological system, lungs, and kidneys (Park & Zheng, 2012; Teixeira et al., 2018).

Methylmercury is more dangerous than inorganic mercury due to its ease of acceptance by organisms (Pandey et al. 2014). United States Centres for Disease Control and Prevention (CDC) reported that in fact, everyone has a certain amount of methylmercury in their body as a reflection of pervasive environmental occurrence. People are most typically exposed to methylmercury when they consume seafood (such as fish) with high amounts of methylmercury in their tissues (Hong et al. 2012). Severe exposure to methylmercury causes Minamata disease, known with symptoms including sensory disturbances, ataxia, dysarthria, auditory disturbances, and tremor (rhythmic shaking of one or more parts of the body). Higher levels of exposure can potentially result in memory problems, brain and kidney damage, respiratory failure, and death (Hong et al. 2012).

Cadmium toxicity occurs when a person inhales high levels of cadmium from the air, eats cadmium-contaminated food, or cadmium-bearing drinks (Hallenbeck et al., 1984). It is poisonous and non-essential and can lead to kidney disease, bone fragility, lung cancer, and other diseases(Genchi et al., 2020; Schoeters et al., 2006). Exposure comes especially from smoking, nutritional deficiency of essential elements (Zn, Ca, Fe), and remains in hazardous environments, such as smelters and waste disposals. Long cadmium ingestion causes the most severe form of chronic cadmium poisoning, called Itai-Itai (which means “it hurts” in Japanese) disease. A kidney is the main target organ in this illness, with tubular and glomerular failure as symptoms (Baba et al., 2013).

2.5. Soil microbial community and the metal(loid) resistance

The rapid development of industry has resulted in increased pollution of the environment by heavy metal(loid), which causes a potential threat to ecosystems (Wong et al. 2006; Sun and Chen, 2016; Mohammad Ali et al., 2021). The accumulation of chemical and biological

contaminants in soils alters the physicochemical and biological properties of soils and disturbs the ecological balance (Akinola et al., 2021; Friedlová, 2010)

The elevated levels of metal(loid)s in soils have significant impacts on the structure and overall activity of the soil microbial communities. However, it is quite difficult to predict how microbial communities will react to metal(loid)s, as diversity (i.e., the richness and evenness of species within a sample) and microbial biomass have been observed to decrease in some cases, while they have shown no correlation in others (Sheik et al., 2012).

The most difficult problem associated with the contamination of soils with metal(loid)s is that they cannot be naturally degraded like organic pollutants, and they can be accumulated in different parts of the food chain (Huseen & Mohammed, 2019; Shahid, 2017). Metal(loid)s can slow down the speed of growth and reproduction of living microorganisms, including microbes, through functional disturbance, protein denaturation, or the destruction of the integrity of cell membranes (Table 2; Ghorbani et al. 2002). Studies have shown that the toxicity exerted by metal(loid)s may suppress or can kill sensitive members of the microbial community and lead to a shift in community structure.

Table 2. Effect of the selected metal(loid) toxicity on microorganisms.

PTEs	Effect on microbes	Citation
Arsenic	Deactivation of enzymes, respiration, and cellular functions	(Ghosh et al., 2004)
Lead	Destroyed nucleic acid and protein, inhibiting enzyme actions and transcription	(Fashola et al., 2016)
Mercury	Denature protein, inhibit enzyme function, disrupt the cell membrane	(Fashola et al., 2016)
Cadmium	Denature protein, destroy nucleic acid, hinder cell division and transcription	(Fashola et al., 2016; Sankarammal et al., 2014)

The toxicity is primarily concerned with the bioavailability of metal(loid)s, that is, the amount of species that are eventually absorbed into the body by absorption, migration, and transformation (Lu et al., 2017; Tamayo-Figueroa et al., 2019). The bioavailability of PTE and associated toxicity to soil biota vary with time, soil type, speciation, aging, sources, organisms, and other environmental factors. The available fraction of PTE (not the total concentration) seems to correlate well with the toxicity parameters (Takáč et al., 2009). Therefore, long-term

metal(loid) contaminated soil will choose those who can specifically adapt to polluted soil by developing various mechanisms to resist the pollution (Nies, 1999; Silver & Phung, 1996). High concentrations of metal(loid)s on the toxicity of microorganisms may have two reasons, metal(loid)s and microorganisms have a strong affinity, and it is easy to bind with some biological macromolecules such as enzyme activity centre, and electron-donating groups, which is resulting in the inactivation of them (Busenlehner et al., 2003; Kim et al., 2015). Metal(loid) pollution leads to the degradation of microbiological diversity of those who lack the pressure on the outside world, and at the same time leads to those who can adapt to the increased pressure.

The development of molecular techniques facilitated the identification of microorganisms in diverse environments. Ribosomal DNA gene analysis is the frequently used method and relies on polymerase chain reaction (PCR) amplification and comparison with assigned taxonomic groups of 16S rDNA sequences from ambient microorganisms. The advantage of using 16S rDNA sequences is they exist in all bacterial cells with a high level of structural and functional preservation. Thus, various regions of this gene allow them to be used in identifying closely related organisms (Schöler et al., 2017).

2.6. Resistance mechanisms of bacteria to PTE

To define their interaction with the environmental components, especially metal(loid)s, it is necessary to understand the bacterial resistance mechanisms. The main strategies through which they resist high concentrations of metal(loid)s include efflux mechanisms, extracellular sequestration, biosorption, precipitation, alteration in cell morphology, enhanced siderophore production, intracellular bioaccumulation, etc. (Figure 2) (Naik & Dubey, 2013; Silver & Phung, 1996; H. C. Yang & Rosen, 2016).

To maintain intracellular homeostasis, the level of toxic metal(loid) ions have to be strictly controlled. This process is managed by an active efflux mechanism, which involves three groups of proteins in the transport of metal(loid)s outside the cell membrane, and governs bacterial metal(loid) resistance (Monchy et al., 2006; Naik & Dubey, 2013). Among them, P-type ATPases and cation diffusion facilitator (CDF) transporters export metal(loid) ions from the cytoplasm to the periplasm; meanwhile, CBA transporters (consisting of subunits C, B, and A), chemiosmotic ion-proton exchangers extrude metal(loid)s from cytoplasm or periplasm to outer membrane (Nicholls & Ferguson, 2013). All the three transporter proteins prevent over-accumulation of highly toxic and reactive metal(loid) ions such as Pb^{2+}, Cu^{+}, Ag^{+}, Zn^{2+}, Cd^{2+},

Hg^{2+}, As^{3+}, etc. in prokaryotic cells. Passive diffusion, facilitated diffusion, and active transport are three processes for metal transport into the bacterial cell. Metal selectivity is a feature of active transport systems, however, toxic metal(loid)s use transporters that carry essential elements to penetrate the cell (e.g., Cd use Zn transporters) (Nicholls & Ferguson, 2013).

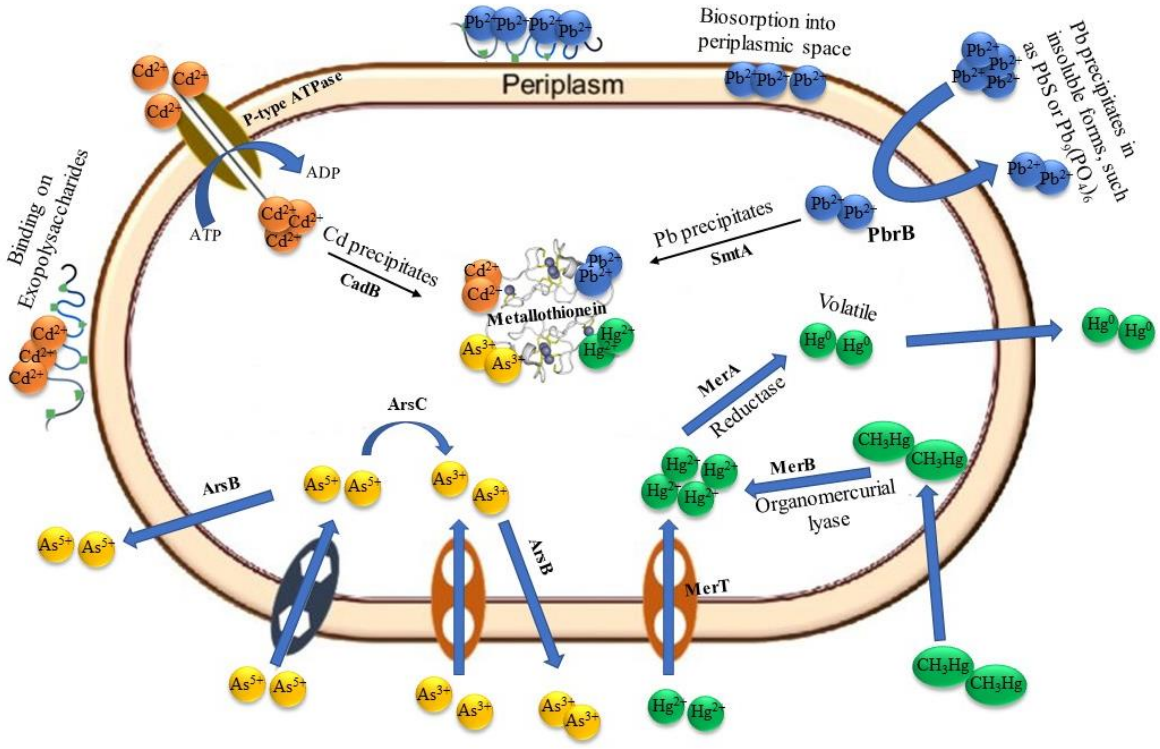

Figure 2. Possible microbial metal(loid) resistance mechanisms in the schematic cell. The resistance mechanisms reported by Jarosławiecka & Piotrowska-Seget, 2014; Nies, 1999; Silver & Phung, 1996, 2005.

One another essential and common metal(loid) resistance mechanism is bioaccumulation, which involves specific metal(loid) binding proteins to sequester/bioaccumulate toxic metal(loid)s in the cell (Wang, 2016). Those proteins are referred to as metallothioneins (MTs) and play an important role in the immobilization of toxic metal(loid)s, thus protecting enzyme-catalysed metabolic processes (Genchi et al., 2020; Leiva-Presa et al., 2004). Metallothioneins are cysteine-rich (20-30%) polypeptides that can bind both essential (Zn) and non-essential metal(loid)s. However, there are reports that certain microorganisms immobilize metal(loid)s by bioprecipitation in extra and intracellular areas (Mugwar, 2015; Rene et al. 2017). For example, when these microorganisms release high concentrations of $HPO4^{2-}$ through

phosphatase activity, a class of enzymes that catalyse phosphate donors for precipitation, such as $PbHPO_4$, $CdHPO_4$, etc. (Mugwar, 2015). Additionally, intracellular accumulation and precipitation of $Pb_3(PO_4)_2$ by *Staphylococcus aureus* grown in the presence of high concentrations of soluble lead nitrate were reported (Nies, 1999).

The bioavailability of toxic metal(loid)s is also important in regulating metal(loid) toxicity. Therefore, microorganisms apply a metal(loid) immobilization strategy to prevent the impact of metal(loid)s, and this process is called extracellular sequestration (Naik & Dubey, 2013). Several microbial biopolymers have already been discovered with their specificity and affinity for metal(loid)s. Exopolysaccharides (EPS) are highly viscous carbohydrate polymers secreted by microbial cells that contain various macromolecules/functional groups, such as hydroxyl, carboxyl, amides, and phosphoryl that have a high affinity for metal(loid)s (Vicentin et al., 2018; Xie et al., 2014). Thus, the mobile metal(loid) compounds can be attached to EPS matrix to immobilize and protect the cells from metal(loid) toxicity.

Using the metal(loid) resistance mechanisms of microorganisms to reduce, eliminate or transform toxic compounds in soil, sediment, etc. is a type of bioremediation, and the method requires the presence of favourable environmental conditions and enough nutrients (Gadd & Pan, 2016; Omokhagbor Adams et al., 2020). Furthermore, successful remediation depends on using microorganisms with remediation and survival capabilities in contaminated environments (Lyon & Vogel, 2011; Omokhagbor Adams et al., 2020).

Chapter 3. MATERIAL AND METHODS

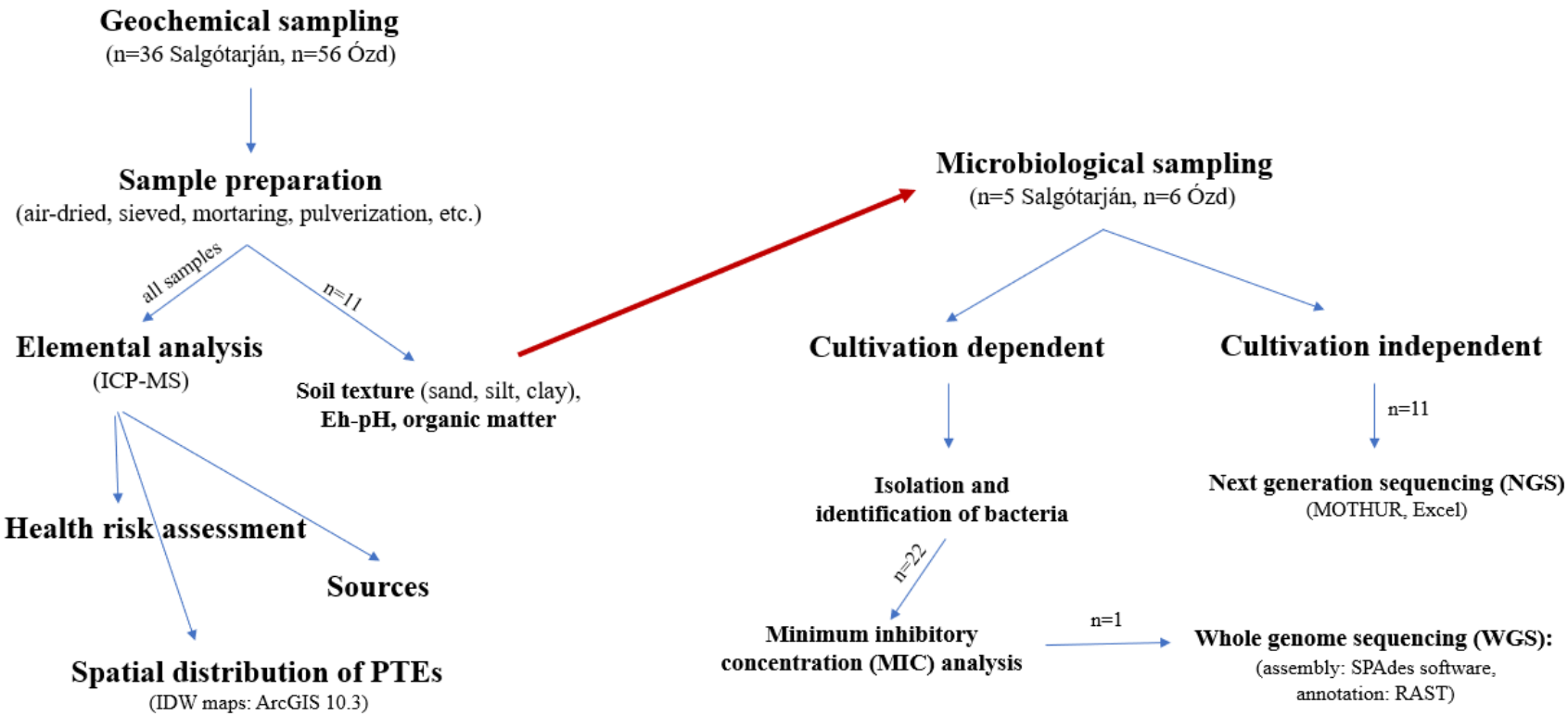

Figure 3. Graphic workflow; showing the sequence of the work and used methods. More details are given in the relevant section. (n=number of given samples; used methods are given in brackets).

Chapter 3. MATERIAL AND METHODS

3.1. Description of the study areas- Salgótarján and Ózd

Sampling was performed (see section 3.2) in two former highly industrialized cities, Salgótarján and Ózd, located in a hilly area approx. 40 km distance from each other, where the region was significant brown coal, iron, and steel supplier. High hills and valleys characterize the region with several creeks, and the wind is dominantly northern directed. The elevation ranges from 200 to 500 m.a.s.l. for Salgótarján and 120-250 m.a.s.l. for Ózd, and the highest elevations are framed at the northern margins of the cities. The forested area is covered mainly by brown forest soil. Salgótarján and Ózd cities cover 103 km^2 and 92 km^2 areas with approximately 32,000 populations, respectively (Figure 5). The foundation and development of ironwork started in the mid-18^{th} century when brown coal deposits were discovered nearby both cities. In Salgótarján, behind the iron and steel manufacturing, glassworks, mining machine factory, stove factory, and later ferroalloy factory functioned along the East-West and North-South main roads. The city and its adjacent area were provided by energy from the coal-fired power plant, which was supplied by the local brown coal mines (Figure 5B). In Ózd, the iron and steelwork were established in the city centre, which was ~100 years later extended to the north-eastern part of the city, and its activity continues even today as Ózd Steelworks Ltd. (Figure 5C). Local brown coal deposits yielded the necessary supply for the energy-consuming steel metallurgy. In the 1980s, industrial production started to decrease, and after the collapse of the communist system, the shutdown of coal mines and industries (exception of the stove factory in Salgótarján and the small and recent modern Ózd Steelworks Ltd. In Ózd) dramatically changed the whole region in employment rate, life standard, and population. This economic and social shift resulted in remarkable changes in the landscape of the cities, where the reconstruction of commonwealth establishments (particularly buildings of schools and Kindergartens), and open recreation areas (playgrounds and parks) have been started. However, the footprint of the significant and long-term (at least 150 years) anthropogenic industrial activities (coal mining, heavy industry, and later road and train transportation) can be recognized even today in both cities due to the presence of potential contamination sources (e.g., ruins of former smelters, coal mines, coal-fired power plant, slag hill, fly ash cone, etc.).

3.2. Urban soil geochemical analysis

3.2.1. Sample collection

The urban areas for sampling were selected for this study due to the industrial activities, and productions occur mostly in urban areas, and the byproducts (contaminants) are deposited in the surrounding areas. The abundance of industrial sources requires certain studies to identify potential sources which pose a high risk to the residents and the environment.

Urban soil samples[3] were collected in residential areas of Salgótarján (STN) and Ózd (I), including samples from surrounding sites, like steel factories, coal mines, dumps, coal-fired power plants, and forests (Figure *4* and Figure 5). A 'zig-zag' sampling strategy (Alloway, 2013) was followed from each 1x1 km grid for both cities, where randomly picked points based on the availability of desired site categories as kindergarten, playground, park, and 'other' (i.e., roadsides, cemeteries, soccer pitch, and gardens) were selected for urban soil sampling. A total of 39 urban soils from Salgótarján and 64 urban soils from Ózd, including coal, slag, and local geochemical background (control) samples, were collected from 5–15 cm depth to study.

A local coal ash sample from the cone of the former coal-fired power plant in Salgótarján (Figure 5A), and three smelter slag samples from former and the recent smelter dumps in Ózd (Figure 5B) were taken. Moreover, brown coal samples from the same Neogene geological formations were acquired from the former coal mines (i.e., Inászó, part of Salgótarján, and Farkaslyuk, a former part of Ózd, from the collection of the Department of Physical and Applied Geology of Eötvös Loránd University, Budapest. Brown forest soils as local geochemical background samples, brown forest soils, were taken from the nearby forest area, far (~7 km away) from all potential contamination sources (e.g., former iron and steel works, road systems) in both cities.

[3] Each sample represents sampling site (location) and shown by STN/OZD and relevant sample numbers.

Figure 4. Collection of urban soil samples at roadside (A), kindergarten (B), park (C), and playground (D). E, G- sampling sites containing oxidized slag below surface. F- slag deposit in Ózd city

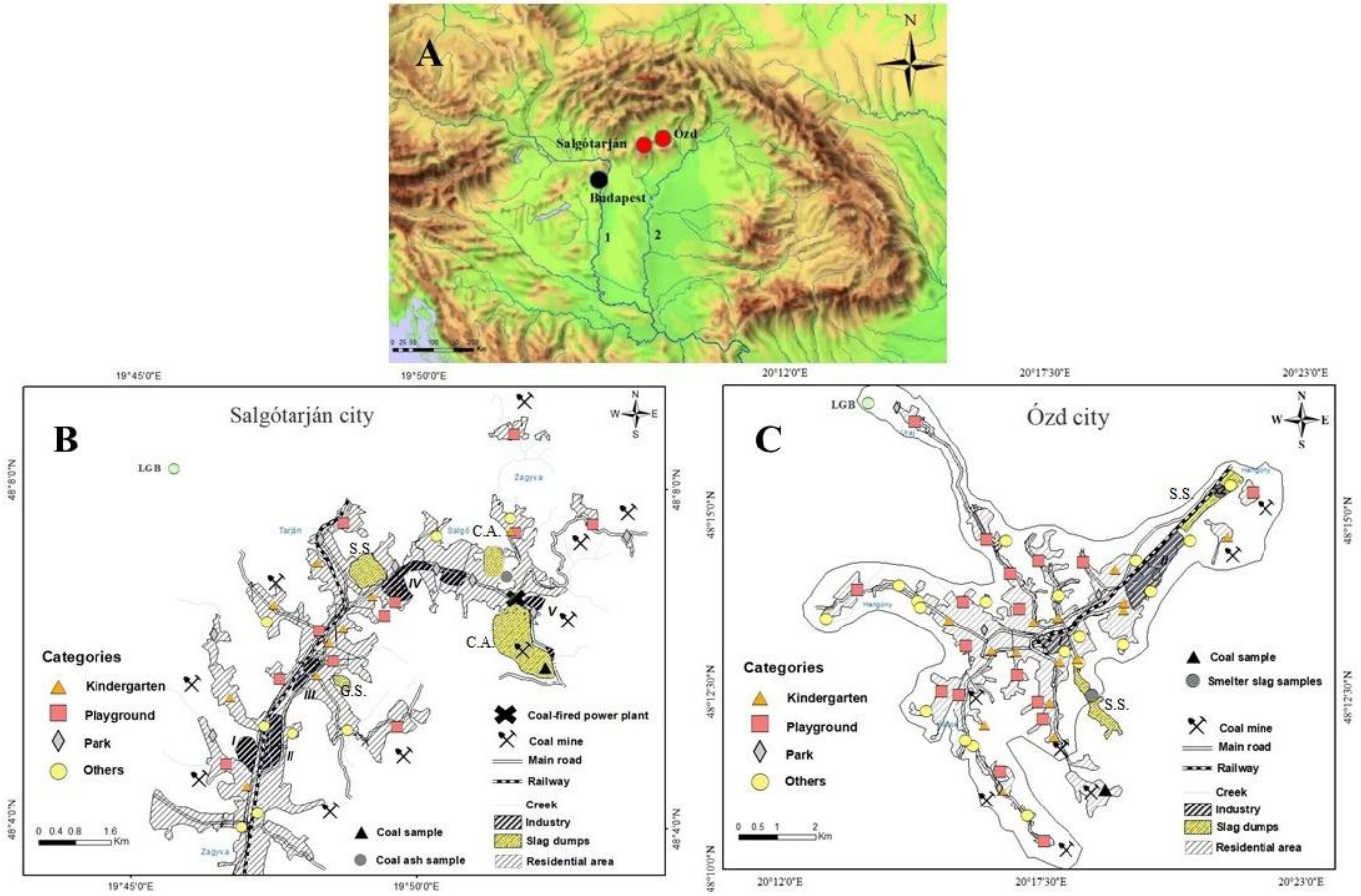

Figure 5. A. Carpathian-Pannonian region shows the geographic environment of the two studied cities (Salgótarján and Ózd). Brown colour - mountains (like the Carpathian Chain), green colour - plains (Pannonian Basin), blue colour - major rivers (Danube -1 and Tis–a - 2). B. Map of Salgótarján and C. Map of Ózd, showing the sampling sites and their categories, residential areas, locations of the industry and coal mine, slag landfills, and coal-fired power plant. Abbreviation for Salgótarján: I - former mining machine factory, II - former glassworks, III - stove factory, IV - former steelworks, V - former ferroalloy factory, and C. Map for Ózd: I - former steelworks, II- Ózd present steelwork. GS-glass slag, SS-steel slag, CA-coal ash.

3.2.2. Sample preparation

Our urban soil sampling followed the EuroGeoSurveys Geochemistry Expert Group Sampling Protocol (Demetriades & Birke, 2015). Cross-contamination was avoided during the sampling, and samples were collected and delivered to the laboratory in plastic bags. The urban soils were air-dried in the laboratory and passed through 2-mm sieves to obtain a representative portion. For homogenization, the coning and quartering procedures were applied (Hooda, 2010). Visible organic materials (e.g., worms, grasses, roots) and urban debris (e.g., bricks, concrete, waste) were removed before grinding at Eötvös Loránd University. The rest of the sample preparations (such as mortaring, pulverization, etc.) were performed at Bureau Veritas Global Company[4] in Canada (described below) (Bureau Veritas, 2021).

3.2.3. Elemental analysis

The modified aqua regia digestion (1:1:1 HNO_3: HCl: H_2O) method was used at 95 °C on 15 g of < 0.075 mm milled aliquots for low to an ultra-low determination of As, Pb, Hg, and Cd (additionally, Fe and Mn to identify their role in PTE mobility) in soils (Reimann et al., 2009) and were analysed by quadrupole-based ICP-MS (detection limit is 0.01 mg/kg) at the Bureau Veritas Global Company in Canada (Bureau Veritas, 2021). For homogeneity and heterogeneity identification of the measurements, a total of 10 (7 from Salgótarján and 3 from Ózd) urban soil duplicate samples were used. The analytical quality was controlled using certified reference materials (DS11, NIST981, and NIST-983). To correct mass bias and dead-time effects, calibration against reference materials was performed after every sample. In all cases, the relative standard deviation (RSD) for elemental concentration measurements was <3% RSD.

3.2.4. Grain size analysis

Prior to the particle analysis, around 0.5 g of urban soil was mixed with an optimal amount of Na-pyrophosphate ($Na_4P_2O_7$) to disaggregate particles (Abdulkarim et al., 2021) which was further performed by applying to ultrasonic cleaner. The mixture was kept overnight so that the aggregates were detached and then was analysed by Laser Scattering Particle size distribution analyser PARTICA 950-V2 LA instrument at the Research and Instrument Core Facility of Sciences, Eötvös Loránd University, to identify soil texture. Laser diffraction is the most often used technology to identify size and size distribution of particles quickly and

[4] A global leader in Testing, Inspection and Certification of geochemical, geo-analytical and mineral analysis

accurately with diameters ranging from tens of nanometres to a few millimetres. Based on measurements, urban soil particle sizes were assessed in three size categories: <8 µm (clay), 8-63 µm (silt), and >63 µm (sand) (Konert & Vandenberghe, 1997).

3.2.5. Eh-pH analysis (redox potential and acidity)

The air-dried urban soil samples were mixed with 10 ml of distilled water for Eh-pH analysis. The mixture was kept rotating for 30 min. Soil pH and conductivity (Eh) were tested in a prepared solution in a 1:10 soil-water ratio with a digital Eijkelkamp 18.52.01 Multimeter instrument (Yu & Rinklebe, 2015) at Eötvös Loránd University.

3.2.6. Organic content (SOC) analysis

The organic content (total organic carbon, total nitrogen, ammonia, nitrate) of the urban soil samples was analysed at the Institute for Soil Sciences and Agricultural Chemistry, Budapest. The analysis was performed by the method of Hargitai/Tyurin (Molnár et al., 2019) and the method of Kjeldahl (Alfred R. Conkinlin, 2014) for organic carbon and nitrogen species, respectively.

3.3. Enrichment factor analysis

The enrichment factor (EF) of each PTE to estimate the enrichment levels of the selected hazardous four metal(loid)s in the urban soil samples was calculated by the following equation (Dragović et al., 2008; Z. Wang et al., 2018):

$$EF = \frac{(Ci/Cref)sample}{(Ci/Cref)background^{5}} \qquad \text{(eq. 1)}$$

where C_i is the hazardous metal(loid) concentration in mg/kg and C_{ref} is the content of the reference element in mg/kg. Because of their low variability in urban soil samples, K, Al, Fe, Mn, Ti, and Sr are usually applied as reference elements in EF calculations (Cui et al., 2014; Gąsiorek et al., 2017). Considering the industrial production in Salgótarján and Ózd contained a huge amount of Fe and other transitional metals, the reference aluminium (Al) was considered the best candidate. The enrichment levels of toxic metal(loid)s in the samples were classified as follows: deficiency to minimal enrichment (EF≤2), moderate enrichment (2<EF≤5), significant enrichment (5<EF≤20), very high enrichment (20<EF≤40), and extremely high

[5] In the thesis the term background is equivalent of control/non-contaminated

enrichment (EF>40) based on the calculated EF values (Khademi et al., 2019) which can reflect the origin of the toxic metal(loid)s as well (Gąsiorek et al., 2017; Zacháry et al., 2015).

3.4. Microbiological analysis

3.4.1. Sample collection for microbiological studies

Based on the urban soil elemental analysis (see section 3.2), the most PTE-contaminated areas (sometimes for only one selected element) were identified and subjected to microbiological analysis (Figure 6). The samples were obtained by scraping away the upper 5 cm surface of the soil (due to plant roots and residues) with a sterile knife, and the samples were placed into sterile plastic tubes (from the upper 10 cm) and transported to the laboratory at 4°C and then kept at -20°C until the analysis (described below) at Department of Microbiology, Eötvös Loránd University.

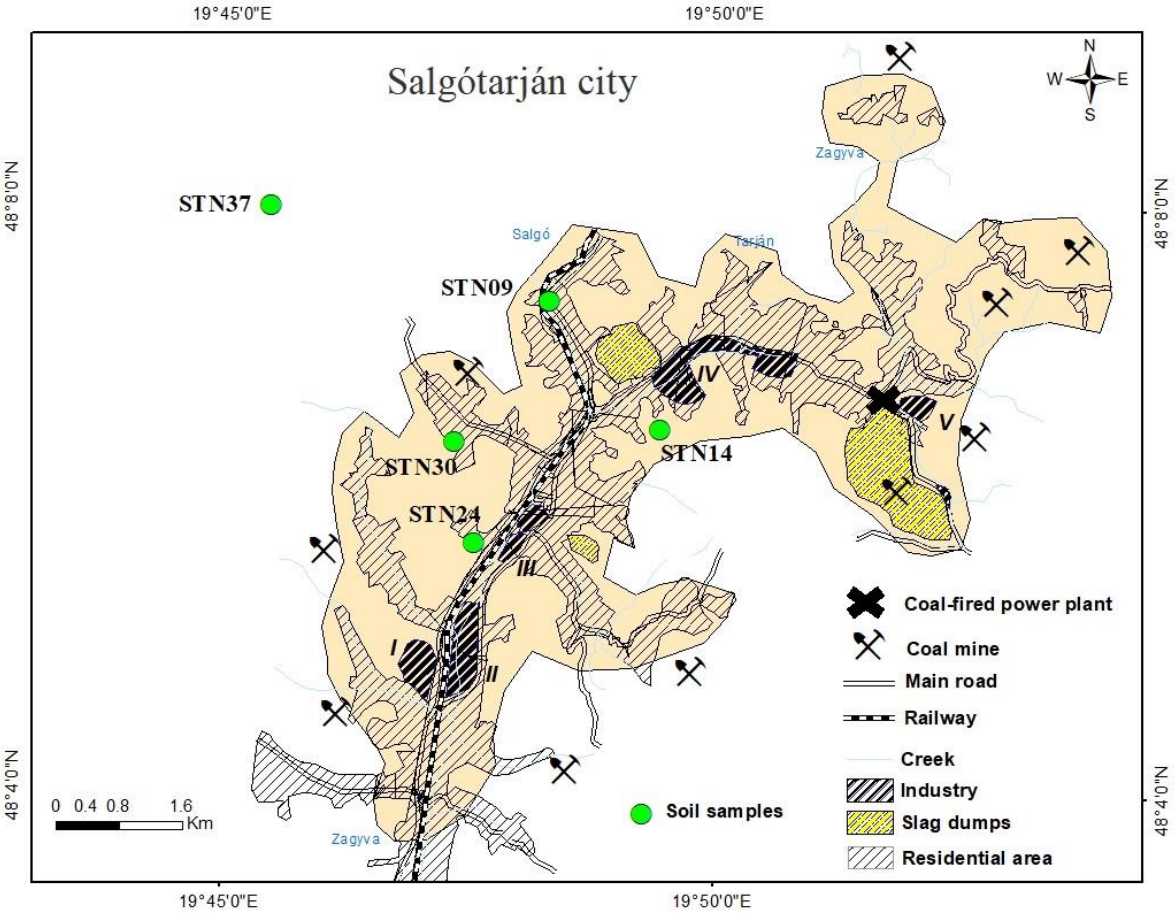

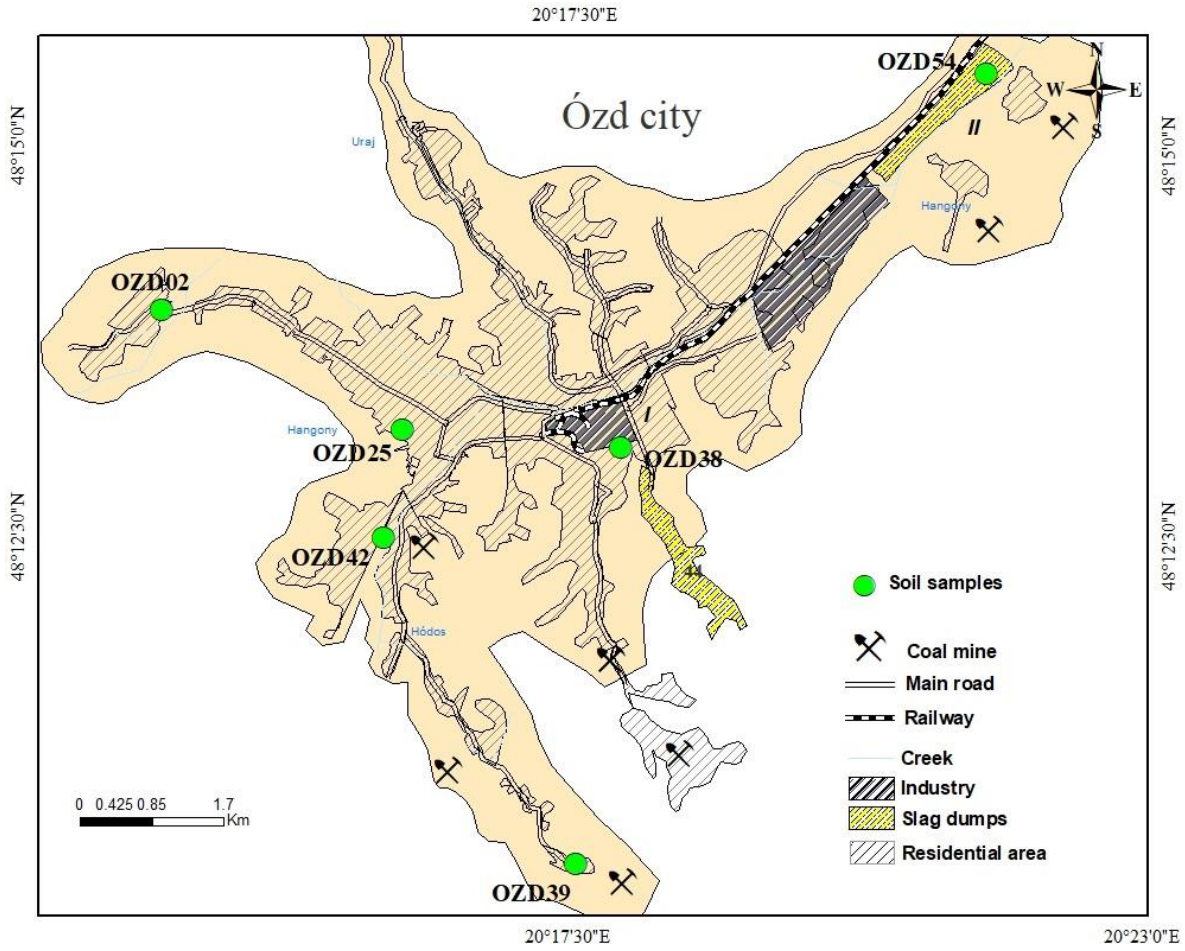

Figure 6. Simplified map of Salgótarján (A) and Ózd (B) showing sampling sites for microbiological study and positions of the local anthropogenic sources (industries, slag dumps, coal mines). Sample STN37- brown forest soil and OZD02 – agricultural soil are considered as uncontaminated or control samples.

3.4.2. Isolation and identification of bacteria

Bacterial strains were cultivated on nutrient agar medium (5g/L peptone, 3g/L meat extract, 10 g/L Agar; DSM medium 1) supplemented with 200 µg/ml of respective metal salt compounds ($CdSO_4$, $HgCl_2$, $Pb(NO_3)_2$). The number of metal tolerant bacteria determined CFU values after the dilution series method. Bacterial strains were randomly isolated from all plates.

After purification, bacterial strains were identified based on 16S rRNA gene sequencing: the genomic DNA of the isolates was extracted using a DNA extraction kit (DNeasy Power Lyzer Microbial Kit, Qiagen, Germany). The 16S rRNA gene of the bacterial strains was amplified (PCR) from the extracted genomic DNA using the universal primers 27f (5′-AGAGTTTGATCCTGGCTCAG-3′) and 1492r (5′-GGCTACCTTGTT ACGACTT-3′) (LGC Genomics, Berlin, Germany). The 16S rRNA gene sequence of the strains was compared with

references in the EzTaxon database (Yoon et al., 2017) to identify closely related bacteria. The obtained 16S rDNA gene sequences were deposited in the National Centre for Biotechnology Information (NCBI) under accession number MT765153 - MT765173.

3.4.3. Minimum Inhibitory Concentration (MIC) analysis

In order to obtain metal(loid) resistant isolates, a minimum inhibitory concentration (MIC) analysis was performed (Maity et al., 2019; Neethu et al., 2015). Bacterial strains were transferred to elevated concentrations of metal(loid) salts ($CdSO_4$, $HgCl_2$, $Pb(NO_3)_2$ and As_2O_3) on the nutrient agar medium (DSM medium 1) that contains 200 µg/ml, 500 µg/ml, 800 µg/ml, 1000 µg/ml, 1500 µg/ml, 2000 µg/ml, 2500 µg/ml, 3000 µg/ml, 5000 µg/ml, 10000 µg/ml, 15000 µg/ml of Pb, Cd, Hg and As. Besides the individual effect, isolates were exposed to the complex effect of metal(loid) salts (900 µg/ml Pb, 600 µg/ml Cd, and 600 µg/ml Hg) to check their multi tolerance, as well. Additionally, MIC values were checked by low phosphate Tris-salt mineral medium supplemented with heavy metal(loid) salt additives ($CdSO_4$, $HgCl_2$, $Pb(NO_3)_2$, or As_2O_3,) in various concentrations (500 - 800 µg/ml for Pb, 500 - 1500 µg/ml for Cd, 300 - 500 µg/ml for Hg, 100 - 220 µg/ml for As).

3.4.4. Next-Generation Sequencing (NGS)

Soil community analysis were performed on the selected eleven sampling sites (including control samples) to be able to compare the effect of the metal(loid) contamination on the microbial community. The isolation of the community DNA from the soil samples was conducted according to the manufacturer's instructions via Ultraclean® PowerSoil DNA Kit (MoBio, Carlsbad, CA, USA). The cell walls were destroyed mechanically by Retsch Mixer Mill MM400 (Retsch, Germany), shaking at 30 Hz for 2 min. The Bacteria and Archaea communities were identified based on the partial 16S rDNA gene sequence after the PCR amplification of V3-V4 regions by universal primers (S-D-Bact-0341-b-S-17 forward (5′-CCT ACG GGN GGC WGC AG-3′) and S-D-Bact-0805-a-A-21 reverse (5′-GAC TAC HVG GGT ATC TAA TCC-3′) for Bacteria, and S-D-Arch-0519-a-A-19 (5' – CAG CMG CCG CGG TAA – 3') and S-D-Arch-0787-a-A-20 (5' – TCC CCC GCC AAT TCC TTT AA – 3') for Archaea in triplicate and the mixture was used for sequencing (Srinivasan et al., 2012). The DNA sequencing was fulfilled at the Michigan State University (USA) by Genomics Research

Technology Support Facility (RTSF). Identification of genomic bases and FastQ format conversion were performed by Illumina Real-Time Analysis (RTA) v1.18.54 and Illumina Bcl2fastq v2.19.1, respectively.

The bioinformatic analysis of raw sequencing reads was executed with MOTHUR v.1.40.5 software (Kozich et al., 2013) using the MiSeq SOP protocol (accessed in 2019). After a quality trimming (deltaq=10) the raw reads were dereplicated, and the sequences were aligned against SILVA template alignment; then, the desired aligned region was screened. Following filtering gaps, the potentially chimeric sequences were detected via chimera.vsearch tool and removed. Additional reduction of sequence noise with pre-clustering followed the taxonomic classification using the SILVA taxonomy database (https://mothur.org/wiki/silva_reference_files/) with a greater than 80% bootstrap support value considered for the successful classification.
Species richness and diversity indices were assessed with inverse Simpson (1/D) (Simpson, 1949), Shannon-Weaver (Shannon, 1948), Chao1(Anne Chao, 1984), and ACE (Hughes et al., 2016) indices, as well as depicted with rarefaction curves based on the subsampled reads from MOTHUR. The sequence raw reads were deposited under the BioProject PRJNA643801 accession number in the NCBI SRA database.

3.4.5. Whole-genome sequencing (WGS)

The whole genome sequence of bacterial strain S14E4C (NCBI GenBank accession MK660715) was analysed. The BLAST search results based on EzTaxon and GenBank databases both indicated that strain S14E4C belongs to the genus *Cupriavidus* and it is 100% identical to *Cupriavidus campinensis* WS2 (Goris et al., 2001). The whole-genome shotgun and paired-end sequencing were performed by the Genomics Research Technology Support Facility (RTSF), Michigan State University (USA), on an Illumina MiSeq platform using the MiSeq standard v2 chemistry. Sequence read quality was checked by the FastQC tool, and the low-quality reads, with excess "N" and low-quality scores, duplication reads, and adaptor contamination was filtered out from the sequence set. Subsequently, the de-novo assembly of high-quality reads was made using the SPAdes v3.10.0 assembler (Bankevich et al., 2012) in careful mode, and the existence of plasmids in the genome was identified by the plasmid SPAdes (v3.5.0) tool. The assembly quality and coverage value were calculated by QUAST v2.3 (Gurevich et al., 2013), and contigs shorter than 500 bp were removed from the

assembly, which resulted in 52 contigs with 6,322,653 bp lengths (66.3 % GC), 290,832 bp N50 value, and 78.3 × genome coverage. The possible genome contamination was checked based on the 16S rRNA on the ContEst16S platform (Yoon et al., 2017). The replicons were identified by the PlasmidSPAdes v.3.5 software that the algorithm using contigs' read coverage information, estimates median coverage, builds assembly graph and generates plasmidic contigs (Antipov et al., 2016). To validate the obtained results, the draft genome sequence (52 contigs) and putative plasmids of the S14E4C strain were aligned by Mauve v.2.4 software (Darling et al., 2004) with the whole genome, chromosome, and plasmid sequences of the known *Cupriavidus* species (mainly *C. metallidurans*).

The nearly full-length 16S rRNA gene sequence of strain S14E4C obtained by the Sanger method was compared with the obtained 16S rRNA gene sequence from the genome assembly and showed 100% similarity. The Whole Genome Shotgun project of strain S14E4C has been deposited at DDBJ/ENA/GenBank under the accession VCIZ00000000 (the described version is VCIZ01000000). The strain S14E4C has been accessioned into the National Collection of Agricultural and Industrial Microorganisms under the accession number NCAIM B.02650.

3.4.6. Genome annotation and analysis

Genome annotation, prediction of genome features, and functions were analysed by RAST (Rapid Annotation using Subsystem Technology), PATRIC 3.5.38, and DDBJ Fast Annotation and Submission Tool (DFAST) web interfaced pipelines (Brettin et al., 2015; Tanizawa et al., 2018). The annotation results of different tools were combined to cover all parts of the genome. Additionally, after submission, the NCBI Prokaryotic Genome Annotation Pipeline (PGAP) (https://www.ncbi.nlm.nih.gov/genome/annotation_prok/) was ordered to annotate the genome. Functional genes that were looked into for potential involvement in metabolic pathways were examined by the KEGG database on PATRIC 3.5.38. Phylogenetic classification of proteins encoded in the S14E4C genome was based on clusters of orthologous groups (COG) functions.

3.4.7. Phylogenetic and phylogenomic analysis

To determine the phylogenetic relationships among *Cupriavidus* species, the public and completed 16S rRNA gene sequences of the corresponding *Cupriavidus* type strains were gathered from the Arb-Silva database (Yilmaz et al., 2014) and aligned by SINA 1.2.11 aligner

in SILVA ACT (Alignment Classification and Tree Service) service before creating Maximum Likelihood (ML) tree. A rooted phylogenetic tree based on 16S rRNA gene sequence similarity of the genus *Cupriavidus* was created using CIPRES Science Gateway's MrBayes tool (Ronquist et al., 2012) and the closely related bacterium *Polynucleobacter cosmopolitanus* CIP 109840T (AJ550672) was used as an outgroup. The phylogenetic tree was visualized by FigTree v1.4.4 (Patrício et al., 2012). In addition, PATRIC (Wattam et al., 2017) presents the reference and representative genomes and uses them as part of the Comprehensive Genome Analysis in phylogenomic analysis. The closest reference and representative genomes have been identified by Mash/MinHash (Ondov et al., 2016). The phylogenetic position of the genome was identified by PATRIC based on chosen global protein families (PGFams) (Davis et al., 2016) from these genomes. Then these protein sequences were aligned with MUSCLE (Edgar, 2004), and the nucleotides were plotted to the protein alignment of each sequence. The amino acid and nucleotide alignments were linked into a data matrix and the RaxML tool (Stamatakis, 2014) was used to analyse this matrix using quick bootstrapping (Stamatakis et al., 2008) and produce support values in the tree.

3.5. Human health risk assessment

Non-carcinogenic and carcinogenic human health risk assessment based on the geochemical dataset (Table S1 and S2) was calculated by a health risk model suggested by the US Environmental Protection Agency (RAIS, 2017; US EPA, 1989b, 1989a). The study covers the ingestion, inhalation, and dermal pathway exposure for PTE, which can result from hand-to-mouth action, dropped food, direct soil or dust consumption and inhalation, dermal contact, etc.

The non-carcinogenic risk assessment was done by the following equations (RAIS, 2017):

$$ADI_{\text{children/adults}} = (C*EF*ED*IR*CF) / (AT*BW) \quad \text{(eq. 2)}$$

$$HQ^i = ADI^i / RfD^i \quad \text{(eq. 3)}$$

ADI represents the average daily intake of metal(loid)s; C - concentration of PTE at sampling site (mg/kg); EF - exposure frequency, 350 days/year; ED - exposure duration that is considered 6 years for children and 30 years for adults; IR - ingestion rate that is 200 mg/kg for children and 10 mg/kg for adults; AT - average time = 365*ED; BW - average body weight which is

15 kg for children and 70 kg for adults. Hazard quotient (HQ)>1 indicates possible adverse health effects, whereas HQ<1 means no adverse health effect. The oral reference dose (RfD) of PTEs is shown in Table 3 (RAIS, 2017; US EPA, 1989a, 1989b).

The non-carcinogenic effect on the population for n number of PTEs is the sum of all the HQs owing to individual heavy metal(loid)s. According to the USEPA, this is referred as the Hazard Index (HI) and is represented by the following equation:

$$HI=\sum_{k=1}^{n} HQk \qquad \text{(eq. 4)}$$

where HQ_k is a value of heavy metal(loid) k. The exposed population is unlikely to suffer negative health impacts if the HI value is less than one. If the HI value is more than one, there may be cause for concern about non-carcinogenic effects (US EPA, 1989a).

The carcinogenic risk was assessed by the equations below for a probable appearance of any kind of cancer when PTE was orally ingested in an individual lifetime (LT=70) (RAIS, 2017; US EPA, 1989a, 1989b):

$$LADD_{ing}=\frac{C*EF*CF*RBA}{AT*LT}*\left(\frac{ED*IngR}{BW}\right) \qquad \text{(eq.5)}$$

$$OralRisk=LADD_{ing}*CSF \qquad \text{(eq. 6)}$$

where RBA is the relative bioavailability factor (1 for all metals and 0.6 for As); CSF is the oral carcinogenic slope factor, and values for PTE are shown in Table 3. The carcinogenic risk levels considered as < 10^{-6} very low, 10^{-6} – 10^{-5} low, 10^{-5} – 10^{-4} medium, 10^{-4} – 10^{-3} high and > 10^{-3} very high level (US EPA, 1989a, 1989b).

Table 3. Reference dose (RfD) and cancer slope factor (CSF) values (US EPA, 1991, 2011).

	Ingestion RfD	Dermal RfD	Inhalation RfD	Ingestion CSF
As	3.00E-04	3.00E-04	3.00E-04	1.50E+00
Pb	3.60E-03	-	-	8.50E-03
Hg	3.00E-04	3.00E-04	8.60E-05	-
Cd	5.00E-04	5.00E-04	5.70E-05	-

3.6. Statistical analysis

3.6.1. Mapping of PTE distribution

The spatial distribution maps of PTE in Salgótarján and Ózd urban soils were created by the Inverse Distance Weighting (IDW) method, which is considered to be interdependent on the basis of distance (Achilleos, 2011) and generated by ArcGIS v10.3 software. The method transforms the values from the erratically distributed sampling points to regular grid-based variograms. Class divisions for PTE distribution colour maps are based on a manual classification to compare elemental data in the cities and indicate the internationally accepted soil PTE threshold values (Table 4).

3.6.2. Basic and descriptive statistics

Using descriptive statistics, the minimum, maximum, average, standard deviation, standard skewness, and standard kurtosis were determined on urban soil PTE. The summary statistics were performed by using original data. The elemental data were analysed and displayed by R v4.0.2 (R Core Team, 2020) and Past4 software.

3.6.3. Hypothesis tests

Since environmental data series often display nonnormality, heterogeneity, and outliers, the Shapiro-Wilk hypothesis test (Shapiro & Wilk, 1965) was performed to assess the normality and lognormality of the elemental data. The p-value less than 0.05 rejected the null hypothesis and indicated the data was not normally distributed. Normalization and transformation (Box-Cox) of the data were fulfilled by PAST4 software to minimize redundancy, and the obtained data was used in further statistical analysis. The Mann-Whitney (Wilcoxon) homogeneity test (Neuhäuser, 2011) based on the comparison of medians confirmed differences between sample groups at the 95 % confidence level.

3.6.4. Univariate analysis

Spearman's correlation coefficient (Spearman, 1904) was conducted to examine the relationships between the potentially toxic elements (non-linear), as well as their relationship with community structure and diversity indices (see section 4.2.2). Correlations = or > 0.7 were considered important and in all cases $p<0.05$ was considered significant.

3.6.5. Multivariate analysis

To extract a reduced number of independent PTE components in soils, principal component analysis (PCA) was performed. PCA eligibility for the analysis of the dataset (soil physicochemical parameters and PTE) was determined by the Kaiser-Meyer-Olkin measure (Kaiser, 1974) of sampling adequacy and the Bartlett test (Arsham & Lovric, 2011) of sphericity. In both cases, the data met the threshold requirements (0.65 and $p<0.001$, respectively). The relationship between soil microbial community and PTE/physicochemical parameters was examined and illustrated by R 2.5.1 (R Core Team, 2020) via vegan (Oksanen et al., 2019) and ggplot2 packages (Wickham, 2010). The dissimilarity of the bacterial communities (using OTU data) was visually interpreted by non-metric multidimensional scaling (NMDS) based on the Bray-Curtis similarity method. The relationship between operational taxonomic units (OTU[6]) and environmental factors was analysed by the Envfit function using the vegan package (Oksanen et al., 2019). Differences in the environmental factors (soil organic content, soil texture, Eh-pH) and PTE in sampling areas were checked by one-way ANOVA ($p<0.05$ considered significant). The OTU dissimilarities between sampling sites/cities were analysed by the Simper test on PAST4 software. Community structure differences were checked by the PERMANOVA test, using Adonis with 9999 permutations on the vegan package (Anderson, 2001).

[6] An Operational Taxonomic Unit (OTU) classifies organisms at any taxonomic level based on their sequence similarity.

Chapter 4. RESULTS

4.1. The concentration and spatial distribution of PTE in the soil samples

The statistical characteristics of the urban soil PTE content are listed in Table 4 (details in Table S1 and Table S2). There is a heterogeneous distribution of PTE in both cities. The concentration ranges for As, Pb, Hg, and Cd are 3.7-73.6 mg/kg, 8.5-1692 mg/kg, 0.03-0.5 mg/kg, 0.1-1.6 mg/kg in Salgótarján, and 2.7-35.9 mg/kg, 6.6-1673.5 mg/kg, 0.015-4.9 mg/kg, and 0.11-62.89 mg/kg in Ózd samples, respectively. In Salgótarján, 50% of samples for As, 75% for Pb, 61% for Hg, and 64% for Cd, whereas in Ózd, 58% for As, 91% for Pb, 55% for Hg, and 98% for Cd exceeded their corresponding local geochemical background values (Table 4).

The spatial distribution of As, Pb, Hg, and Cd in urban soils is shown in Figure 7. It can be observed that except for Hg in Salgótarján, all the selected PTE in both cities exceeded the maximum permissible soil values for PTEs (Table 4) which indicates significant PTE contamination in the cities (Figure 9). Among them, the concentration of 20% of the samples for As and 6% for Pb and Cd in Salgótarján exceeded the assigned Hungarian pollution limit (Table 4). In Ózd samples, these values are less than 10% for selected PTEs.

Due to its multi-industrial background, Salgótarján urban soils depicted irregular distribution of PTE. In certain parts of the city, however, there was a similar pattern of elevated As and Hg, as well as Pb and Cd concentration (Figure 7). Therefore, the identified patterns might suggest the origin of the contaminants. Despite that, the detected high PTE contents in Ózd urban soils showed clear patterns, particularly around former and recent industrial sites, smelter slag contaminated soils, and coal mining areas. In addition, elevated mercury distribution was observed almost in all parts of Ózd, except western and north-western parts (Figure 7).

Table 4. Summary statistics of selected PTE concentration in the studied 36 (STN) and 55 (OZD) urban soil samples.

	Salgótarján				**Ózd**			
	As mg/kg	Pb mg/kg	Hg mg/kg	Cd mg/kg	As mg/kg	Pb mg/kg	Hg mg/kg	Cd mg/kg
n	36	36	36	36	55	55	55	55
Minimum	3.7	8.5	0.03	0.1	2.7	6.6	0.015	0.11
Maximum	73.6	1692	0.5	1.6	35.9	1673.5	4.9	62.89
Average	11±2	82±47.4	0.1±0.02	0.36±0.06	8.4±0.8	80±31.6	0.23±0.09	1.77±1.14
Standard deviation	12	285	0.1	0.34	6.1	234.6	0.66	8.4
Median	6.85	20.5	0.07	0.23	6.4	29.8	0.084	0.38
25 percentiles	5.43	16.35	0.05	0.17	5	21.7	0.05	0.29
75 percentiles	12.95	31.08	0.1	0.39	8.3	46	0.13	0.57
Standard skewness	4.3	5.5	2.2	2.5	2.8	6.23	6.76	7.3
Standard kurtosis	21.8	31.5	4.4	6.5	8.8	41.4	48.1	53.9
Coefficient of variation	108.4 %	347 %	100.6 %	94.2 %	72.5%	293.4%	292.7%	477.2%
Confidence level (95%)	1.86	52.91	0.11	1.37	1.64	63.43	0.18	2.28
Local geochemical background	6.8	16.65	0.05	0.18	6	17.49	0.079	0.13
FOREGS topsoil mean value	6	15	0.037	0.15	6	15	0.037	0.15
Hungarian pollution limit	15	100	0.5	1	15	100	0.5	1

- European mean topsoil value published in FOREGS Geochemical Atlas of Europe (Salminen et al., 2005)
- Hungarian pollution limit value is declared by the Hungarian environmental legislation (HUGD, 2009) on the environmental standards for Earth materials, pollution threshold, red colour)

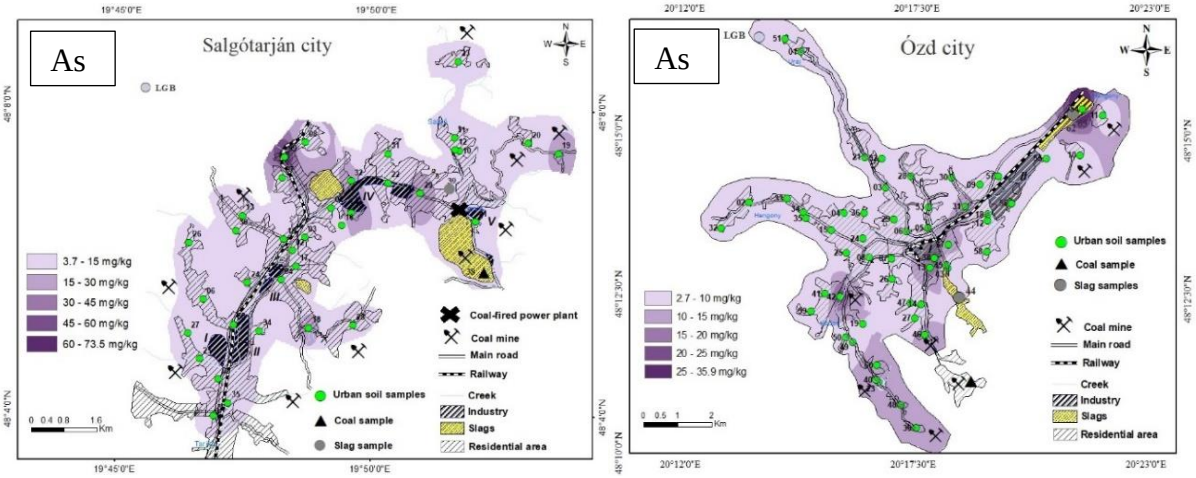
As
Salgótarján city
LGB
3.7 - 15 mg/kg
15 - 30 mg/kg
30 - 45 mg/kg
45 - 60 mg/kg
60 - 73.5 mg/kg
Coal-fired power plant
Coal mine
Main road
Railway
Creek
Industry
Slags
Residential area
Urban soil samples
Coal sample
Slag sample
As
Ózd city
2.7 - 10 mg/kg
10 - 15 mg/kg
15 - 20 mg/kg
20 - 25 mg/kg
25 - 35.9 mg/kg
Urban soil samples
Coal sample
Slag samples
Coal mine
Main road
Railway
Creek
Industry
Slags
Residential area

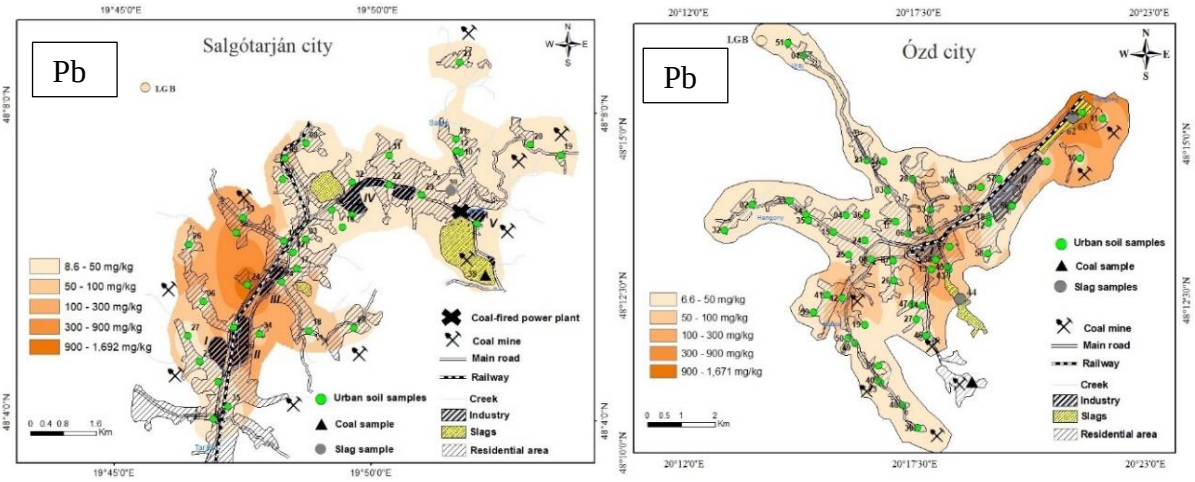
Pb
Salgótarján city
LGB
8.6 - 50 mg/kg
50 - 100 mg/kg
100 - 300 mg/kg
300 - 900 mg/kg
900 - 1.692 mg/kg
Coal-fired power plant
Coal mine
Main road
Railway
Creek
Industry
Slags
Residential area
Urban soil samples
Coal sample
Slag sample
Pb
Ózd city
6.6 - 50 mg/kg
50 - 100 mg/kg
100 - 300 mg/kg
300 - 900 mg/kg
900 - 1,671 mg/kg
Urban soil samples
Coal sample
Slag samples
Coal mine
Main road
Railway
Creek
Industry
Slags
Residential area

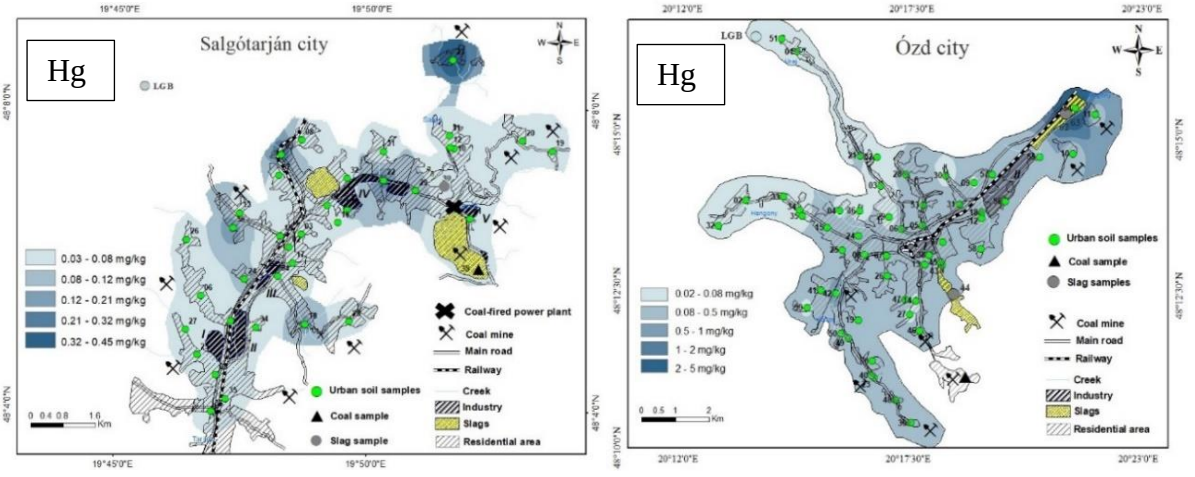
Hg
Salgótarján city
LGB
0.03 - 0.08 mg/kg
0.08 - 0.12 mg/kg
0.12 - 0.21 mg/kg
0.21 - 0.32 mg/kg
0.32 - 0.45 mg/kg
Coal-fired power plant
Coal mine
Main road
Railway
Creek
Industry
Slags
Residential area
Urban soil samples
Coal sample
Slag sample
Hg
Ózd city
0.02 - 0.08 mg/kg
0.08 - 0.5 mg/kg
0.5 - 1 mg/kg
1 - 2 mg/kg
2 - 5 mg/kg
Urban soil samples
Coal sample
Slag samples
Coal mine
Main road
Railway
Creek
Industry
Slags
Residential area

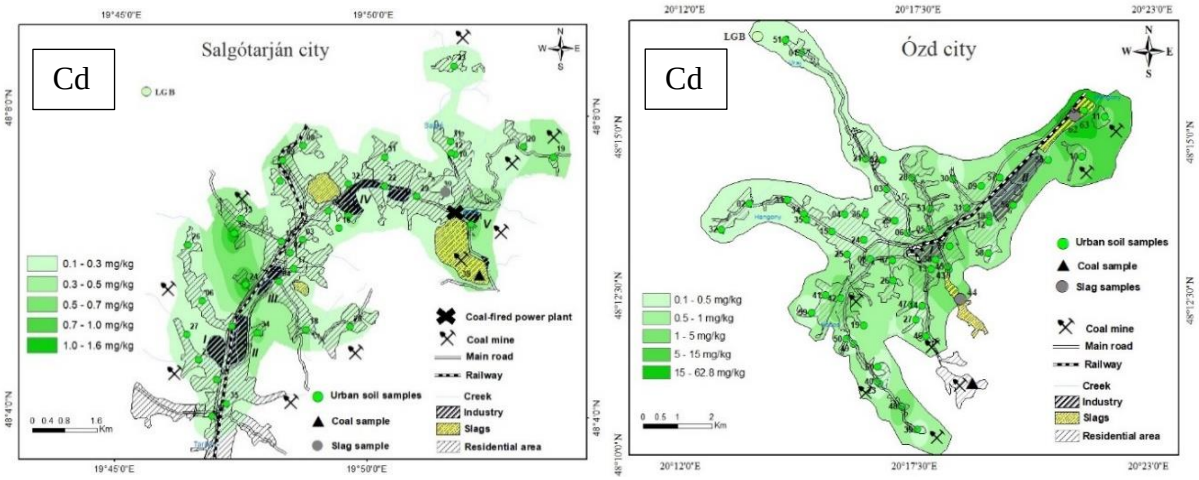

Figure 7. Spatial distribution of As, Pb, Hg, and Cd in Salgótarján and Ózd urban soils. The figures show sampling sites, locations of the slag, coal, brown forest soil (as local geochemical background - LGB), and relative information from Figure 5. In some cases, the concentration patterns on maps were made comparable. The class divisions are set on manual classification involving the Hungarian and internationally accepted soil PTE threshold values (Table 4; (CSTEE, 2000; HUGD, 2009).

4.1.1. Enrichment factor

The enrichment factor (EF) values of the analysed PTE were calculated for urban soil samples in both cities relative to the local geochemical background value of the soil, and the results are presented in (Figure 8). The mean EF values decreased in the order of Pb>Cd>Hg>As in Salgótarján and Cd>Pb>Hg>As in Ózd. The average Salgótarján urban soil enrichment values showed a minimal enrichment of PTE; however, in three samples (STN09, STN24, and STN30), we observed moderate As, Hg, and Cd and significant to very high enrichment of Pb (max. 35 times). These values are much higher in Ózd urban soils: 3 urban soils showed significant enrichment for As (max. 6.4 times enrichment), 6 samples significant to extremely high enrichment for Pb (max. 100 times enrichment), 8 samples significant to extremely high enrichment for Hg (max. 65 times enrichment), and 24 samples significant to extremely high enrichment for Cd (max. 500 times higher) (Table S3). On the other hand, the average cadmium enrichment is 16 times higher than the relative local geochemical background sample (Figure 8).

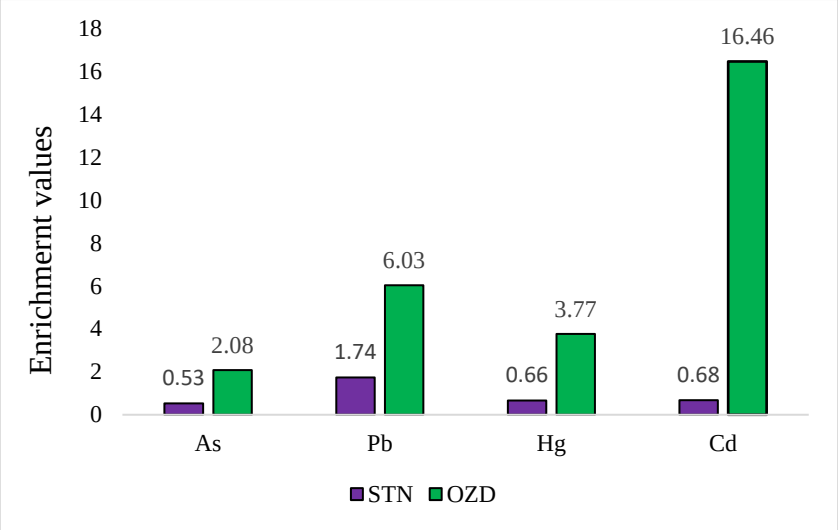

Figure 8. The average PTE enrichment factor in Salgótarján and Ózd urban soils. Enrichment levels are as following: deficiency to minimal enrichment (EF≤2), moderate enrichment (2<EF≤5), significant enrichment (5<EF≤20), very high enrichment (20<EF≤40), and extremely high enrichment (EF>40)

4.1.2. PTE distribution by sampling site category

As samples were collected mainly from public areas (kindergarten, playground, park, and others: roadside, garden, etc.) to assess the contamination and the relative risk for residents (especially children), the distribution of PTE content by sampling site categories were analysed. The results were depicted in log scale to be able to compare the data from both cities and are shown in Figure 9. In both cities, most of the sampling sites show a low to moderate enrichment of As, Pb, Hg, and Cd along the categories. The outlier samples with the highest PTE concentrations (samples exceeding the soil allowable PTE concentration; Table 4) were separated by red line and are encountered at kindergarten (OZD13: 16.8 mg/kg As, 173.1 mg/kg Pb, 2.9 mg/kg Cd), park (STN09: 73.6 mg/kg As), playground (STN14: 26.1 mg/kg As; STN24: 1692 mg/kg Pb, 1.4 mg/kg Cd; OZD42: 23.8 mg/kg As, 250.1 mg/kg Pb, 0.9 mg/kg Hg, 3.03 mg/kg Cd), roadside (STN30: 433 mg/kg Pb, 1.6 mg/kg Cd), and industrial areas (OZD38: 27.1 mg/kg As, 596.4 mg/kg Pb, 0.7 mg/kg Hg, 5.2 mg/kg Cd; OZD54: 35.9 mg/kg As, 1674 mg/kg Pb, 4.9 mg/kg Hg, 62.9 mg/kg Cd) of Salgótarján and Ózd (Figure 7 and Figure 9; Table S1 and Table S2). The overlap of outlier samples indicates several-fold higher PTE contents at the same sampling sites. In general, except for As, the concentration of all PTE in Ózd is relatively higher than in Salgótarján urban soil samples (Figure 8). In the contaminated sites (in the case of both cities), the PTE content is at least 10 times, and in industrial areas

around 500 times higher than the local geochemical background value (Figure 7 and Figure 9).

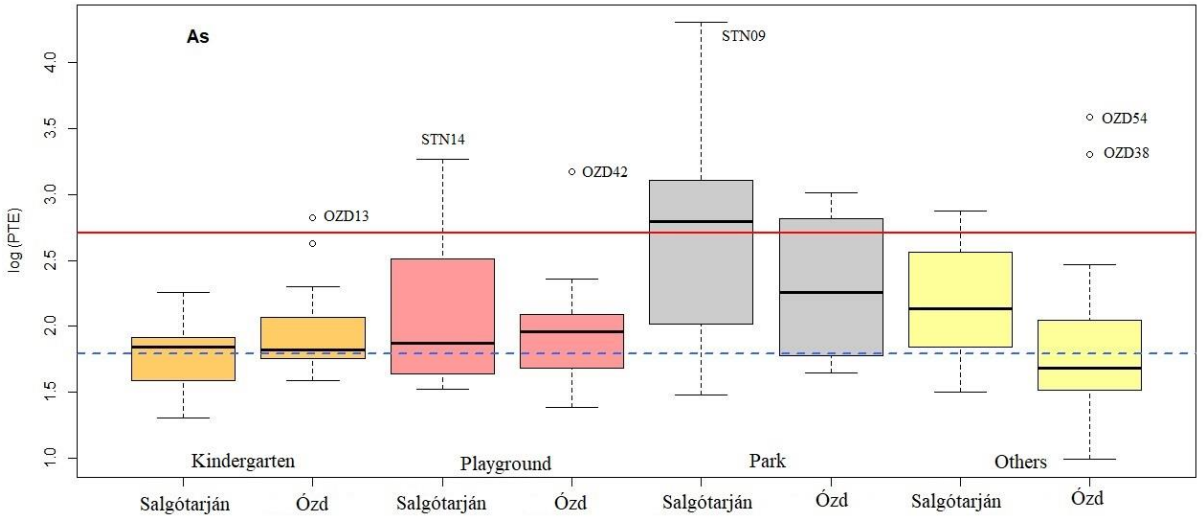

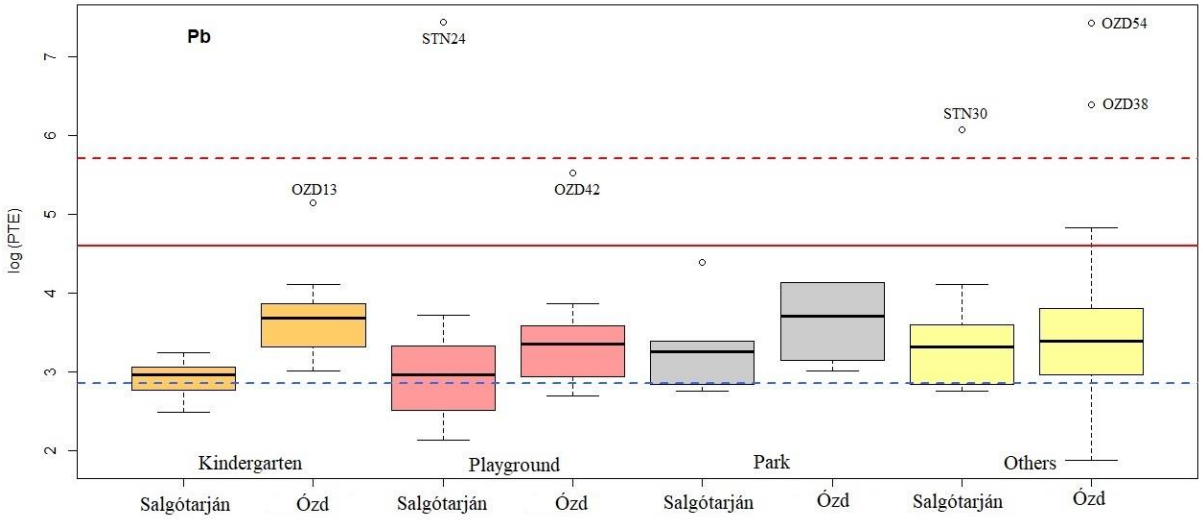

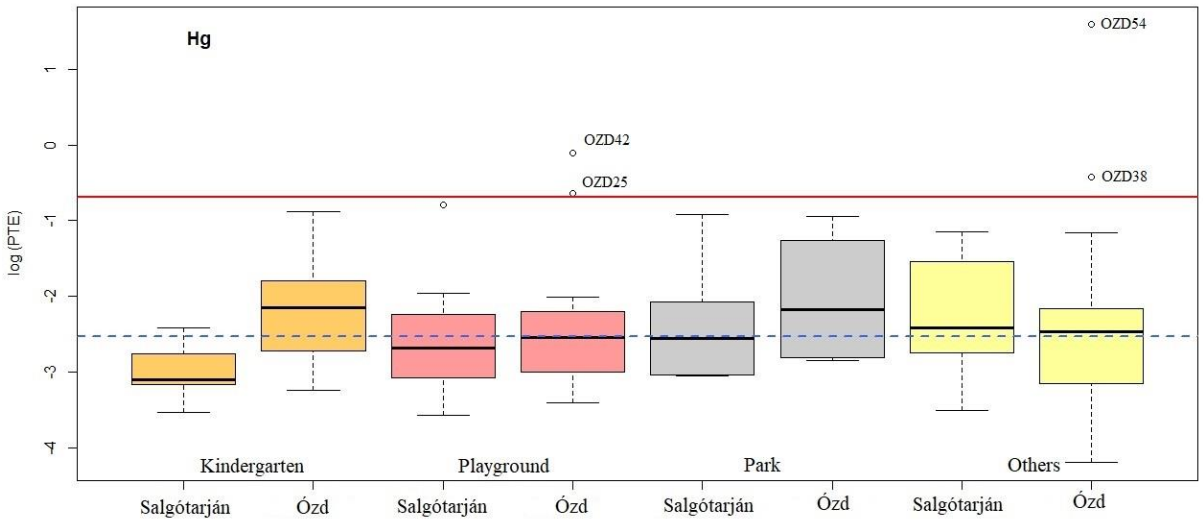

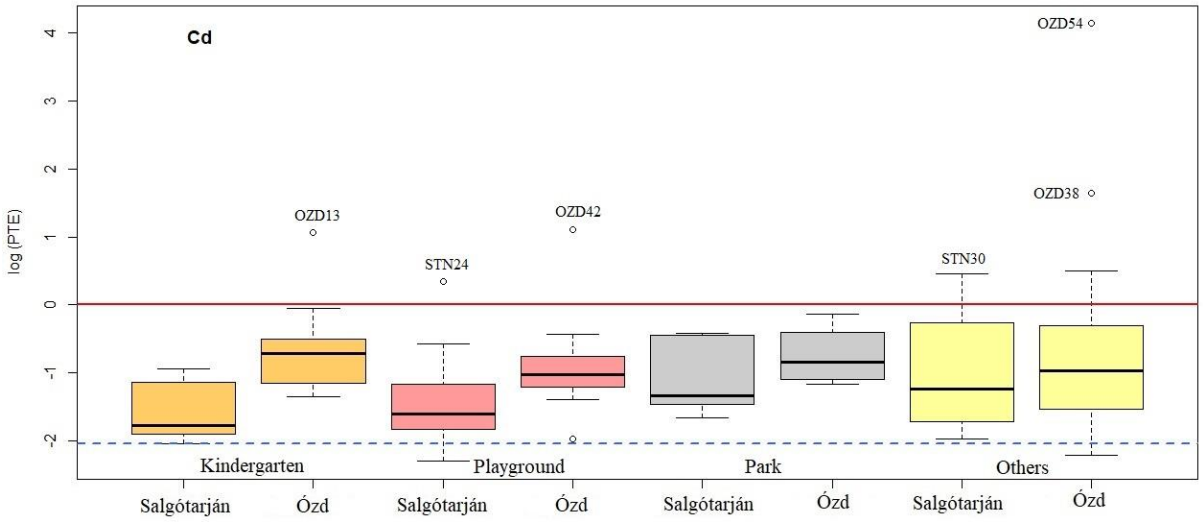

Figure 9. Box and whiskers diagrams showing PTE (As, Pb, Hg, Cd) concentration (in mg/kg) distribution in Salgótarján (STN) and Ózd (OZD) urban soil based on sampling categories in the log scale. Blue dashed line represents brown forest soil (local geochemical background: LGB) for both cities, red and red-dashed lines indicate the maximum allowable PTE limit in soil by Hungarian and European legislations (for Pb), respectively(CSTEE, 2000; HUGD, 2009). The outlier samples are shown with sample numbers.

4.1.3. PTE concentration in local coal, coal ash, and smelter slags

Both studied cities are well-known for their former coal mining and iron-steel industry. Therefore, the PTE content was analysed in local coal, coal ash, and slag samples (Table 5). In Salgótarján, the coal ash sample originated from coal combustion at the coal-fired power plant; however, Ózd smelter slag is a byproduct of the former (slag1) and recent (slag 2-3) iron-steel industry. Results show that Salgótarján coal is enriched with As (5.2 mg/kg), Hg (0.44 mg/kg), and Cd (0.18 mg/kg), whereas STN coal ash with As (35.7 mg/kg). The coal sample collected from Ózd showed similar As and Pb, less Hg, and Cd values compared to Salgótarján coal. On the other hand, Ózd smelter slag samples are characterized by high Pb, Hg, and Cd content (Table 5), especially the sample collected from slag dump site of the former iron-steel industry (OZD slag 1).

Table 5. The concentration of the selected PTE in local coal, coal ash, and smelter slag of Salgótarján (STN) and Ózd (OZD).

	As (mg/kg)	Pb (mg/kg)	Hg (mg/kg)	Cd (mg/kg)
STN coal	5.2	1.28	0.44	0.18
OZD coal	1.2	1.86	0.074	0.01
STN coal ash	35.7	14.19	0.097	0.08
OZD smelter slag 1	6.7	202.2	0.421	1.5
OZD smelter slag 2	1.7	28.48	0.005	0.73
OZD smelter slag 3	0.5	3.21	0.005	0.1

The principal component analysis of Salgótarján and Ózd urban soil samples and local coal, coal ash, smelter slags, and brown forest soils demonstrated one component (PC1) with an eigenvalue more than one and was responsible for 74% of the variance. The loading of As, Pb, Hg, and Cd in PC1 was approximately 50%/each, and among them, Pb and Cd correlated with Ózd smelter slag samples. However, As and Hg showed a high connection to Salgótarján coal, mainly to coal ash. The PC2 was responsible for 14% of variables, with the As and Hg loading of 60% and 40%, respectively (Figure 10).

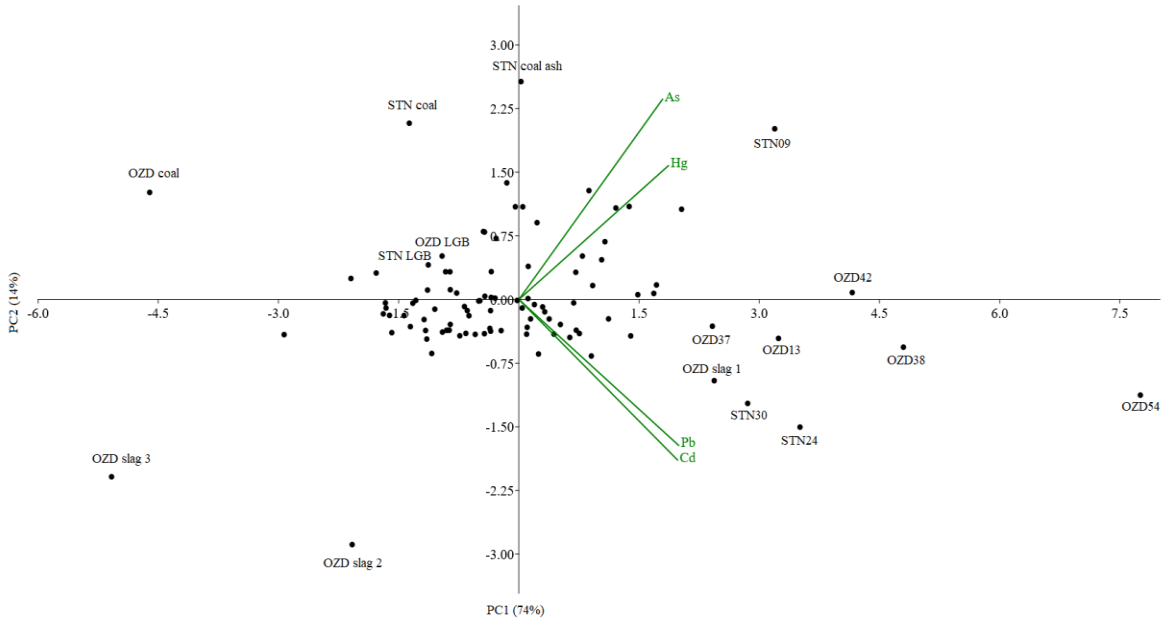

Figure 10. The principal component analysis of Salgótarján and Ózd urban soil samples and coal, coal ash, smelter slags and brown forest soils (local geochemical background- LGB). The used data was transformed by Box-Cox method. LGB- Local Geochemical Background (brown forest soils). The sample numbers are shown for outlier sampling sites.

4.1.4. Influencing factors on PTE distribution

To identify and highlight the strength of interrelationship between selected PTE concentration of the studied urban soils and physicochemical parameters of urban soils (Table S4) Spearman rank correlation coefficients were calculated for Salgótarján and Ózd samples and the results are shown on Table 6 and Table 7, respectively. A significant ($p<0.05$) positive correlation was found between PTE content and physicochemical parameters of urban soils, which show their strong impact on PTE mobility. Notably, Spearman's correlation coefficient indicated a significant correlation between Fe and As; total organic carbon and Pb; Pb and Cd; and As with Pb and Hg in Salgótarján urban soils (Table 6), whereas in Ózd urban soils, significant ($p<0.05$) correlation was observed between all the selected PTE (also with each other) and Fe content (Table 7). Based on the average pH values (7.2 in Salgótarján and 7.5 in Ózd), the urban soil samples are slightly alkaline, and it is relatively high in PTE elevated sites (Table S4). No significant correlation was noted between pH, Eh, soil texture (clay, silt, and sand), and PTE content in the urban soils of the current study.

Table 6. Spearman correlation coefficient between soil physicochemical parameters and PTE in urban soils from Salgótarján. TN-total nitrogen, NH_4^+ - ammonia, NO_3^- -nitrate, TOC-total organic carbon. The significance values were obtained after Bonferroni correction and shown by the * sign (*<0.05, **<0.001). Values higher than ~0.7 (bold) were considered important.

STN	TN	NH_4^+	NO_3^-	TOC	CO_3^{2-}	pH	Eh	clay	silt	sand	Fe	Mn	**As**	**Pb**	**Hg**	**Cd**
TN																
NH_4^+	0.55															
NO_3^-	0.27	0.45														
TOC	**0.95***	0.58*	0.27													
CO_3^{2-}	-0.26	-0.21	0.23	-0.24												
pH	-0.54	-0.40	-0.05	-0.48	0.55											
Eh	0.54	0.40	0.06	0.47	-0.55	**-1.00***										
clay	-0.35	-0.11	-0.21	-0.36	-0.11	-0.08	0.07									
silt	0.43	0.28	0.19	0.43	-0.34	-0.49	0.49	0.07								
sand	-0.20	-0.28	-0.05	-0.18	0.41	0.47	-0.47	**-0.66***	**-0.73***							
Fe	0.11	-0.12	-0.33	0.12	-0.15	-0.16	0.15	0.12	0.04	-0.07						
Mn	0.47	0.26	-0.11	0.51	-0.43	-0.27	0.27	-0.12	0.19	-0.09	0.38					
As	0.32	-0.01	-0.13	0.45	-0.09	-0.16	0.16	-0.23	0.03	0.13	**0.65***	0.39				
Pb	0.58*	0.13	-0.03	**0.65***	-0.26	-0.29	0.28	-0.34	0.13	0.06	0.45	0.60*	**0.71***			
Hg	0.49	0.05	-0.03	0.56*	-0.05	-0.23	0.23	-0.46	0.15	0.14	0.40	0.33	**0.73***	0.64*		
Cd	0.56	0.11	-0.12	0.64*	-0.20	-0.19	0.19	-0.20	0.10	0.07	0.38	0.57*	0.63*	**0.78***	0.57*	

Table 7. Spearman correlation coefficient between soil physicochemical parameters and PTEs in urban soils from Ózd. TN-total nitrogen, NH_4^+ -ammonia, NO_3^- -nitrate, TOC-total organic carbon. The significance values were obtained after Bonferroni correction and shown by the * sign (*<0.05, **<0.001). Values higher than ~0.7 (bold) were considered important.

OZD	TN	NH_4^+	NO_3^-	TOC	CO_3^{2-}	pH	Eh	clay	silt	sand	Fe	Mn	**As**	**Pb**	**Hg**	**Cd**
TN																
NH_4^+	**0.81***															
NO_3^-	0.33	0.23														
TOC	**0.95***	**0.76***	0.27													
CO_3^{2-}	-0.17	-0.23	0.05	-0.12												
pH	-0.31	-0.41	0.18	-0.25	**0.73***											
Eh	0.43	0.48*	-0.13	0.36	**-0.69***	**-0.91***										
clay	-0.12	-0.09	-0.09	-0.23	-0.31	-0.22	0.24									
silt	0.36	0.27	0.22	0.23	-0.18	-0.10	0.24	0.49*								
sand	-0.17	-0.12	-0.09	-0.03	0.32	0.19	-0.30	**-0.82***	**-0.88***							
Fe	-0.13	-0.20	0.11	0.01	0.23	0.40	-0.35	-0.23	-0.30	0.30						
Mn	0.05	0.03	0.04	0.19	0.17	0.40	-0.35	-0.30	-0.11	0.20	0.64*					
As	0.25	0.08	0.09	0.42	0.14	0.17	-0.12	-0.35	-0.21	0.30	**0.76***	0.57*				
Pb	0.03	-0.18	-0.02	0.18	0.26	0.35	-0.30	-0.36	-0.22	0.33	**0.75***	0.60*	**0.80***			
Hg	-0.06	-0.21	-0.13	0.09	0.30	0.36	-0.31	-0.32	-0.27	0.35	**0.72***	0.53*	**0.76***	**0.88***		
Cd	0.03	-0.15	0.06	0.17	0.45	0.46	-0.41	-0.35	-0.22	0.34	**0.80***	0.61*	**0.79***	**0.93***	**0.86***	

4.2. Characterization of soil microbial community

4.2.1. The relation of environmental factors and PTE content in eleven sampling sites selected for microbiological analysis

As the soil microbial community analysis was performed on eleven sampling sites, the distribution of environmental factors in these sampling sites was checked, and their relations were analysed (Table 8; Figure 11). The soil physicochemical parameters and metal(loid) contents (Table *8*) in the two city soil samples were distributed heterogeneously and formed three groups (Figure 11). Group 1 contains samples STN24, OZD38, OZD42, and OZD54 and is considered a high metal(loid)-enriched group (Figure 11). Group 2 includes sample STN09 and STN14, where moderate metal(loid) enrichment, the lowest pH, high Eh, and clay fraction was noted (Figure 11). However, the rest of the samples (STN30, OZD25, OZD39), together with control samples (STN37 and OZD02), formed a distinct group 3, showing moderate or low metal(loid) enrichment and high organic content (Figure 11), clarified by PCA analysis. It is observed that the sampling sites OZD02 (control sample) and OZD39 are characteristic with high ammonia content (7.8 mg/kg and 10.4 mg/kg, respectively), meanwhile the samples STN30 and OZD02 with high nitrate content (10.5 mg/kg and 20.7 mg/kg). The lowest organic carbon (0.9%) and nitrogen (0.05%) were observed in the highest metal(loid) enriched sampling site (OZD54) with the highest sand fraction (72.2 wt%).

Differences in the environmental factors of the sampling sites were tested by one-way ANOVA ($F=5.9$) and were considered significant at $p<0.05$. The Simper test showed that the concentrations of metal(loid)s in control and metal(loid)-enriched (Salgótarján and Ózd soil) samples were significantly ($p<0.05$) different (53.5%), where the Ózd soil samples showed higher enrichment than Salgótarján samples. This was proved by the principal component analysis (Figure 11), which explained 46.8% (PC1) and 16.9% (PC2) of the variables, and most of the metals indicated a correlation with metal(loid) enriched Ózd urban soil samples.

Table 8. Physicochemical parameters and PTE contents in the selected soil samples of Salgótarján and Ózd. TN -Total Nitrogen, TOC – Total Organic Carbon, C_i – inorganic carbon ($CaCO_3$).

			STN09	STN14	STN24	STN30	**STN37**	**OZD02**	OZD25	OZD38	OZD39	OZD42	OZD54
	units												
Pb		mg/kg	80	60	1692	433	16	14.8	36.3	596.4	23.5	250.9	1673.5
Cd		mg/kg	0.7	0.6	1.4	1.6	0.2	0.1	0.4	5.2	0.4	3	62.9
Hg		mg/kg	0.4	0.1	0.1	0.3	0.1	0	0.5	0.7	0.1	0.9	4.9
As		mg/kg	8.5	73.6	26.1	15.7	6.8	4	7.7	27.1	10.3	23.8	35.9
NH_4^+		mg/kg	3.3	2.1	1.6	2.8	1.6	7.8	5.2	3.6	10.4	5.9	2
NO_3^-		mg/kg	4.4	5.3	4.9	10.5	2.1	20.7	7.2	2.1	7.7	4.3	0.5
TN		wt%	0.2	0.2	0.4	0.3	0.2	0.2	0.1	0.1	0.3	0.2	0.05
TOC		wt%	1.7	1.7	1.9	4	2.8	1.3	1.2	1.9	2.9	1.4	0.9
C_i		wt%	1.8	0.1	0.6	0.6	4.5	0.5	4.2	16.4	0.4	9.2	8.1
pH			5.9	6.6	7.6	7.4	7.7	7.6	7.6	7.9	7.5	7.7	8.3
Eh			59	20.1	-29.4	-22.6	-35.5	-41.2	-36.4	-55.2	-32.8	-44.7	-77.5
Soil texture	Clay	V%	20	13.4	12.3	7.1	10.9	9.8	14	6.6	11.2	11	4.7
	Silt	V%	48.7	45.9	42.5	59.2	39.9	46.2	52.5	33.6	45.8	39.7	23
	Sand	V%	31.3	40.8	45.2	33.8	49.2	44	33.5	59.8	43	49.3	72.2

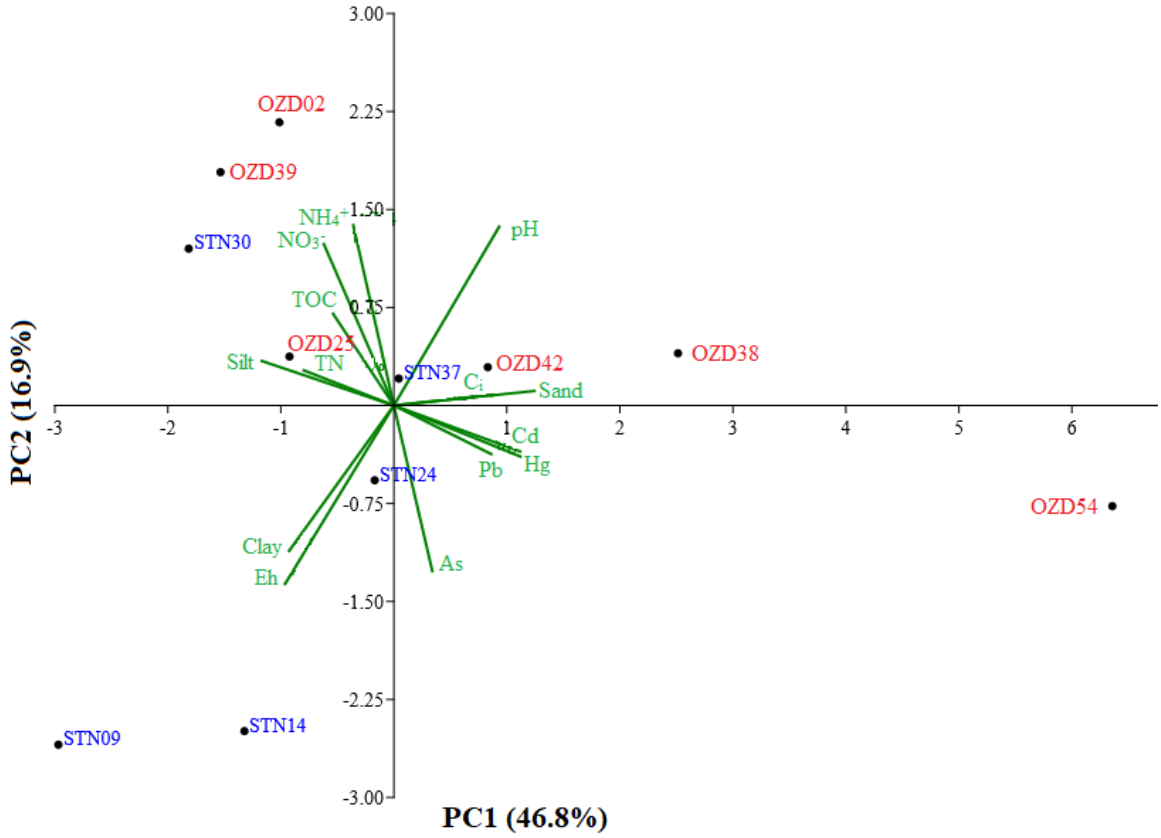

Figure 11. Principal component analysis (PCA) of the soil physicochemical parameters and PTE (As, Pb, Hg, Cd) content. The figure illustrates the possible effects of the environmental factors (see Table 8) on sampling sites.

4.2.2. Molecular studies (NGS) of the microbial community in Salgótarján and Ózd soil samples

4.2.2.1. Diversity indices

The alpha diversity of the 16S rRNA gene sequencing was used to calculate the bacterial richness and diversity (Table 9) in the sampling sites (due to the low diversity of archaea, the calculations could not be performed). Bacterial OTU ranged from 1701 to 2349. It is revealed that only 37-53% of the total bacteria community is abundant more than 1% in all soil samples. Among the diversity indices, the Chao1 and ACE are particularly effective in estimating the species richness. The Chao1, ACE, Shannon, and inverse Simpson indices ranged from 1704-2406, 1722-2557, 6.49-7.03, and 128-485, respectively. It is observed that compared to the control sample, the Shannon, and Inverse Simpson diversity indices of Salgótarján metal(loid)-enriched samples are high, however, the opposite was observed in the case of Ózd samples (Table 9). The Simper test showed that the dissimilarity in diversity between control and

metal(loid)-enriched samples is significantly low (9.5%). Archaea OTU ranged from 18 to 91. The highest archaeal OTU number was found in sample OZD25 (91 OTU), whereas the lowest value was defined in samples OZD38 and OZD54 (15 and 18, respectively). The correlation analysis between the diversity indices and As, Pb, Hg, and Cd (also the environmental factors) showed no significant correlation.

Table 9. The number of operational taxonomic units (OTUs) for Bacteria and Archaea, estimated species richness, and diversity indices for Bacteria. The species richness and diversity indices are shown only for Bacteria (due to the low abundance of Archaea).

Sample	No of observed OTUs	Species richness		Diversity indices	
	Bacteria /Archaea	Chao1	ACE	Shannon	Inverse Simpson
STN09	2117 / 33	2153	2253	6.77	325
STN14	2313 / 52	2393	2528	6.91	456
STN24	2349 / 39	2406	2530	6.96	389
STN30	2272 / 50	2292	2361	7.03	485
STN37 (control)	1701 / 51	1704	1722	6.63	309
OZD02 (control)	2133 / 27	2138	2184	6.96	484
OZD25	1933 / 91	1933	1939	6.68	150
OZD38	2317 / 15	2405	2557	6.49	128
OZD39	1997 / 32	1997	1999	6.83	200
OZD42	2023 / 52	2036	2086	6.77	294
OZD54	1810 / 18	1844	1905	6.55	206

4.2.2.2. Soil microbial community composition

Analysis indicated that in all the sampling sites on the level of the phyla, the bacterial community was dominated by Proteobacteria, which constituted 20-22.8 % of the total soil bacterial community in Salgótarján and 25-28% in Ózd soil samples, independently from PTE (though, characteristic differences could be observed at lower-level taxonomic units). In Salgótarján samples, the abundance was followed by Acidobacteria (9.8-14.4%), Actinobacteria (9.1-12.6%), Bacteroidetes (8.3-12.3%), Planctomycetes (8.9-12%), Patescibacteria (7.1-10.2%), Verrucomicrobia (4.1-9%), and Chloroflexi (4-7%) (Figure 12A). In Ózd samples, however, the abundance was followed by Planctomycetes (10-13.8%), Acidobacteria (7.7-13.1%), Bacteroidetes (7-12.3%), Actinobacteria (7.6-11.7%), Patescibacteria (2-11.7%), Verrucomicrobia (3.6-7.3%), and Chloroflexi (2.5-7.1%) (Figure 12A). The abundance of unclassified bacteria ranged between 3.6-7.1% in Salgótarján and 3.6-

12% in Ózd soil samples. The above-mentioned phyla cover 91% of the soil community (Figure 12A). The relative abundance of each phylum varied among the sampling sites, and the overall average dissimilarity of phyla was only 15% between control and metal(loid) enriched samples. Compared to the control samples, the metal(loid)-enriched samples were characterized by a low abundance of Acidobacteria and a higher abundance of Patescibacteria in both city samples (Figure 12A).

The archaeal community in all sampling sites of Salgótarján and Ózd was dominated by Thaumarchaeota (19.6-62.5%), Nanoarchaeota (6.7-60.8%), and Euryarchaeota (6.25-28%), and these phyla covered the 95% of the archaeal communities (Figure 12B). Among all the sampling sites, Crenarchaeote appeared only in the sampling site STN30, one of the low metal(loid) and high organic content sites (roadside sample). The highest number of OTU (at the level of phyla) was observed in sample OZD25, however, the lowest number of archaeal phyla was observed in sampling sites OZD38 and OZD54 of Ózd (Figure 12B), and the most PTE enriched sites. The average dissimilarity, based on the Simper test, of archaea phyla in control and metal(loid) enriched samples was 35%.

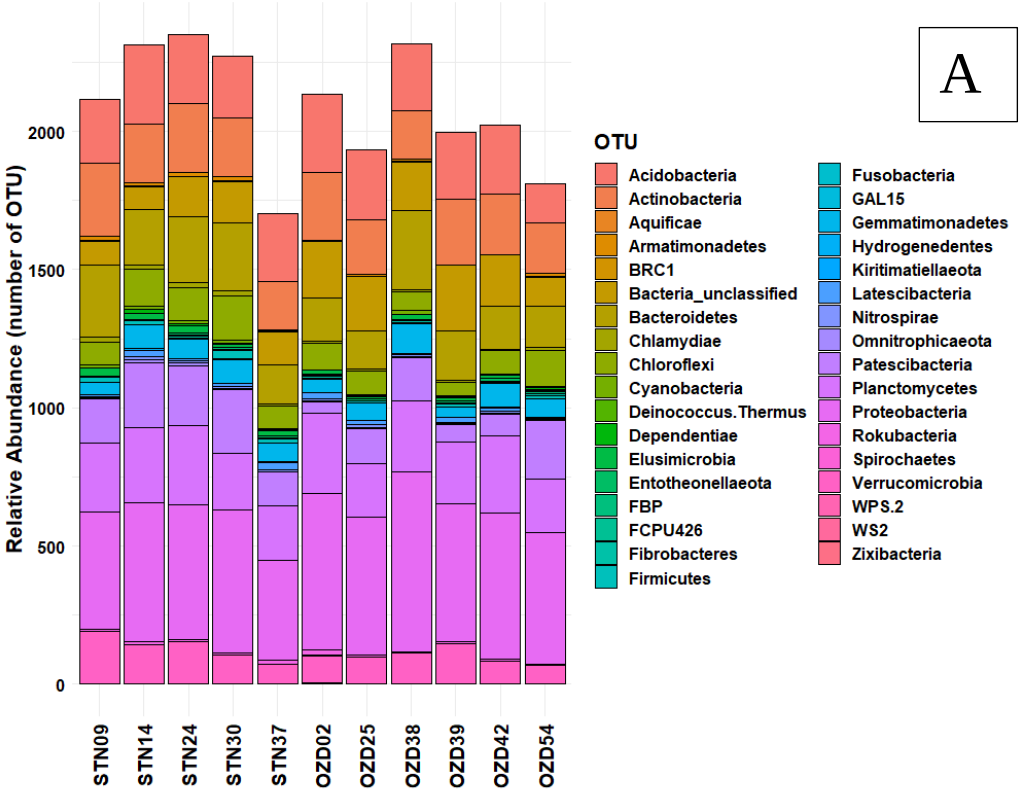

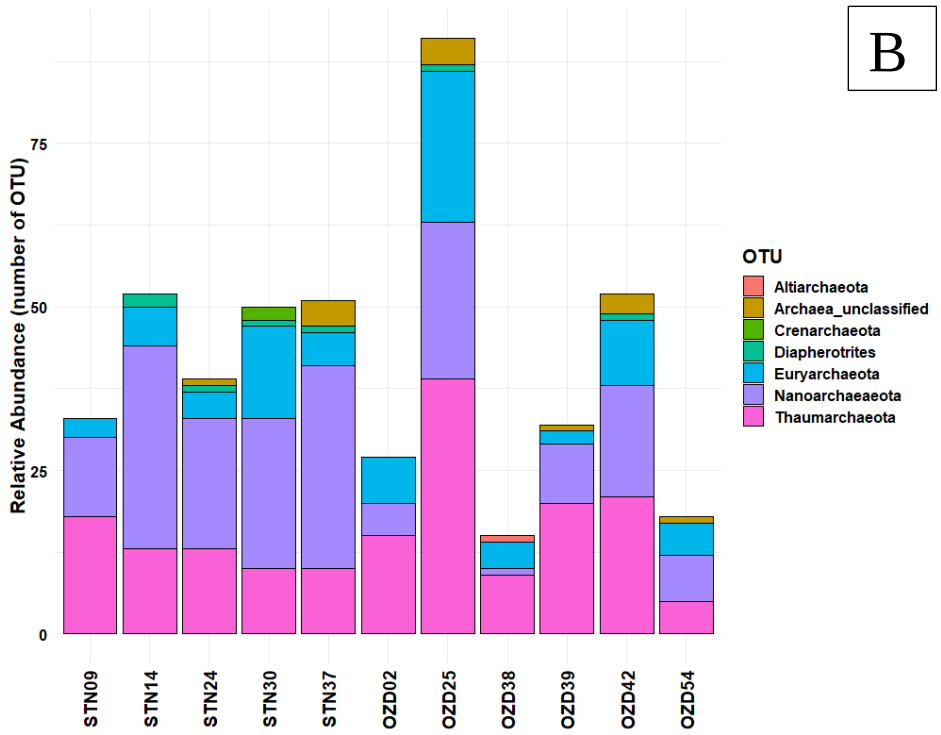

Figure 12. The results of NGS analysis (see section 3.4.4) shows the distribution of Bacteria (A) and Archaea (B) phyla in Salgótarján (STN) and Ózd (OZD) soil samples. STN37 and OZD02 are control samples.

The taxonomic differences between metal(loid)-enriched and control sampling sites were especially visible at class and genus level. In contrast to the control sample, a significant increase of Gammaproteobacteria, Deltaproteobacteria, Planctomycetacia, and Actinobacteria was observed in Salgótarján urban soils (metal(loid)-enriched), whereas in Ózd urban soils the OTU number of Deltaproteobacteria, Planctomycetacia, and Actinobacteria considerably decreased. The characteristic abundance of Subgroup_6 and Latescibacteria_cl in control samples, on the other hand, Parcubacteria and Saccharimonadia in urban samples (metal(loid)-enriched) of both cities (Table S5).

In the case of Archaea, the most abundant classes belong to Thermoplasmata, Woesearchaeia, and Nitrososphaeria, typically observed in control or low metal(loid)-enriched samples. Among the sampling sites, in the sample OZD25, one of the low PTE containing Ózd urban soil, the number of Thermoplasmata and Nitrososphaeria is highest. The lowest number of the mentioned Archaea classes were observed in the most PTE-enriched sites (Table S6).

At the genus level, more than 1 % of genera represented the 37-53 % of the total community. Among them, *Subgroup_6_ge* are the most abundant genera in all sampling sites (both cities),

followed by *Saccharimonadales_ge* (Figure 13). Analysis indicated clear differences that emerged at the genus level where certain taxa decreased or increased significantly in metal(loid)-enriched samples. It is noticed that the relative abundance of *Subgroup_6_ge* and *Latescibacteria_ge* in control and *Saccharimonadales_ge* and *Parcubacteria* in the metal(loid)-enriched samples are substantially high. Additionally, an increase of *Pedosphaeraceae_ge* and *Haliangium* in Ózd control sample and *Pedosphaeraceae_ge* and *Flavobacterium* in Salgótarján urban soils was observed (Figure 13).

The Simper test proved the significant OTU dissimilarity among urban soils (metal(loid)-enriched) and control samples with 72.16 %. Main contribution was from the genus *Pseudomonas* (Proteobacteria), *MB-A2-108_ge* (Actinobacteria), *RB41* (Acidobacteria). The biggest variation (83.83%) was observed in sample OZD54, which is enriched in metal(loid) concentration. It was observed that the number of Alphaproteobacteria (*Ellin6055* genus) and Blastocatellia (*RB41* genus) in sample OZD54, meanwhile Gammaproteobacteria (*Burkholderiaceae_unclassified* genus) in samples OZD38 and OZD54 (two highly metal(loid)-enriched samples) are abundant than other sampling sites.

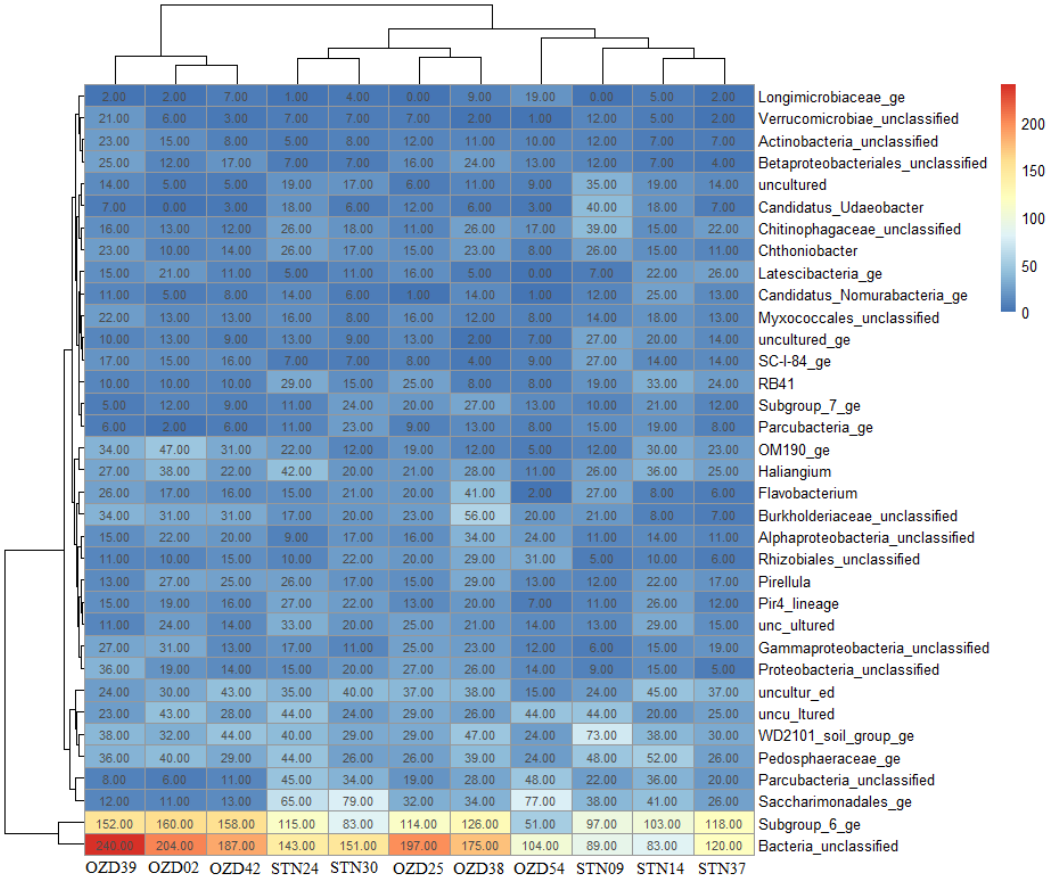

Figure 13. The most abundant (>1%) bacterial OTUs (genus level) in Salgótarján and Ózd soil samples. The plot shows the number of OTUs in each sample. STN37 and OZD02 are control samples.

The most abundant Archaeal genera were *Woesearchaeia_ge, Nitrososphaeraceae_ge and unclassified Thermoplasmata* in both cities representing 6.7-60.8%, 11.1-53.1%, and 3-14.3% of the communities, respectively. The number of abundant Archaeal genera at the sampling sites does not follow any patterns, however, there is a significant decrease of *Nitrososphaeraceae_ge, Woesearchaeia_ge* in the metal(loid)-enriched sites (OZD38 and OZD54) (Figure 14). The most abundant Archaeal OTU was encountered at the sample OZD25, which contains low metal(loid) and high organic content, which was observed in higher taxonomic levels as well (Figure *14*).

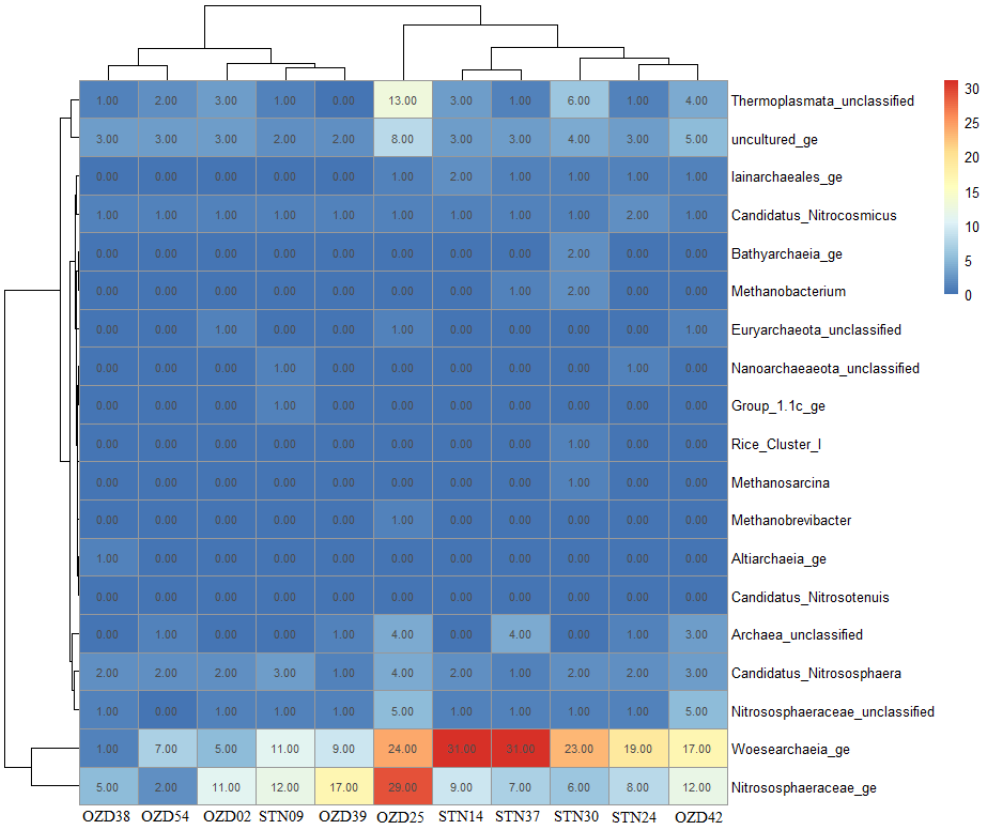

Figure 14. The present archaeal OTU (genus level) in Salgótarján and Ózd urban soil samples. The number of OTUs in each sample is shown in the plot. STN37 and OZD02 are control samples.

As the abundance of the rare genera (abundance less than 1%) was responsible for 47-63% of the total community, their potential impact on soil processes cannot be ignored. Analysis showed that in Salgótarján and Ózd soils, some of the rare taxa (at genus level) exist either only at the metal(loid)-enriched or control soil samples (Figure 15A and B). Among them

Sulfurifustis, and Candidatus Moranbacteria, together with other rare genera (Figure *15*), exist only in the urban samples (metal(loid)-enriched). On the other hand, genera, such as *Nitrobacter*, *Filomicrobium*, *Lactobacillus*, etc. (Figure 15A) and *Azomonas*, *Methyloterrigena*, *Emticicia*, etc. (Figure 15B) were found only in in Salgótarján and Ózd control samples.

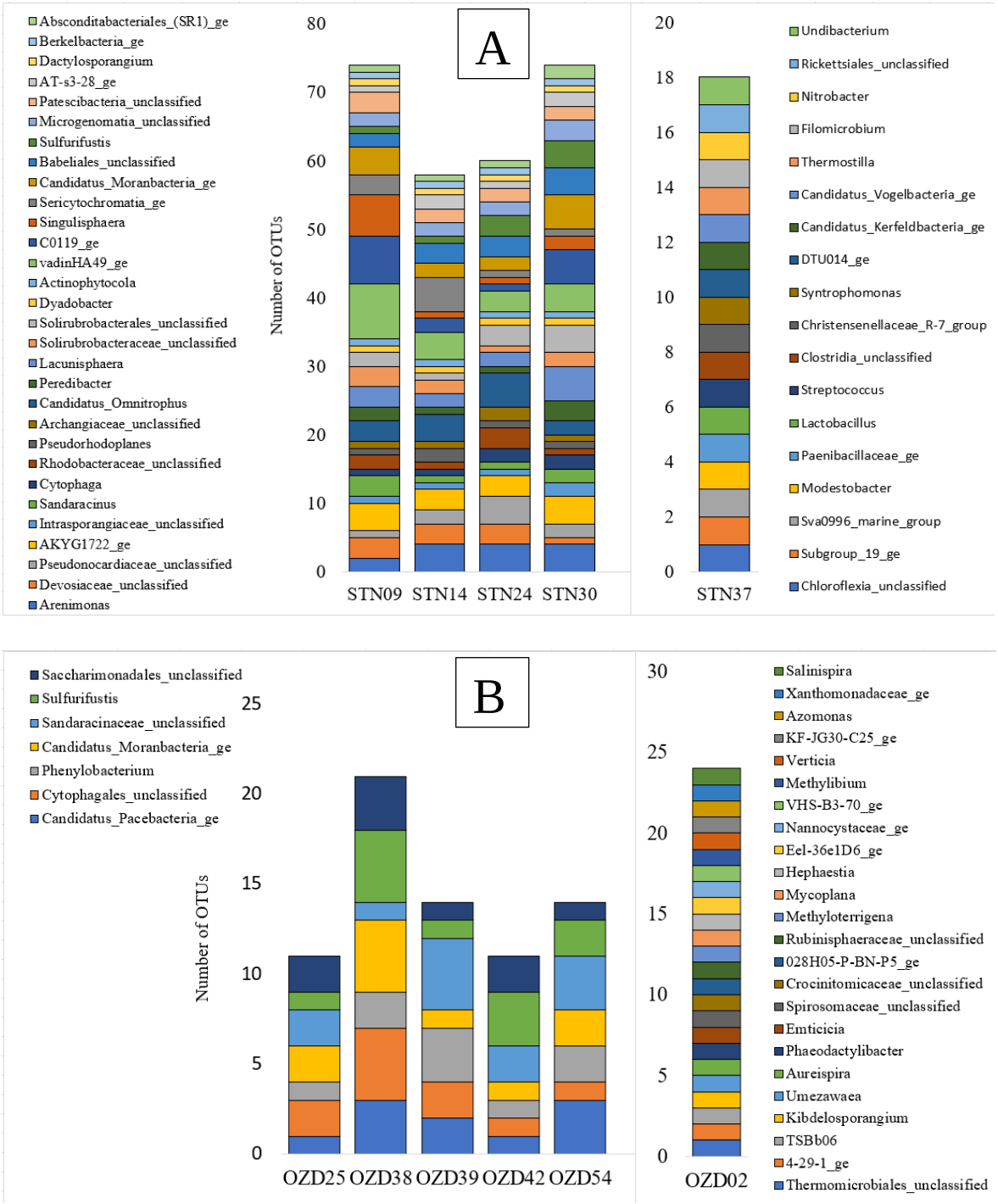

Figure 15. Identified rare taxa (at genus level) in Salgótarján (A) and Ózd (B) urban soil samples. Sample STN37 and OZD02 represent control samples.

4.2.2.3. The relative impact of environmental parameters and heavy metal(loids) on community composition

Based on the nonmetric-multidimensional scaling (NMDS) ordination analysis (see section 3.6.5), the enrichment of the selected PTE significantly affected the diversity of prokaryotic communities (OTU assemblies) at the sampling sites (Figure 16). Among PTE, Cd and Hg were found to have a significant positive connection with microbial communities. Soil physicochemical parameters, such as Eh (NMDS2=-86.9%, r^2=0.74, p<0.006), pH (NMDS2=86.8%, pH- r^2=0.7, p<0.01), clay fraction (NMDS2=-80.9%, r^2=0.82, p<0.01), sand fraction (NMDS2=78.5%, r^2=0.74, p<0.007) significantly correlated with NMDS2, whereas, Cd (NMDS1=99.4%, r^2=0.75, p<0.002) and Hg (NMDS1=98.0%, r^2=0.77, p<0.007) significantly correlating with NMDS1 (Figure 16). Especially, the impact of the selected metal(loid)s on the samples STN30, OZD38, and OZD54 is very strong, whereas the community in the STN09 sample is mainly affected by low soil pH value and clay fraction. The taxonomic differences (OTU) were identified by the Simper test, and taxa with high load for each sampling site were shown in Figure 16, which revealed minor clusters indicate the similarity of the OTUs in the Salgótarján and Ózd urban soils. However, among them, samples STN09, OZD25, STN30, OZD38, and OZD54 represented higher dissimilarities than the other samples (showing similarity). One of the biggest variations (OTU difference) was observed in sample OZD54, where the anthropogenic metal(loid) input (from industry) altered the soil texture and became rather sand fraction dominated compared to other samples. A huge shift in Proteobacteria (*Ellin6055_ge*, *unclassified Burkholderiaceae*) and Acidobacteria (*RB41_ge*) was observed at this site (Figure 16). Besides, other moderate metal(loid)-enriched samples (STN09, OZD25, STN30, and OZD38) indicated additional patterns with a shift in Bacteroidetes (*Flavobacterium*), Actinobacteria (*Aeromicrobium, unclassified Micrococcaceae*), Proteobacteria (*Pseudomonas, Sphingomonas*) and Verrucomicrobia (*Candidatus Udeobacter*). Though the samples STN14, STN24, OZD39, and OZD42 are moderately or highly enriched with various metal(loid)s (including PTEs), they show an OTU similarity to control samples (STN37 and OZD02) (Figure 16).

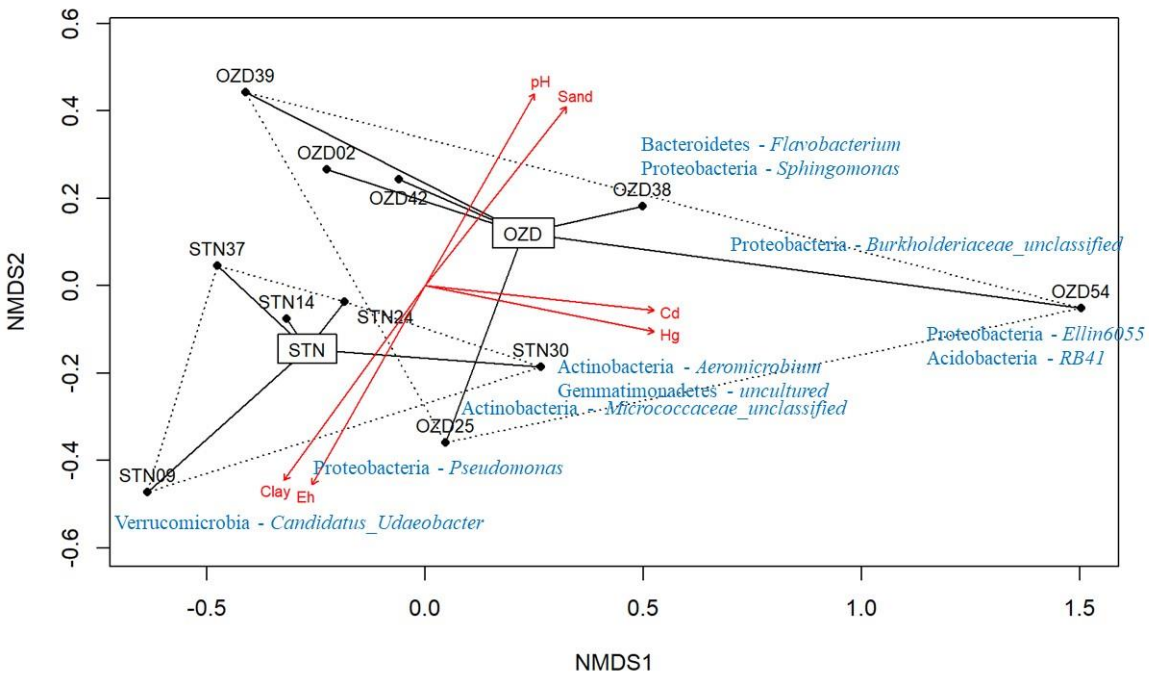

Figure 16. Results of NMDS analysis based on bacterial OTUs and environmental factors ($p<0.05$). The stress level is 0.08 (a fair stress value is one that is equal to or lower than 0.1, whereas a good fit is one that is equal to or lower than 0.05). The unique phyla and genera in sampling sites are shown next to the sampling sites. The studied Salgótarján (STN) and Ózd (OZD) microbiological samples are connected by dotted lines separately. Sample STN37 and OZD42 are control samples.

According to Spearman correlation analysis, soil microbial communities respond differently to environmental factors (Figure 17A and B). It is noticed that the content of heavy metal(loid)s significantly correlated with 9 bacterial phyla (Figure 17A) and 7 abundant bacterial genera ($p < 0.05$) (Figure 17B). In particular, Patescibacteria, Armatimonadetes, Dependentiae, Fibrobacteres, and Gemmatimonadetes showed positive ($p<0.05$) correlation with As, Cd, and Pb, respectively. A strong negative correlation was also observed between Rokubacteria, Latescibacteria vs. Hg, Cd, and Pb (Figure 17A).

At the level of bacterial genera, *Saccharimonadales_ge*, *Longimicrobiacea_ge*, and *Parcubacteria_ge*, as well as unclassified Rhizobiales, and Parcubacteria were significantly related to Hg, Cd, Pb, and As, respectively. It is observed that among the genera, the heavy metal(loid)s, particularly Hg, Cd, and Pb, are negatively influencing OM190_ge and Latescibacteria_ge (Figure 17B).

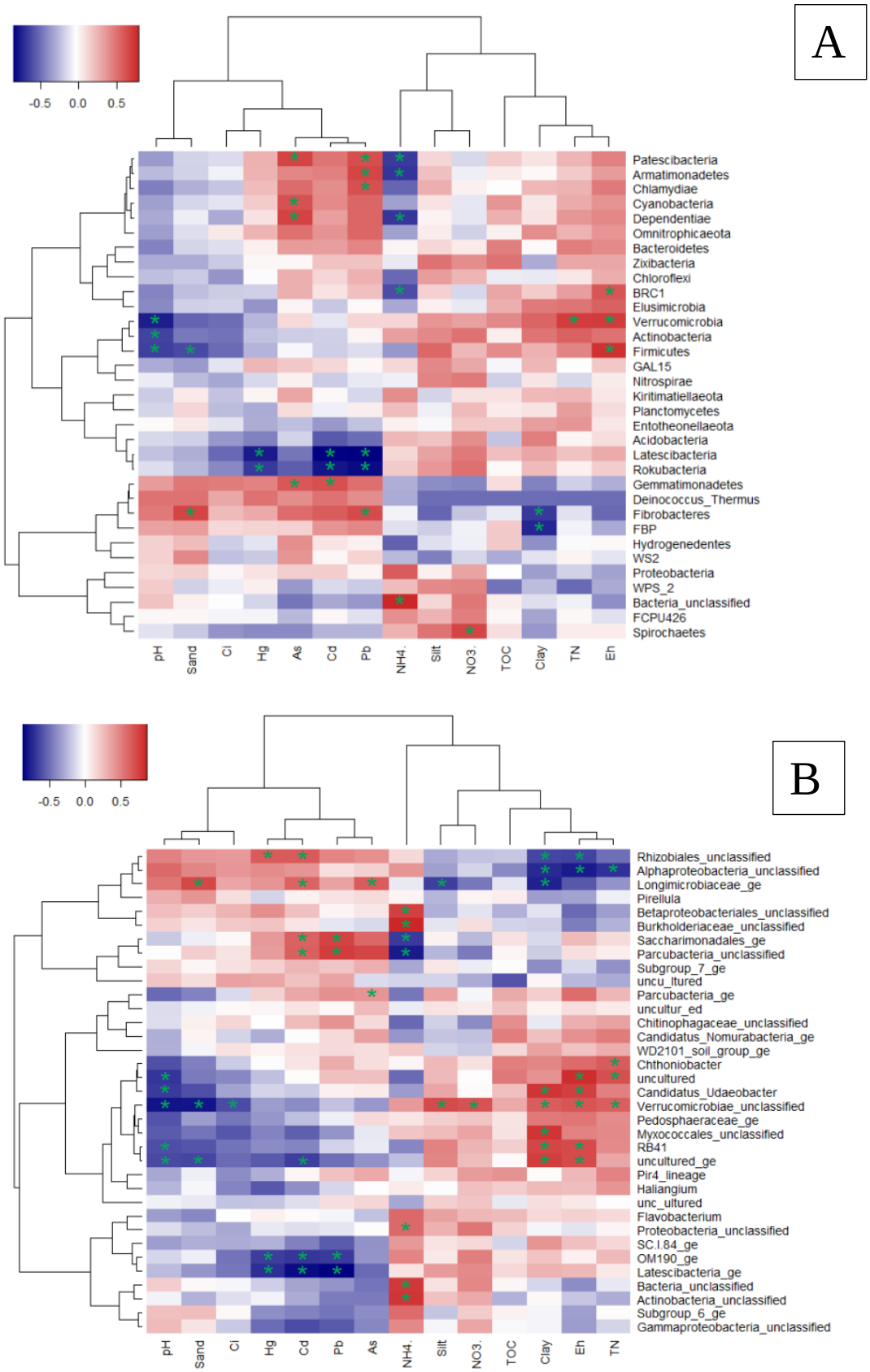

Figure 17. Spearman correlation heatmap shows the connection between environmental factors, PTE, and Bacteria phyla (A) or genera (B). Stars show correlation significance values ($p<0.05$).

Though the analysis for Archaeal phyla also indicated two clusters, a significant positive correlation could be observed only between Thaumarchaeota and soil ammonia content and clay fraction (Figure 18). There is no sign of the connection between soil PTE content and Archaea phyla.

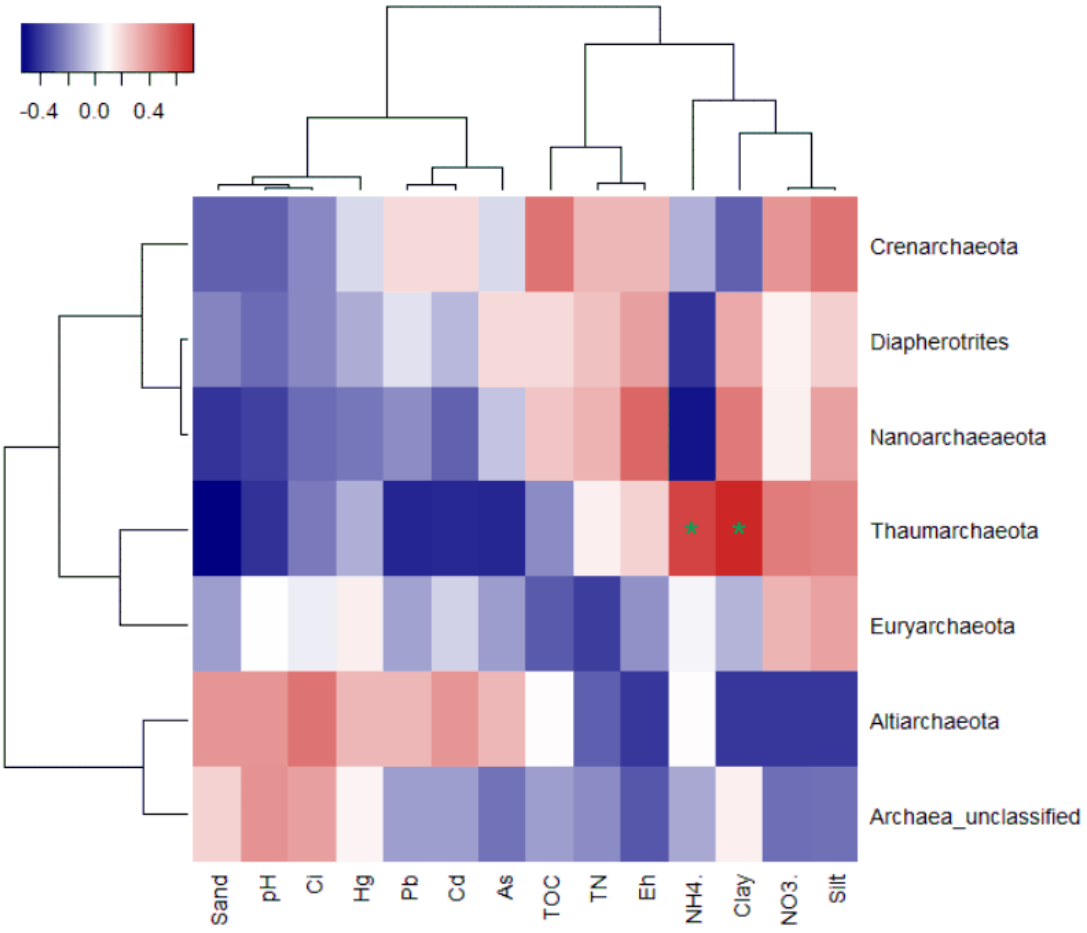

Figure 18. Spearman correlation heatmap showing the connection between environmental factors, PTE and Archaea phyla. Correlation significance values ($p<0.05$) are shown by stars.

4.2.3. Cultivation of metal(loid) tolerant/resistant Bacteria

Cultivation (see section 3.5.1) revealed a high number of bacteria tolerant to 200 µg/ml Pb and Cd salts, ranging from $0.5*10^{\wedge 4}$ to $16.2*10^{\wedge 4}$ for Pb and from $0.007*10^{\wedge 4}$ to $1.5*10^{\wedge 4}$ for Cd. However, there is very less or no growth on Hg and As salts amended plates (Figure 19). In total, 220 isolates were obtained from the plates and exposed to elevated concentrations of the PTE salts to identify minimum inhibitory concentration (MIC) values. From them, 21 bacterial strains were studied based on their tolerance to separate and complex effects of PTEs (Table 10).

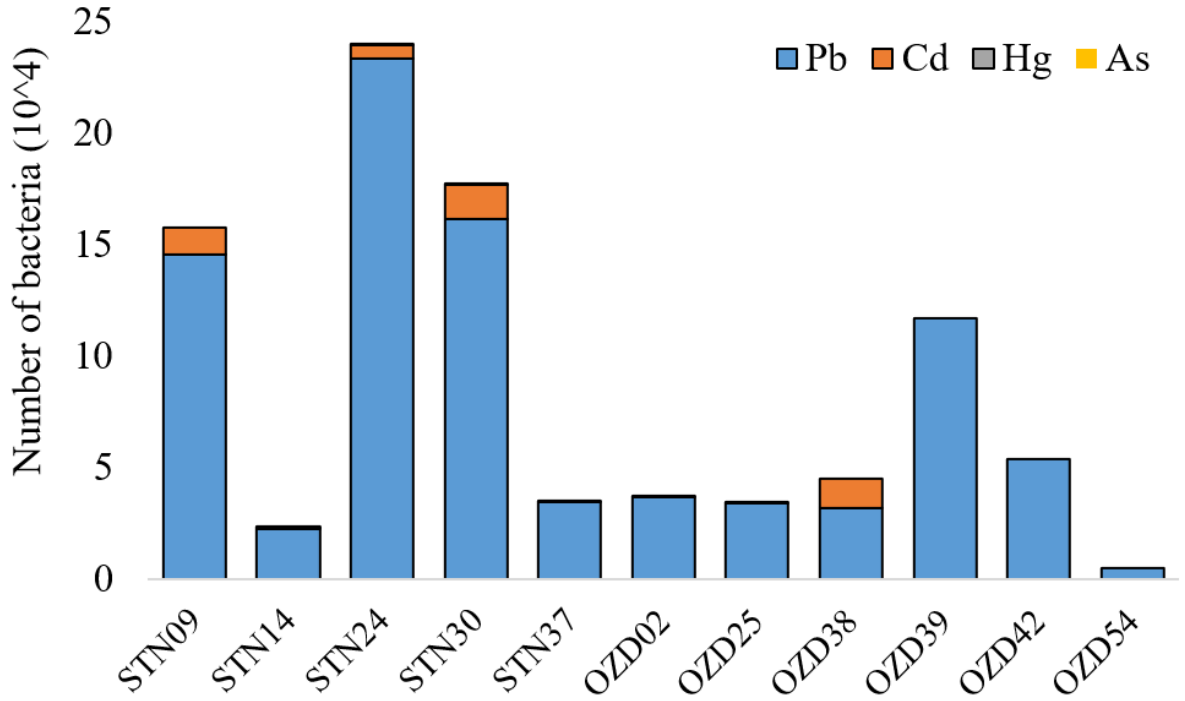

Figure 19. Resistant colony forming unit (CFU) counts in Pb, Cd, Hg, and As salt amended nutrient media plates. The number of Hg and As resistant bacteria are very low (or there is not); thus, it cannot be seen in the figure. The samples STN37 and OZD02 are control samples. The details are in Table S7.

The selected 21 PTE-resistant bacterial strains were identified by 16S rRNA gene sequence, and the minimum inhibitory concentrations (MIC) connected to four toxic compounds (Table 10). These values change for different bacterial species and strains, ranging between 1300 – 3000 µg/ml for Pb, 600 – 15000 µg/ml for Cd, 600 – 1500 µg/ml for Hg, and 100 – 1000 µg/ml for As. Remarkable differences among species in terms of metal(loid) tolerance were observed. A single *Delftia acidovorans* strain S24E7C and *Pseudomonas* spp. depicted considerable resistance to Pb, Cd, and Hg, whereas significant As tolerance was observed only in the case of the strains of *Bacillus* species. Due to their sensitivity, certain strains did not grow in the As salt-containing medium (Table 10).

Table 10. Isolated bacterial strains and their tolerance to selected metal(loid) salts. All listed strains resisted the complex effect of metals (Pb-900 µg/ml, Cd-600 µg/ml, Hg-600 µg/ml).

Strain ID	Species	NCBI accession number	PTE			
			Pb (µg/ml)	Cd (µg/ml)	Hg (µg/ml)	As (µg/ml)
S9E8P	*Bacillus pseudomycoides*	MT765153	1600	600	600	800
S14E3P	*Bacillus pseudomycoides*	MT765154	1600	600	600	400
S14E4P	*Aminobacter aminovorans*	MT765155	1600	600	600	-
S14E6H	*Azospirillum brasilense*	MT765156	1300	600	800	-
S14E9P	*Ochrobactrum lupini*	MT765157	1600	800	600	1000
S3010P	*Arthrobacter gyeryongensis*	MT765158	1600	600	600	100
S9E3P	*Bacillus mobilis*	MT765159	1600	600	600	600
S9E4H	*Bacillus megaterium*	MT765160	1500	2000	1200	1000
S14E1C	*Cupriavidus campinensis*	MT765161	3000	15000	1400	200
S14E3C	*Cupriavidus campinensis*	MT765162	3000	10000	1400	200
S14E4C	*Cupriavidus campinensis*	MT765163	3000	15000	1500	400
S14E6C	*Cupriavidus campinensis*	MT765164	3000	15000	1500	200
S24E2P	*Bacillus mobilis*	MT765165	1600	600	600	600
S24E3C	*Cupriavidus campinensis*	MT765166	3000	4500	1400	100
S24E7C	*Delftia acidovorans*	MT765167	3000	3000	1400	200
S24E7H	*Pseudomonas frederiksbergensis*	MT765168	1500	2000	1200	-
S24E9P	*Brevibacterium frigoritolerans*	MT765169	1600	600	600	600
S30E2H	*Pseudomonas kunmingensis*	MT765170	1500	2000	1200	-
S30E3H	*Pseudomonas kunmingensis*	MT765171	1500	2000	1200	100
S303Pb	*Bacillus idriensis*	MT765172	1600	600	600	800
SK27P	*Bacillus simplex*	MT765173	1600	600	600	800

- No bacterial growth

Among all the identified strains, *Cupriavidus campinensis* strain S14E4C tolerated extremely high concentrations of the metal(loid) salts and therefore were picked for further analysis, including whole genome sequencing (see section 3.5.4), to identify its potential in PTE resistance (Table 10 and Table 11). Additionally, to compare its metal(loid) resistance to other *Cupriavidus* sp., the strain was exposed to metal(loid) salts in two different media. The nutrient and Tris-salt mineral medium indicated a significant difference in terms of growth inhibition. Resistance to heavy metal(loid)s in the nutrient medium was extremely high, on the contrary, resistance to metal(loid) salts of the strain S14E4C in low phosphate Tris-salt mineral medium was lower, and obtained values are not considerably high compared to other *Cupriavidus* species, though the Hg resistance is noticeable (Table 11).

Table 11. Comparison of different *Cupriavidus* strains based on their minimum inhibitory concentration (MIC) values. The values for *C. campinensis* S14E4C are from this study.

MIC (µg/ml) [#]					
Metal(loid) ionic form	Compound*	*C. gilardii* CR3	*C. metallidurans* CH34	*C. campinensis* S14E4C	*C. campinensis* S14E4C
Cd	$CdCl_2*5H_2O$	1000	1000	-	-
	$CdSO_4*3/8H_2O$	-	-	15000	1500
Hg	$HgCl_2$	100	100	1200	500
Pb	$Pb(NO_3)_2$	1300	300	3000	800
As	As_2O_3	-	800	500	200
Used media		Tris-buffered mineral salt medium	Tris-salt mineral medium	Nutrient medium	Tris-salt mineral medium

[#]MIC values of *C. gilardii* CR3 and *C. metallidurans* CH34 are from reference (Janssen et al., 2010; Monsieurs et al., 2011; Wang et al., 2015), *C. campinensis* is from the present study.
[*]*C. gilardii* CR3 and *C. metallidurans* CH34 cadmium resistance were checked by $CdCl_2*5H_2O$, whereas in *C. campinensis* S14E4C by $CdSO_4*3/8H_2O$ salt.

4.2.4. Whole-genome sequencing (WGS) of Cupriavidus campinensis S14E4C

4.2.4.1. Genome structure and general features of Cupriavidus campinensis strain S14E4C

The genome of S14E4C is 6,322,653bp long with a GC content of 66.3% after assembly to 52 contigs (contigs shorter than 500 bp were removed) with a 78.3x coverage value. A total of 5,968 putative coding sequences (CDSs) were validated by homology, and 4,460 CDSs were assigned to one or more functional classes (Table 12), whereas 1,508 CDSs are identified as hypothetical based on functional annotation. The draft genome contained 49 tRNA and 7 rRNA genes (including 5S, 16S, and 23S rRNA) and is displayed in Figure 20.

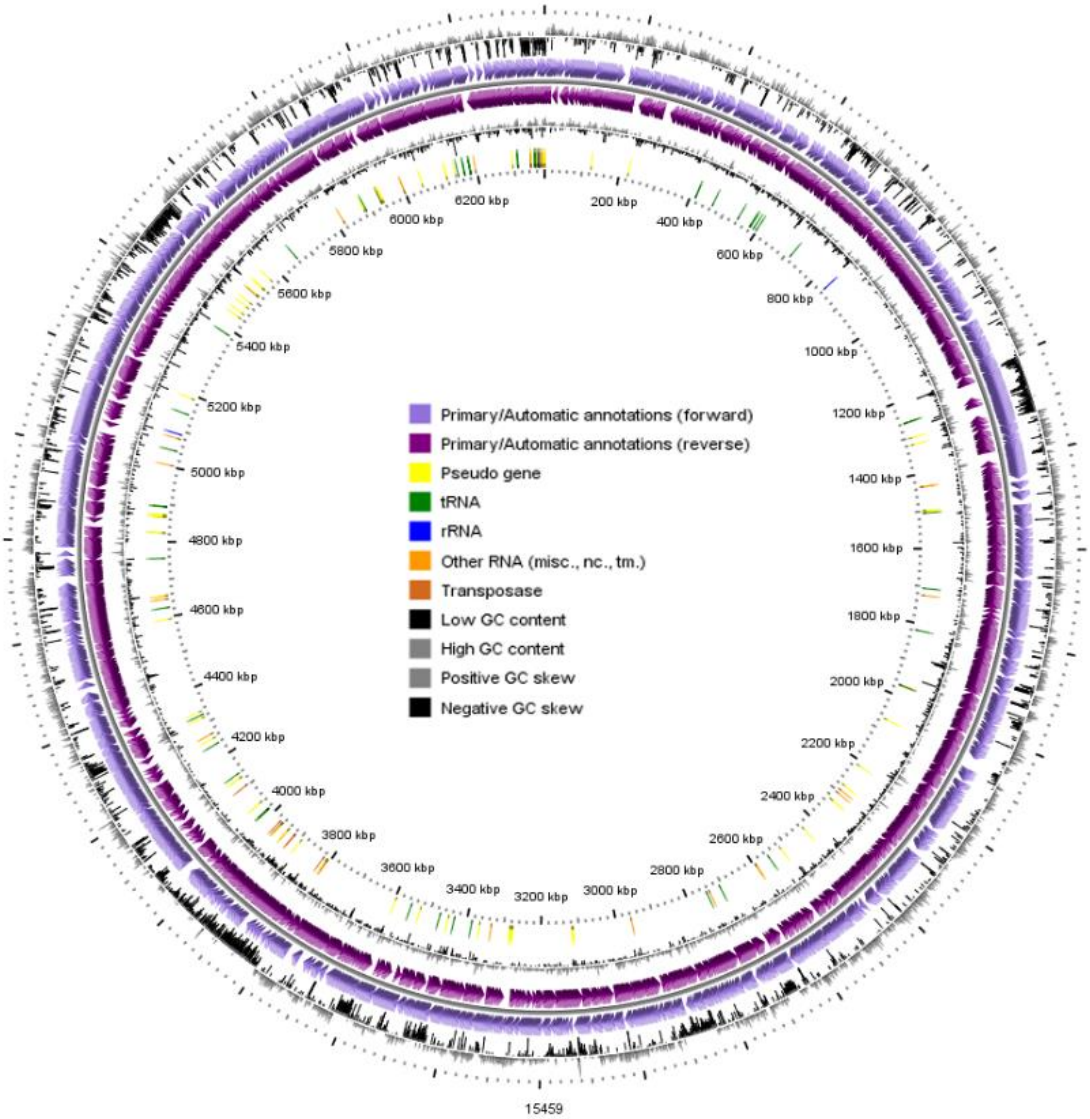

Figure 20. A circular graphical display of the *C. campinensis* S14E4C genome (contains chromosome and plasmid contigs) and applicable genes. This includes CDS on the forward strand, CDS on the reverse strand, RNA genes, Transposase, pseudogene, GC content, and GC skew. The figure was prepared by the CGView circular genome visualization tool.

The analysis resulted in 2 plasmids with the length of 295,460 bp and 50,483 bp and with an average GC content of 59.9% and 63%, respectively. Plasmid 1 contains genes mainly encoding mechanisms of metal resistance (Cd, Hg, Cu, Zn, etc.) and membrane cation transport and additionally genes encoding proteins involved in carbohydrate metabolism and c-type cytochrome biogenesis. Whereas plasmid 2 carries genes for antibiotic resistance (e.g., *tetMOPQST)* and operon for ribosomal protein synthesis (SSU rRNA, LSU rRNA, 5S rRNA).

Table 12. General features of *Cupriavidus campinensis* S14E4C genome. bp- base pairs, GC- Guanin + Citozin, CDS – coding sequences

Features	**Genome**	**Plasmid 1**	**Plasmid 2**
Size (bp)	6,322,653	295,460	50,483
Contigs	52	4	7
Contig L50	7	1	1
Contig N50	290,832	212,313	43,173
GC content	66.3	59.9	63
tRNA	49	0	6
rRNA	7	0	3
Total number of CDSs	5,968	351	43
CDSs with assigned functions	4,460	158	27
Hypothetical proteins	1,508	193	16
CDSs with EC number assignments	1,265	31	9
CDSs with GO assignments	1,091	27	9
CDSs with KEGG pathway assignments	972	17	9

4.2.4.2. Metabolic pathways

The genome of *C. campinensis* S14E4C consists mostly of known genes encoding metabolic modules and various pathways that support its growth. The main metabolic genes are shown in Figure 21. Among them genes of cyanate hydrolysis (*cynRXST* operon), nitrate and nitrite ammonification (*nrf, nar, nit, nat* reductase or transport), nitrate reductase (*narRKGHJIA, nirVK, norDQBCFE, nosXLYFDZR*) and gene clusters responsible for nitrogen metabolism (Figure 21).

The biochemistry of the bacterial sulfur metabolism pathways is quite complex and encoded by *soxABXYZDFCRSWH* gene cluster. In the case of organic sulfur assimilation, alkanesulfonate assimilation and utilization occur by *ssuA* - alkanesulfonates-binding, *ssuB* - alkanesulfonate ABC transporter ATP binding, s*suF* - organosulfonate utilization, *ssuC* - alkanesulfonates transport system permease, *ssuD* - alkanesulfonate monooxygenase, etc. proteins.

The strain S14E4C implements phosphate metabolism with *ptsS* (putative periplasmic phosphate-binding protein), *ptsA* (phosphate transport system permease protein), *ptsB* (phosphate transport ATP binding protein), *oprO* and *oprP* (pyrophosphate and phosphate specific outer membrane porins) genes. The spectrum of carbohydrate metabolism is broad, and several operons are responsible for maltose and maltodextrin utilization (*malEFGKMPRAZ*), and mannose metabolism (*manYZBCEFGKL*, *mtpEFGKL*) (Figure 21).

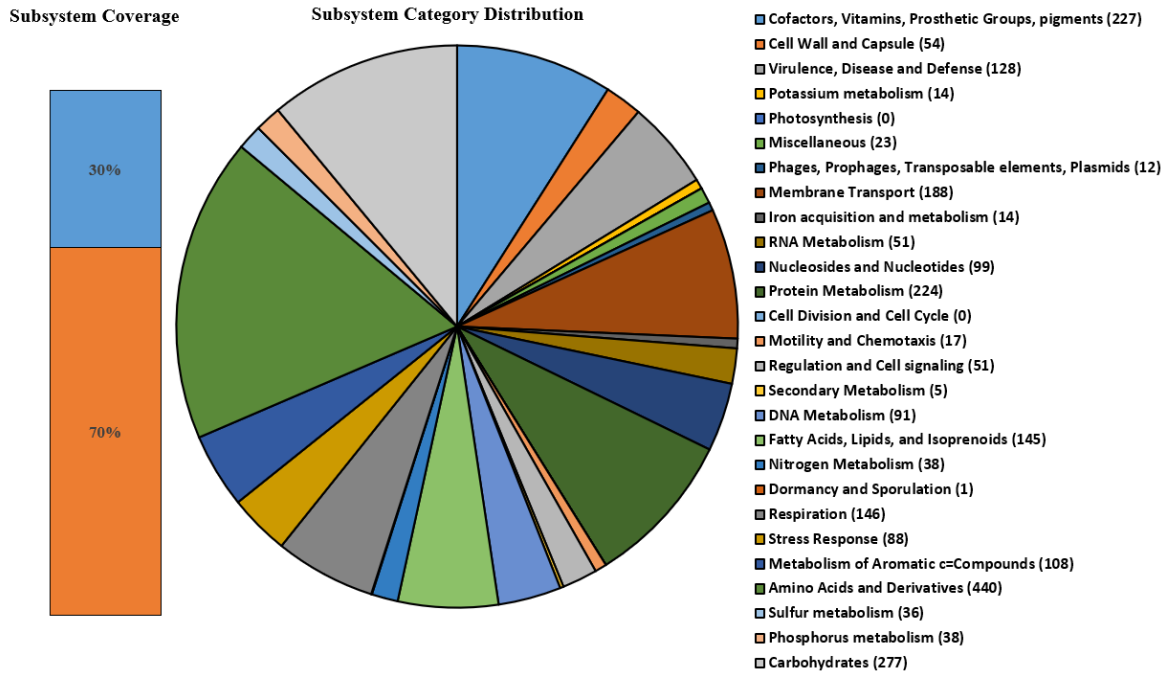

Figure 21. Subsystem coverage and category distribution of the genome of S14E4C strain. The pie chart demonstrates the counts for each subsystem feature and the subsystem coverage. The number of genes for each category was shown in brackets. Subsystem coverage represents the percentage of annotated and remaining genes.

4.2.4.3. Genes/gene clusters of metal(loid) resistance

Referring to the genome annotation analysis *Cupriavidus campinensis* strain S14E4C possesses an extensive number of heavy metal(loid) resistant genes and gene clusters (Table 13). The genome also carries genes and gene clusters involved in the transport and resistance of Cd^{2+}, Pb^{2+}, such as *czcABCREI*, *cadAR*, *ctpD*, plasmid-mediated *trcD*, etc. The Hg^{2+} resistance system at strain S14E4C consisted of *merR* gene, which activates transcription of *mer* operon (*merRTPCADE*) in elevated concentrations of Hg. The operon is located on contig twelve with the gene order shown in Figure 22, and delimited by transposon sequences.

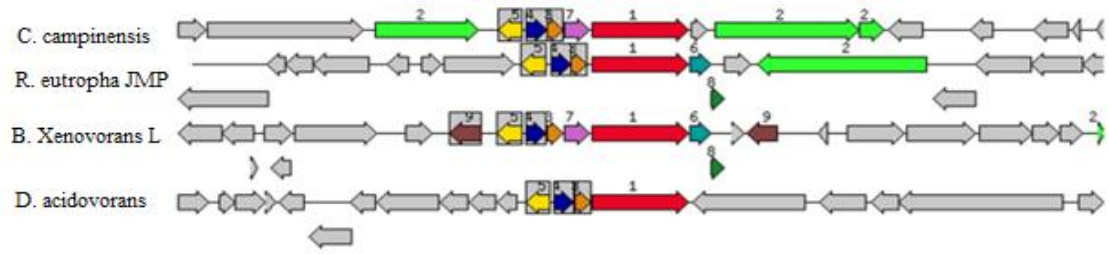

Figure 22. Mercury resistance gene cluster: The chromosomal region of the focus gene (top) is compared with three similar organisms. The graphic depicts the focus gene, which is red and numbered 1. Sets of genes with similar sequences are grouped with the same number and colour (1- mercuric ion reductase, merA; 2- TnpA transposase (left), Transposase Tn3 (right); 3- periplasmic mercury (2+) binding protein merP; 4- mercuric transport protein merT; 5- transcriptional regulator merR family; 6- mercuric resistance operon coregulator merD; 7- mercuric transport protein merC; 8- mercuric transport protein merE; 9- DNA-invertase). Genes whose relative position is conserved in at least three other species are functionally coupled and share grey background boxes

In addition to the cluster elements, several *ars* gene homologs (*arsB*, *arsC*, *arsR*, *arsH*) were identified in the genome of *Cupriavidus campinensis* S14E4C for arsenate (AsO_4^{3-}) resistance, and the strategy followed by bacteria depend on the arsenate reductase (ArsC) protein (Table 13).

Table 13. Genes/gene clusters of metal(loid) resistance (MR) of *Cupriavidus campinensis* strain S14E4C. Some genes exist in multiple copies (locations were shown).

Genes	Functions	Metal(loid)	Locus tag
czcA[# 12]	Cobalt-zinc-cadmium resistance protein	Cd^{2+}, Co^{2+}, Zn^{2+}	FGG12_RS19525
czcB[# 12]	Cobalt-zinc-cadmium efflux RND transporter, membrane fusion protein	Cd^{2+}, Co^{2+}, Zn^{2+}	FGG12_RS19530
czcC[# 12]	Heavy metal RND efflux outer membrane protein	Cd^{2+}, Co^{2+}, Zn^{2+}	FGG12_RS19535
czcR[# 12]	Cobalt-zinc-cadmium resistance protein	Cd^{2+}, Co^{2+}, Zn^{2+}	FGG12_RS19515
czcE[# 12]	CzcE family metal-binding protein	Cd^{2+}, Co^{2+}, Zn^{2+}	FGG12_RS19505
czcI[# 12]	Cobalt-zinc-cadmium regulatory protein	Cd^{2+}, Co^{2+}, Zn^{2+}	FGG12_RS19540
cadA[# 12]	Cadmium-translocating P-type ATPase	Cd^{2+}, Co^{2+}, Zn^{2+}	FGG12_RS19635 FGG12_RS19680
cadR[# 12]	Cobalt-zinc-cadmium transcriptional regulatory protein	Cd^{2+}, Co^{2+}, Zn^{2+}	FGG12_RS19620
merA[# 12]	Mercuric ion reductase	Hg^{2+}	FGG12_RS19735
merC[# 12]	Mercuric transport protein	Hg^{2+}	FGG12_RS19740
merP[# 12]	Periplasmic mercury (+2) binding protein	Hg^{2+}	FGG12_RS19745
merT[# 12]	Mercuric transport protein	Hg^{2+}	FGG12_RS19750
merR[# 12]	Mercuric resistance operon regulatory protein	Hg^{2+}	FGG12_RS19755
arsB[*1]	Arsenic transporter (efflux pump)	As^{3+}, As^{5+}	FGG12_RS00815
arsC[*1]	Arsenate reductase	As^{5+}	FGG12_RS25020 FGG12_RS00810
arsR[*1,4,6]	Transcriptional regulator	As	FGG12_RS00835 FGG12_RS01270 FGG12_RS11920 FGG12_RS09700
arsH[*1]	Organoarsenical detoxification	As^{3+}	FGG12_RS00805

[#] Genes located on plasmid; * genes located on the chromosome; Numbers depict relevant contigs; Locus tags are from NCBI annotation.

4.2.4.4. Phylogenetic and phylogenomic analysis of *C. campinensis* S14E4C

The phylogenetic analysis suggested that the *C. campinensis* S14E4C strain is a member of the *Cupriavidus* genus, and its closest relative was *C. campinensis* LMG 1195^{T} (AF312020) (Figure 23). Besides, strain S14E4C is phylogenetically close to *C. gilardii* and *C. pampae* with a 98 % similarity value. Additionally, some other core genes (e.g. *gyrB, rpoD, recA*, etc.) were concatenated with the 16S rRNA gene and analysed on PATRIC (Wattam et al., 2017). In fact, the precise phylogenetic position of *C. campinensis* S14E4C was placed by genome sequence and depicted in Figure 24. These results are supported by the tree generated on TYGS database (based on genome signatures), which depicted similar results to Figure 24 (Meier-Kolthoff & Göker, 2019). The genome-wide Average Nucleotide Identity (gANI) value between strain S14E4C and *C. metallidurans* CH34 was identified (Yoon et al., 2017) as 81.98% to confirm the genomic relatedness (80–100% ANI; Jain et al., 2018).

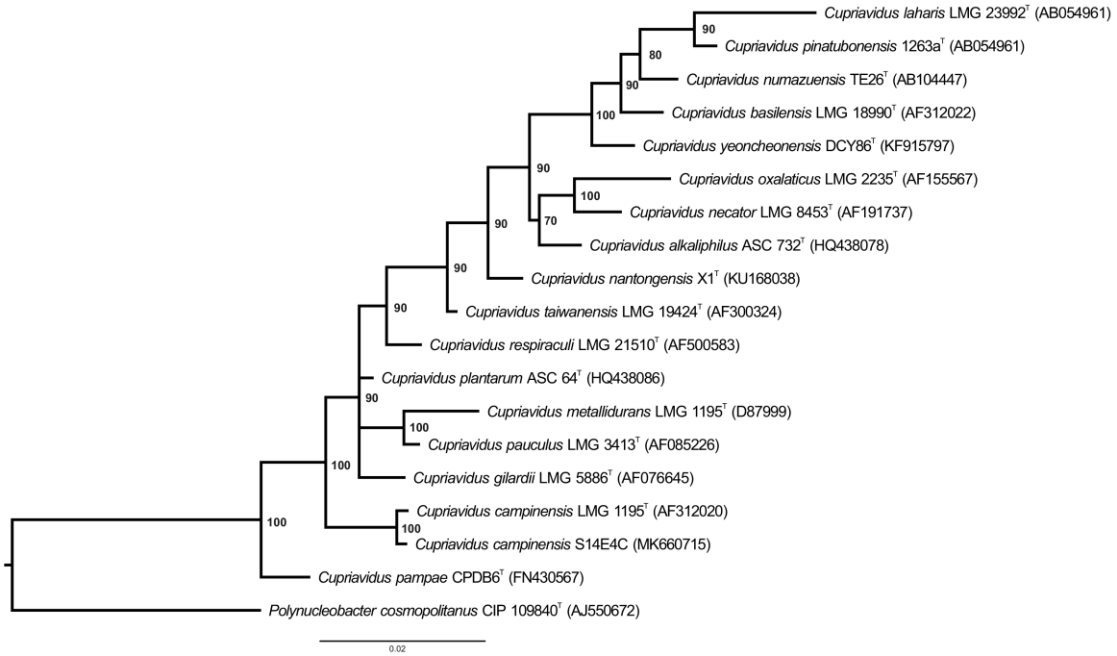

Figure 23. Phylogenetic relationship of *Cupriavidus campinensis* S14E4C strain and the members of *Cupriavidus* species based on 16S rRNA gene sequence. Cluster analysis was based upon the neighbor-joining method with *Polynucleobacter cosmopolitanus* CIP 109840T (AJ550672) as the outgroup root. The MrBayes method was used to generate the tree and its support values (only values above 50% are presented). Bar, 0.02 substitutions per nucleotide position. The tree was visualized by FigTree v1.4.4.

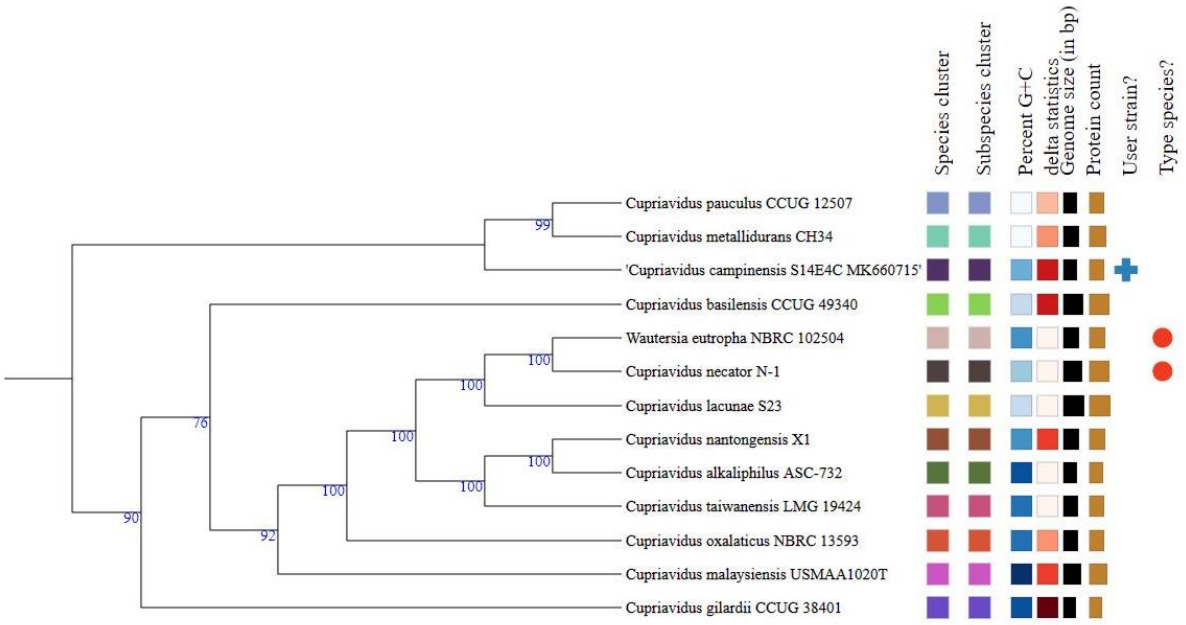

Figure 24. Phylogenomic tree predicted on TYGS database. Genomic G + C content (63.53–68.47%), δ values (0.08–0.2), overall genome sequence length (5,783,696–9,185,558 bp), number of proteins (5142–7932). Values increase based on the colour range (from white to black).

4.5. Human health risk assessment

4.5.1. Non-carcinogenic risk

The non-carcinogenic risk was calculated with the reference dose (RfD) (Table 3) and average daily intake (ADI) values of PTEs for adults and children based on equations 2, 3, and 4 (Table 14). The results for ingestion, inhalation, and dermal pathways show (Figure 25) that hazard quotient (HQ) and hazard index (HI) values of more than 1 represent a potential non-carcinogenic risk for adults and children. The average HQ values for children exceed HQ values for adults from the ingestion pathway for all PTEs (Table S8). The highest HQ_{ing} value for children was 0.47 for As and 0.29 for Pb in Salgótarján and 0.36 for As and 0.29 for Pb in Ózd soil samples (Table S8). According to the results, the average HQ and HI values do not exceed the threshold value (1) in any city and can be considered safe for adults and children (Figure 25).

Table 14. Summary of average daily intake (ADI) of the selected PTE through ingestion (ing), inhalation (inh), and dermal (derms) pathways for adults and children in Salgótarján and Ózd urban soils. The exposure duration for non-carcinogenic (chronic) risk was considered 30 years for adults and 6 years.

		Salgótarján				Ózd			
		As	Pb	Hg	Cd	As	Pb	Hg	Cd
Non-carcinogenic	ADI-ing	1.52E-05	1.12E-04	1.41E-07	4.87E-07	1.14E-05	1.13E-04	3.14E-07	2.41E-06
Adults	ADI-inh	2.33E-09	1.73E-08	2.17E-11	7.49E-11	1.76E-09	1.73E-08	4.84E-11	3.72E-10
	ADI-dems	3.76E-06	2.78E-05	3.50E-08	1.21E-07	2.83E-06	2.79E-05	7.79E-08	5.98E-07
Non-carcinogenic	ADI-ing	1.42E-04	1.05E-03	1.32E-06	4.55E-06	1.07E-04	1.05E-03	2.93E-06	2.25E-05
Children	ADI-inh	5.45E-09	4.03E-08	5.07E-11	1.75E-10	4.10E-09	4.04E-08	1.13E-10	8.67E-10
	ADI-dems	1.81E-05	1.34E-04	1.69E-07	5.82E-07	1.37E-05	1.35E-04	3.76E-07	2.89E-06
Carcinogenic	ADI-ing	6.50E-06	4.81E-05	6.05E-08	2.09E-07	4.90E-06	4.82E-05	1.35E-07	1.03E-06
Adults	ADI-inh	1.00E-09	7.41E-09	9.31E-12	3.21E-11	7.54E-10	7.42E-09	2.07E-11	1.59E-10
	ADI-dems	1.61E-06	1.19E-05	1.50E-08	5.17E-08	1.21E-06	1.19E-05	3.34E-08	2.56E-07
Carcinogenic	ADI-ing	6.07E-06	4.49E-05	5.65E-08	1.95E-07	4.57E-06	4.50E-05	1.26E-07	9.66E-07
Children	ADI-inh	9.34E-10	6.91E-09	8.69E-12	3.00E-11	7.03E-10	6.93E-09	1.93E-11	1.49E-10
	ADI-dems	1.50E-06	1.11E-05	1.40E-08	4.83E-08	1.13E-06	1.11E-05	3.11E-08	2.39E-07

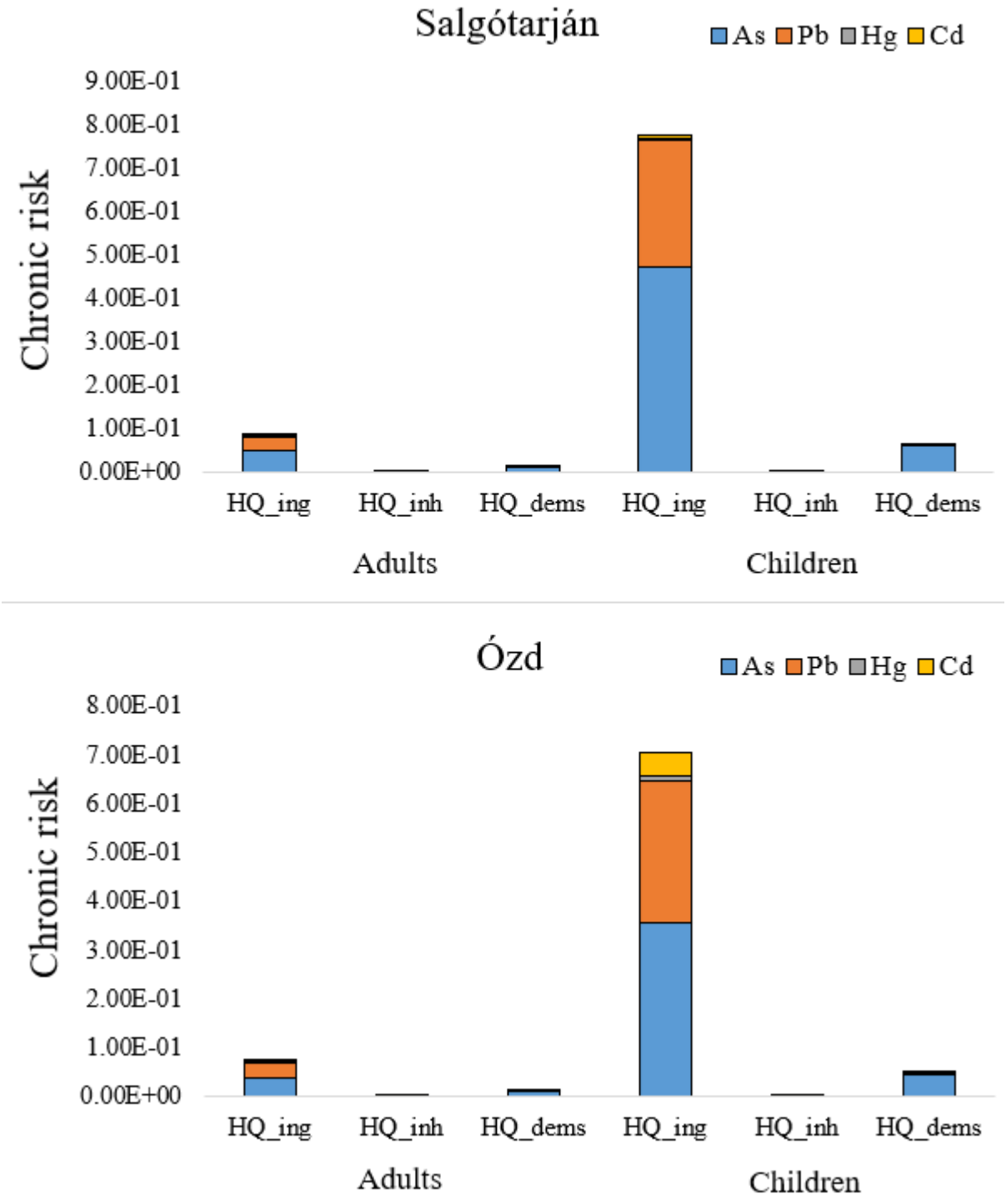

Figure 25. The average non-carcinogenic (chronic) risk assessment values for adults and children in Salgótarján and Ózd soil samples. Table S1 and S2 were used for calculations. Ing – ingestion, inh- inhalation, and dems- dermal pathways

Sampling sites in Salgótarján and Ózd, such as STN24, STN30, OZD13, OZD38, OZD42, and OZD54, depicted a significant non-carcinogenic risk for children's health through the ingestion pathway (HQ_{ing} and HI_{ing}>1) (Figure 26; Table S8).

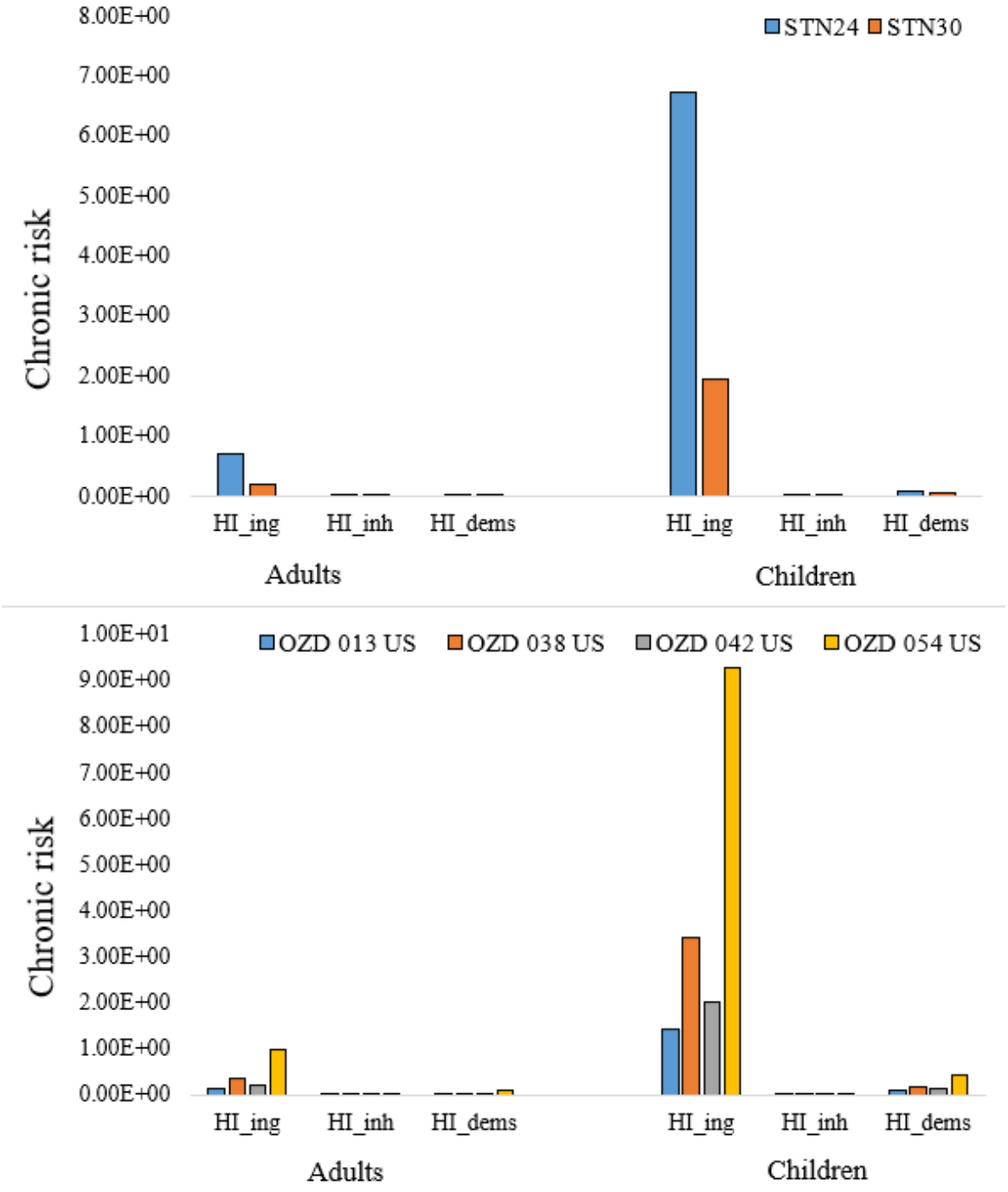

Figure 26. Non-carcinogenic (chronic) risk in sampling sites STN24, STN30, OZD13, OZD38, OZD42, and OZD54 of Salgótarján and Ózd. Ing – ingestion, inh - inhalation, and dems-dermal pathways

4.5.2. Carcinogenic risk

The lifetime carcinogenic risk for adults and children was estimated separately from the average influence of each PTE for all the pathways by using Equations 5 and 6. Based on the calculated carcinogenic risk ADI values (Table 14), the excess lifetime cancer risk values were computed (Table S8). Due to their cancer slope factor values (CSF; Table 3), the carcinogenic risk could be calculated from the ingestion point of Pb and As (adults and children). Results showed that in both cities, the sampling sites exhibit low carcinogenic risk for adults and children (Figure 27; TableS8).

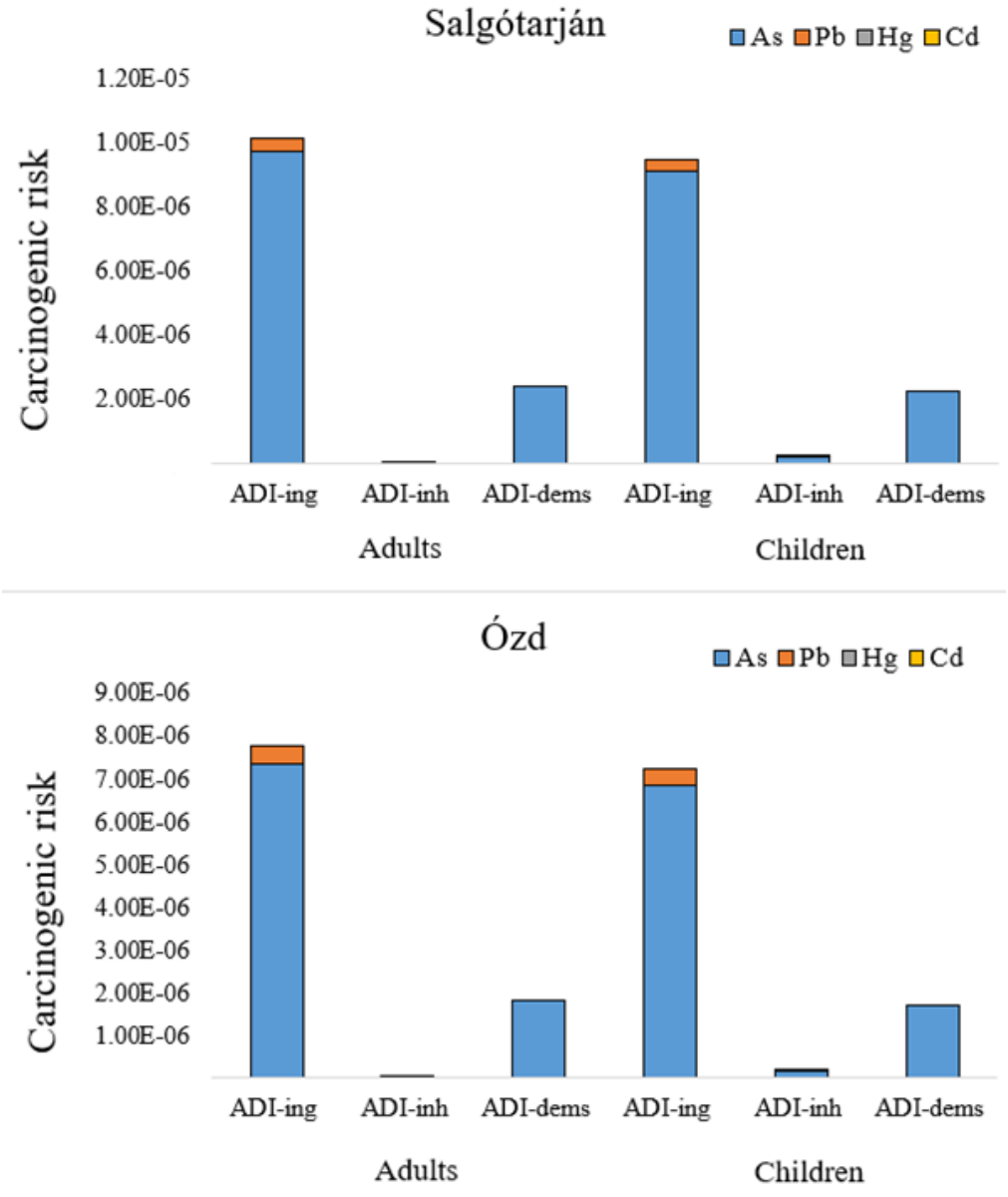

Figure 27. Carcinogenic risk assessment values for adults and children in Salgótarján and Ózd for the selected PTE. Ing – ingestion, inh - inhalation, and dems- dermal pathways

Chapter 5. DISCUSSION

5.1. Metal(loid) contamination in Salgótarján and Ózd soils

5.1.1. Distribution and enrichment of metal(loid)s

The issue of metal(loid) pollution in urban soil is well-known all across the world, and numerous studies have been conducted to investigate their enrichment in many countries (Alloway, 2013; White, 2018). Due to widespread anthropogenic activities, PTE contamination usually coincides in industrial cities. In this study, analysis of selected PTE (As, Pb, Hg, and Cd) content in urban soils showed that the concentration of PTEs exceeded the maximum permissible soil values (Figure 7, Table 4), which indicates significant PTE contamination in the cities. Moreover, Salgótarján urban soils were lesser contaminated with PTEs than Ózd urban soils, whereas in both cities, the enrichment of Pb and Cd was relatively higher than As and Hg (Figure 8). This suggests that Hg and As might have partially originated from a natural source and partially from anthropogenic sources (Figure 10). Hooda, (2010) stated that PTEs in soils might have lithogenic or anthropogenic origins, however, in most sampling sites, high PTE concentrations are linked to human-induced activities, which increases the metal(loid) toxicity and health risk. Though we were not able to observe any direct connection between sampling categories (kindergarten, playground, park, others) and enrichment of the selected four PTE, outlier samples from all categories depicted high PTE concentration (Figure 9). Particularly, the sampling sites STN09, STN24, STN30 in Salgótarján and OZD13, OZD38, OZD42, and OZD54 in Ózd, considered as outliers, show high enrichment of all PTEs (Figure 7), and these samples are located either next to the local industrial sites or rarely in some playground/parks of the studied cities (Figure 9). In the sampling sites, the PTE enrichment is at least 10 times and in industrial areas 100 times higher than the geochemical background value (Figure 7; Figure 9). These findings preliminarily suggest that anthropogenic input from industrial operations was substantial enough to cause significant soil contamination. Comparable results from kindergarten, playground, and park soils of surrounding European countries were published, where the concentration of As, Pb, Hg, and Cd, is either higher or lower than Salgótarján and Ózd soils (Table 15). For example, our results from Salgótarján and Ózd show significantly higher As and Pb content in urban soils compared to those of fifty-nine kindergarten and nineteen park soils of Bratislava (Slovakia; Hiller et al., 2017), one hundred eighteen samples of Maribor (Slovenia) (Gaberšek & Gosar, 2018), and in nine urban parks of Ostrava (Czech Republic) (Galušková et al., 2014) (Table 15). However, in one hundred twenty one Novi Sad urban soils, the concentration of As and Pb, which was published by Mihailović et al., (2015), is slightly similar to our study areas.

Table 15. Summary (minimum, mean, and maximum values) of PTEs in urban soil samples from Salgótarján, Ózd, and other comparative cities.

Cities	Urban soils (mg/kg)												References
	As			Pb			Hg			Cd			
	Min.	Avg.	Max.	Min.	Avg.	Max.	Min.	Avg.	Max.	Min.	Avg.	Max.	
Salgótarján	3.7	11	73.6	8.5	82	1692	0.03	0.1	0.5	0.1	0.36	1.6	This study
Ózd	2.7	8.4	36.9	6.6	80	1674	0.015	0.23	4.9	0.11	1.77	62.9	This study
Bytom	16.9	46.1	138	69	627	5260	-	-	-	0.75	19.6	106	(Ullrich et al., 1999)
Ostrava	11	21	31	27	58	125	-	-	-	0.2	0.44	1.0	(Galušková et al., 2014)
Bratislava	2.69	7.34	14.2	11	26.1	183	0.02	0.12	0.43	0.1	0.23	0.84	(Hiller et al., 2017)
Maribor	5.2	10.1	16.9	19	60.5	626	0.032	0.095	0.81	0.14	0.32	2.28	(Gaberšek & Gosar, 2018)
Berlin	-	5.1	126	-	119	4710	-	0.42	71.2	-	0.92	131	Birke et al., 2011
Novi-Sad	2.1	6.5	11.1	8.9	82.3	999.1	-	-	-	-	-	-	Mihailović et al., 2015

In contrast, the enrichment of selected four PTE in Salgótarján and Ózd never exceeded the values reported from industrial sites of Berlin (Birke et al., 2011) and one hundred twenty-two soil samples in Bytom (Poland), one of the most disastrous industrial areas of Europe (Ullrich et al., 1999) (Table 15). One of the main reasons for high PTE contamination in city parks and playgrounds in many studied cities (mentioned above) is mainly they are open areas and located next to roads, and thus PTE-bearing dust can be accumulated easily. Similarly, Ljung et al. (2006) stated that the oldest playgrounds had the highest multiple metal accumulation in Uppsala; although Uppsala is not an industrial city and does not have many sources of metal pollution, the oldest playgrounds showed a pattern of increased PTE with the age of the site. Thus, these findings clearly show that anthropogenic input from industrial operations was substantial enough to cause significant chemical and/or physical alterations in Salgótarján and Ózd soils.

5.1.2. Connection between environmental factors and PTE distribution

The characteristics of PTE content in urban soils are related to their physicochemical properties (Table 6 and Table 7), which play an essential role in their accumulation and mobility (Csorba et al. 2014; Hiller et al. 2016). In the current study, Spearman rank correlation coefficient analysis revealed a significant correlation between total organic carbon and Pb, as well as Fe and As content in Salgótarján urban soils, indicating the role of these environmental factors on the distribution of the related PTEs (Table 6). The relatively low correlation between As, Hg, and Cd may suggest that As and Hg originated partially from an anthropogenic and partially natural origin, which was consistent with earlier findings (Tepanosyan et al., 2017; Radomirović et al., 2020).

On the other hand, the significant correlation among As, Pb, Hg, and Cd, as well as between these PTE and Fe in Ózd (Table 7), implies that this metal(loid)s in the soil might have originated from the same anthropogenic sources. This finding is consistent with a study by Hiller et al. (2016), which found a link between PTE and Fe/organic matter content in urban soils. Also, previous studies report that the abiotic redox reactions are the main factors controlling the mobility and transformation of PTEs on the surfaces of Fe(III)- and Mn-oxides, as well as ferrous species and humic substances, mainly due to their high affinity and absorption (Alloway, 2013; Caporale & Violante, 2016). These statements suggest that in Salgótarján soils, TOC and Fe whereas, in Ózd soils, Fe most likely constraints on PTE mobility, thus bioavailability in the surface environment. Though the organic content of some

urban soil samples indicates high values in Ózd soils (Table S4), no significant connection was observed between soil organic matter and selected PTE content. This finding is consistent with data that has been published from contaminated urban areas of Naples (Imperato et al., 2003), where the organic content decreased if the metal content increased. This might be the result of the high content of heavy metal(loid)s in polluted soils, which could slow down the mineralization rate of soil organic matter as the experiment of Zhang & Wang, (2007) shows. Additionally, metal(loid)-enriched urban soils are characteristic of high sand fractions, as observed in our study (Table S4). Due to their nature, sandy soils contain less organic material than clay and silt fraction dominated soils, which is the reason for organic content depletion in most urban samples (Seddaiu et al., 2013). The urban soil samples are slightly alkaline, and it is relatively high in PTE elevated sites (Table S4), which were similarly reported in Naples (Imperato et al., 2003), Athens (Kelepertzis et al., 2016), and Maribor (Gaberšek & Gosar, 2018).

5.1.3. Impact of local contamination sources on PTE distribution

Main local contamination sources, coal and coal ash in Salgótarján and smelter slag in Ózd were identified and analysed for their PTE content (Figure *10*). As a dominant energy source, coal played a significant role in the industrial production of Salgótarján and Ózd. It was found that the As, Hg, and Cd content in Salgótarján coal is significantly higher than those of Ózd coal (Table *5*). In all cases, the coal PTE values fall in the range of average world brown coal PTE values (Keegan et al., 2006; Ketris & Yudovich, 2009). Though concentrations of Pb and Cd in Salgótarján coal and four selected PTE in Ózd coal are low, a long period of coal combustion in the coal-fired power plant at Salgótarján and different smelters in both cities, but particularly in Ózd, could accumulate a significant amount of metal(loid)s, in coal ash and smelter slag (Raj et al. 2019). It is known that during the coal combustion process, trace elements evaporate, however, when temperature decreases, they condense back and attach to fine particles (Pudasainee et al. 2020), which explains the impact of coal combustion on the distribution of the studied metal(loid)s in both cities.

Another significant PTE contamination sources were coal ash in Salgótarján and smelter slag in Ózd, characteristic byproducts of heavy industrial activity (Garcia-Guinea et al., 2010; Parzentny & Róg, 2021). Salgótarján coal ash and Ózd smelter slag samples indicated heterogenous PTE content (Table *5*). The elevated As content of Salgótarján coal ash could be associated with local coal, as was reported with its high As content, as Table 5 shows. However,

the low concentration of Pb, Hg, and Cd in Salgótarján coal ash and four PTE in two Ózd smelter slags (2 and 3) samples, from the recent industrial site, could be the result of the long-term physical and chemical weathering process, which was also concluded by Lottermoser, 2004, studying smelter slag dumps in North-Queensland, Australia. Therefore, in Salgótarján, around the former steel factory and coal ash cone (Figure *7*), there is no observable trace of elevated PTE concentration and distribution (Figure 7). However, in Ózd, another smelter slag sample (slag1) from the former iron industry showed an elevated concentration of the studied four PTE (Table 5). The presence of such slag sample allows us to explain the elevated PTE concentration in the urban soils collected in Ózd city centre (where the old factory operated), around the former and recent industrial areas (Figure *7*), showing several folds higher PTE content than the local geochemical background value (Table *4*). Particularly, the high content of Hg in almost all urban soils of Ózd, except western and north-western parts due to the distance to industries, might derive from coal, which was used for the former iron steel industry and most probably distributed as combustion dust.

Additionally, it is observed that in both cities, sites with elevated PTE content are mainly the result of the presence of a slag layer in the urban soil or due to landscape change (Figure 4 E, G; Figure S1), noted during the soil sampling. Slag was used filling up to cover stream beds, holes, mining galleries, openings, etc. This approach was encountered frequently in Salgótarján and Ózd playgrounds and parks, where a significant PTE enrichment was observed (Figure 9; Figure *7*).

Vehicular emissions could be considered an essential origin of Pb contamination (Komárek et al., 2008; Nriagu, 1990). Though the sale and use of leaded gasoline were banned in Hungary in 1999 (e.g., Salma et al. 2000), the burning of leaded gasoline for several decades had left a legacy of alkyl lead additives embedded in the environment. During the 1980s in Europe and North America, engine Pb emissions rapidly dropped after the average Pb content of petrol was decreased from 0.4 g/l to 0.15 g/l (Bollhöfer et al., 2001; Löfgren & Hammar, 2000), resulting in a robust decline of Pb concentration in the atmosphere and hydrosphere (Zhu et al. 2010). Sipos et al., (2013) report that aerosols data collected from Budapest aerosols in the 1990s showed a strong sign of European gasoline. In fact, a general impact of leaded gasoline in Salgótarján and Ózd is expected, but due to a reduced traffic density (following 1990), a ban on leaded gasoline in the past 30 years, local landscape changes, and reconstructions, it was not considered as a significant local pollution source (Abbaszade et al., 2022).

Additionally, atmospheric deposition has an important influence on urban soil as anthropogenic particles can be transferred from other areas to urban soil (Luo et al., 2015; Wu et al., 2021; Zhang

et al., 2018). However, the pollution from atmospheric deposition is secondary pollution and is a combination of different sources. Therefore, atmospheric deposition cannot be thought of as the original source of urban soil in the study area. Taking all previously discussed factors into account, it is considered that in both cities, the PTE concentration is a mixture of various sources, whereas local coal and coal ash, and slag are the predominant pollution sources in the region. This indicates that the primary sources of Pb pollution in Salgótarján and Ózd could not be significantly different, and the possibility of other unidentified minor sources cannot be excluded, as was proved by stable Pb isotopic study in Salgótarján and Ózd soils (Abbaszade et al., 2022).

5.2. Impact of environmental factors and PTEs on microbial community structure

5.2.1. The connection of environmental factors and PTE content in eleven sampling sites, selected for microbiological analysis

The enrichment of the metal(loid)s in the selected 11sampling sites (Table *8*) was identified based on the comparison with the control samples (STN37 and OZD02). Heterogenous distribution of metal(loid)s in the soil samples revealed a significant PTE enrichment, especially around industrial sites (Table 8; Figure 11). Samples with enriched metal(loid) content showed low organic content (Figure 11; Table *8*) that differentiated the metal(loid) contaminated samples from others. Additionally, a significant negative correlation between Eh and pH, as well as soil silt and sand fraction (Figure 11) explain the wide-scale impact of metals and organic content on sampling sites, similarly reported by Lee et al., (2002). Principal component analysis (Figure 11) showed that in the current study, samples STN24, OZD38, OZD42, and OZD54, were in agreement with the statement, meanwhile, the rest of the samples were characterized by their high SOM, low pH, and clay/silt texture (Figure 11A). Wuana and Okieimen (2011) indicated multi-elemental contamination of industries that matches the condition of our metal(loid)-contaminated sampling sites. The similarity in the enrichment of heavy metals indicates they came from the same source, and the soil was polluted during the same period (Figure 11).

5.2.2. Effect of environmental factors on the structure of microbial communities

Among the soil microorganisms, Proteobacteria, Acidobacteria, Actinobacteria, and Planctomycetes are the four most dominant phyla across the world (Janssen, 2006). The current study showed that the top five dominating phyla in 11 urban soil samples were Proteobacteria, Acidobacteria, Planctomycetes, Actinobacteria, and Bacteroidetes (67%–72%; Figure 12A).
In the current study, the observed changes in relative abundance indicated that certain bacterial phyla responded differently to the selected metal(loid)s. Proteobacteria and Patescibacteria indicated a significant increase in the metal(loid)-enriched areas compared to control samples (Figure *12*), though the increase can often be relative: as some members of the prokaryotic community, which is sensitive to metal(loid)s die, on the other hand, can multiply more in the lack of competitors. Similar patterns for Proteobacteria were reported by Sandaa et al. (2001). The reaction of Proteobacteria to heavy metal(loid)s showed different patterns and varied with positive and negative correlations in Salgótarján and Ózd, as was noted by previous studies (Meng, et al., 2017). Compared to the control samples, the Deltaproteobacteria increased in PTE-enriched Salgótarján urban soils but decreased in metal(loid)-enriched Ózd urban soil samples. Studies stated that in metal(loid)-contaminated soils, members of Proteobacteria (e.g. genera *Pseudomonas, Sphingomonas*, etc.) showed high relative abundance and are typically resistant to metals (Yang et al., 2020). Additionally, long-term Cd presence could affect nutrient uptake, reduce microbial diversity, and change community structure. Wang et al. (2019) reported that low levels of Cd (II) appear to increase, whereas higher Cd (II) levels inhibit microbial proliferation. Similar results were observed in the case of Planctomycetacia (Planctomycetes phylum) and Actinobacteria (Actinobacteria phylum) members in our study areas. These varying responses to heavy metal(loid)s may be attributed to varied environmental circumstances and ability to use numerous forms of organic materials such as carbon, nitrogen and energy sources (Bouskill et al., 2010). Meanwhile, a considerable decrease of Acidobacteria (class: *Subgroup_6, genus: Subgroup_6_ge*) and Latescibacteria (class: *Latescibacteria, genus: Latescibacteria_ge*) was observed in metal(loid)-enriched sites which can be associated with their sensitivity to metal(loid)s (Figure 13). As the members of the Acidobacteria are acidophilic and strongly regulated by pH, slightly high pH in metal(loid)-enriched study areas might affect and decrease their abundance (Jones et al., 2008). These dominant phyla were also found in various metal(loid)-enriched soils, including paddy soil, mining sites, and sediment, implying that they are closely related to metal(loid)-enriched soil as well (Yang et al., 2020). Niu et al. (2020) reported that Acidobacteria demonstrates a

significant increase and decrease, respectively, in low and high Pb treated samples. Moreover, the abundance of *Parcubacteria* (Parcubacteria phyla) and *Saccharimonadales_ge* (Saccharimonadia phyla) in all Salgótarján and Ózd metal(loid)-enriched soils indicates their high resistance to different metal(loid) contaminants (Figure 13), especially to As and Cd (Ayala-Muñoz et al., 2020; Yu et al., 2022). These results indicate that environmental factors, particularly the concentration of the studied four PTE, were important for explaining the variations in the bacterial community structure.

Moreover, the impact of rare taxa on soil processes and metal(loid) resistance cannot be ignored as they cover 47-63% (depending on the sampling site) of the total community. Previous studies show that rare and abundant species do not necessarily react to environmental changes in the same way (Liang et al., 2020), and in general, the higher relative abundance of a given taxon is not necessarily connected to increased activity. Compared to rare taxa, abundant species typically occupy a wider range of niches and have access to a wider resource, making them better adaptive to environmental changes. Though the members of "rare taxa" are often relatively slow-growing, they may become active in more advantageous conditions (Shade et al., 2014; Xu et al., 2021). In this study, the growth of bacteria belonging to the rare or less abundant taxa (such as *Nitrobacter, Filomicrobium, Lactobacillus, Azomonas,* etc.) (Figure 15) only at control soils proves this statement, where very low metal(loid) concentration was favourable for growth, however same rare taxa disappeared in urban soils. On the contrary, taxa, such as *Sulfurifustis, Candidatus Moranbacteria*, etc. (Figure 15), could survive in Salgótarján and Ózd metal(loid)-enriched urban soils, which might be due to their gained resistance to the selected metal(loid)s. These taxa might also be present in the control samples, but their quantity is under the detection limits.

Although archaea often make only a small percentage of the microbial community in soils, the archaeal community responded to metal(loid) contamination noticeably. It is observed that in high metal(loid) contaminated sites (OZD38 and OZD54), the number of archaea OTUs (at the level of phyla) is substantially less than in control samples (Figure 12B). The presence of Crenarcheota in sample STN30 can be associated with metal(loid) contamination, as stated by studies (Meng, et al., 2017). An anomaly was observed in sample OZD25, a low metal(loid)-contaminated sample where the number of Thaumarchaeota and Euryarchaeota relatively increased (Figure 12B). At the genus level, the abundance of *Woesearchaeia_ge* and *Nitrososphaeraceae_ge* was particularly noticeable (Figure 14). Due to their membrane structure, extremely diverse energy source, and ability to reduce metal(loid)s by ammonia, sulfide, and sulfur, archaea play an important role in regulating the toxicity of metal(loid)s in

the soils (Meng, et al., 2017). Moreover, according to previous studies, low concentrations of metal(loid)s can promote the growth of communities, whereas higher quantities have an inhibitory effect that frequently results in negative correlated outcomes (Yu et al., 2021). Thus, organic-rich matter and low PTE-containing soils (OZD25 and control samples) might promote the archaea community (Figure 11).

5.2.3. Microbial diversity in the sampling sites and its connection to environmental parameters

Diversity indices of the microbial communities in the control and metal(loid)-enriched samples were relatively similar, despite a high difference in metal(loid) and environmental factors (Table 9). However, environmental parameters in Salgótarján and Ózd urban soils showed different effects, as a diversity increase in Salgótarján and a decrease in Ózd urban soils were observed compared to the control sample. Earlier studies (Luo et al., 2019; Zou et al., 2021) reported that the grade of metal(loid) pollution does not present a simple positive or negative linear relationship with microbial composition and community structure. For instance, the low and medium concentrations of metals can promote, however, long-term metal(loid) exposure can hinder microbial diversity (Luo et al., 2019; Sobolev & Begonia, 2008).

Based on the NMDS results, among the environmental factors and metal(loid)s, Cd and Hg have a significant regulatory effect on community structure in metal(loid)-enriched sampling sites, especially in OZD38 and sample OZD54 (Figure 16). The metal(loid) enrichment and organic content depletion were characteristic in these samples. This finding could imply that the increase in metal(loid)s content altered the community structure and resulted in the relative increase of Proteobacteria, Actinobacteria, and Bacteroidetes. The observed high relative abundance of *Ellin6055* (Proteobacteria) and *RB41* (Acidobacteria) in sample OZD54, *Flavobacterium* (Bacteriodetes) and *Sphingomonas* (Proteobacteria) in sample OZD38, meanwhile unclassified Burkholderiaceae (Proteobacteria) in these two most PTE contaminated samples (Figure 16), confirms that the enrichment of metal(loid)s increases the metal(loid) resistant members in the contaminated sampling sites as was similarly shown by Duan et al., (2021); Luo et al., (2018); and Yu et al., (2021). Moreover, among the communities, taxa at phyla and genus level illustrated a strong correlation with the studied metal(loid)s (Figure 17). Our results suggest that these bacterial phyla and genera are significantly related to the content of PTE, such as As, Cd, and Pb, as was also demonstrated by Liu et al., (2022), which could adapt, adsorb and transfer metal(loid)s until a certain level.

Li et al. (2017) found that soil microorganisms respond to long-term metal(loid) pollution by changing the composition and structure of their microbial communities rather than changing their diversity and evenness. Thus, the abundance of the mentioned genera decreased in low PTE contaminated sampling sites (STN30, OZD25, and STN09), and the community was surpassed by the abundance of *Aeromicrobium*, *unclassified Micrococcaceae* (Actinobacteria), uncultured Gemmatimonadetes, *Pseudomonas* (Proteobacteria) and *Candidatus Udeobacter* (Verrcuomicrobia) (Figure 16). This finding correlates well with the earlier research, which stated that among the community, the members of the class Gemmatimonadetes and genus Aeromicrobium correlate positively with Cd (Sun et al., 2022), as well as *Pseudomonas* species can resist multiple metal ions, including Cd and Hg species in high concentrations (Malik & Jaiswal, 2000). This reveals that the microbial communities of the metal(loid)-enriched samples differed significantly from the control sample locations. However, contaminated samples STN24 and OZD42 showed high OTU similarity to control and low metal(loid) enriched samples (STN37, OZD02, OZD25, OZD39). No any correlation with metal(loid)s was observed in these sampling sites (Figure 16), however, the community similarities can be explained by their adaptation to the contaminants. On the other hand, changes in bacterial community structure are not only influenced by soil metal(loid) content as well as a variety of factors, including soil organic matter, moisture, pH, and soil type. The driving effect of SOM, pH, and redox potential on metal bioavailability and thus on soil microorganisms were reported in a number of studies (Wang et al., 2019; Epp Schmidt et al., 2019; Mhete et al., 2020). Therefore, high soil SOM, silt, and clay fraction, as well as low pH in the studied sampling sites, can be a significant regulator for soil microbial community rather than metal(loid) concentration (Figure 16) (Huang et al., 2021; Nakatsu et al., 2005; Yavitt et al., 2021). Based on the results, the identified phyla and genera were significantly correlated with SOM, pH, Eh, and soil texture (Figure 17) which was consistent with the studies by Mhete *et al.* (2020) and Li et al. (2021) that might explain the relative impact of these parameters. However, in contaminated soils, lower levels of total organic matter were observed and also stated by several studies (e.g., Seddaiu et al. 2013) that can significantly regulate the community. The relative abundances of specific groups of bacteria in soils, such as the Acidobacteria and Proteobacteria (Gammaproteobacteria and Betaproteobacteria), have been demonstrated to be highly influenced by soil pH (Yun et al., 2016). Whereas, except direct effect on the community, changes in pH influence the solubility and bioavailability of metal(loid)s by converting active metal(loid)s into inactive forms or vice versa (Petruzzelli et al. 2020). Lee et al. (2015) reported that a decrease in soil pH and redox potential could increase the metal(loid)

mobility and thus the toxicity. This suggests that the combinations of soil physicochemical parameters (SOM, soil texture, pH-Eh) and metal(loid) content (Pb, Cd, Hg, As, etc) were responsible for alterations in the bacterial community. Studies show that the disturbance of the soil environment by heavy metal(loid)s may result in changes in the microbial compositions and soil microbial activity, such as soil respiration, enzyme activities, microbial metabolic potential, and so on (Chodak et al., 2013).

In the studied urban soils, Archaeal taxa showed a significant correlation only with soil ammonia and clay content. This can be associated with the enrichment of ammonia-oxidizing Thaumarchaeota (Figure *18*) (Brochier-Armanet et al., 2008). In general, Archaea is known for their strong resistance to environmental stress factors (Bini, 2010; Srivastava & Kowshik, 2013), whereas a correlation between archaeal community and metal(loid)s cannot be observed (Figure *18*).

5.2.4. The potential role of genera in geochemical As-, Pb-, Hg-, and Cd-cycle

In the environment, microorganisms are in direct contact with PTE and this threatens their physiological and metabolic functions (Nies, 1999). At high concentrations, PTE can replace the essential nutrients from naturally binding sites, such as Zn, P, Ca, form complex unspecific compounds, disrupt biological processes, and damage DNA. For instance, the metal ions Hg^{2+}, Cd^{2+} tend to attach to the crucial enzymatic sulfhydryl (-SH) groups and so decrease the activity of sensitive enzymes (Kandeler et al., 1996). None of the PTEs are necessary for biological processes, however, they can use the transfer pathways of essential nutrients to access cells and cause toxicity. For this, due to their structural similarity, divalent toxic elements (Pb^{2+}, Cd^{2+}, Hg^{2+}) use the Co^{2+}, Ni^{2+}, Cu^{2+}, Mn^{2+}, Fe^{2+}, and Zn^{2+} pathways. Similarly, chromate and arsenate transport to a cell is fulfilled by sulfate and phosphate transport pathways. To cope with the PTE toxicity, microorganisms developed various methods, including efflux, intracellular and extracellular precipitation, binding to metallothioneins, etc. (Gomathy & Sabarinathan, 2015; Silver & Phung, 1996)

Both the oxidized and reduced forms of arsenic can be used as electron acceptors by a variety of bacteria. After wide genomic analysis, Yang et al. (2012) concluded that almost every prokaryotic organisms carry arsenic resistance genes, particularly, one of the efflux pump genes (*arsB* or *arsY*) to expel As^{3+} from cells. Though, As(III) is more toxic than As(V), both have detrimental effects on microorganisms (Battaglia-Brunet et al., 2002). Some bacteria own the arsenate reductase gene (*arsC*) to reduce As^{5+} to As^{3+}, which is associated with *ars* operons.

Arsenic is taken to cells by a phosphate transport system and can be reduced before effluxed from cells (Li et al., 2014; Yang et al., 2012). Among the identified genera in Salgótarján and Ózd soil samples, the genome of *Aquicella*, *Sphingomonas*, *Solirubrobacter*, members of Subgroup_6, Pedosphaeraceae, unclassified Rhizobiales, and Burkholderiaceae carry arsenate reductase genes and able to reduce As(V) to As(III) (Figure *28*). Besides, genera, such as *Gemmatimonas*, *Sphingomonas*, members of the family Burkholderiacea, order Gaillales, Rokubacteriales, and Parcubacteria can oxidize As(III) to As (V) with arsenite oxidase (*aoxB*) and regulatory *arsR* genes (Figure 28) (Battaglia-Brunet et al., 2002; Shi et al., 2020). Similar studies showed that members of ecologically and metabolically diverse Burkholderiaceae family, Gamma Proteobacteria, Alpha Proteobacteria, Actinobacteria, Firmicutes, etc., are particularly resistant to arsenic and carry many resistant genes (Fekih et al., 2018; Li et al., 2014).

Mercury toxicity is highly complex, and most of the environmental bacteria carry the *mer* operon. In natural waters and soils, Hg can be reduced from Hg(II) to Hg(0) and stays in the atmosphere due to low aqueous solubility. Bacterial Hg reduction is encoded by *merA* gene and regulated by *merR* gene in the cytoplasm (Dash & Das, 2012; Petrus et al., 2015). However, to transfer the Hg^{2+} from outer membrane, additional transport proteins, such as MerC, MerT or MerF are required. The biologically induced Hg(0) oxidation is not widely studied, however, the high Hg(0)-oxidizing activity of *Bacillus* and *Streptomyces* suggest their potential role in Hg cycle (Colombo et al., 2014). Furthermore, rain and snow can precipitate Hg(0) to deep soils or sediments where the microbially mediated transformation of Hg(II) to MeHg occurs (Lin et al., 2021). The process was encoded by *hgcAB* gene pair, and the global biogeochemical cycling takes part in anaerobic and microaerobic conditions by Hg methylators, such as sulfate-reducing bacteria, Fe-reducing bacteria, Chloroflexi, *Nitrospina* , and Verrucomicrobia (Lin et al., 2021; Silver & Phung, 2005). However, some bacteria carry *merB* gene that encodes organomercurial lyase enzyme to reduce organic mercury compounds, such as methyl mercury, phenyl mercury, etc. The process starts with the cleavage of covalent Hg–C bonds and thus releases Hg^{2+} (Nascimento & Chartone-Souza, 2003; Petrus et al., 2015). In this study, *Sphingomonas*, *Rhizobiales*, *Nitrospira*, *Solirubrobacter*, members of Burkholderiaceae, Pedosphaeraceae, and Gaiellales possess reductase genes and take part in the mercury cycle by reducing Hg(II) and MeHg (Figure 28).

Lead, and cadmium resistance to PTEs have many similarities, and they interact with the metabolism of divalent essential metals: Ca, Zn, Fe, etc., and can disrupt bacterial respiratory

proteins and physiological cell functioning (Jarosławiecka & Piotrowska-Seget, 2014). It differs from Hg and As resistance because there are no oxidation/reduction processes or enzymatic transformations. In microbial cells, Pb and Cd resistance is accomplished by energy-dependent active efflux pump, P-type ATPase, chemiosmotic pumps, or metallothionein proteins to extrude or bind Pb and Cd cations to cell components (Figure 2; Silver & Phung, 2005).

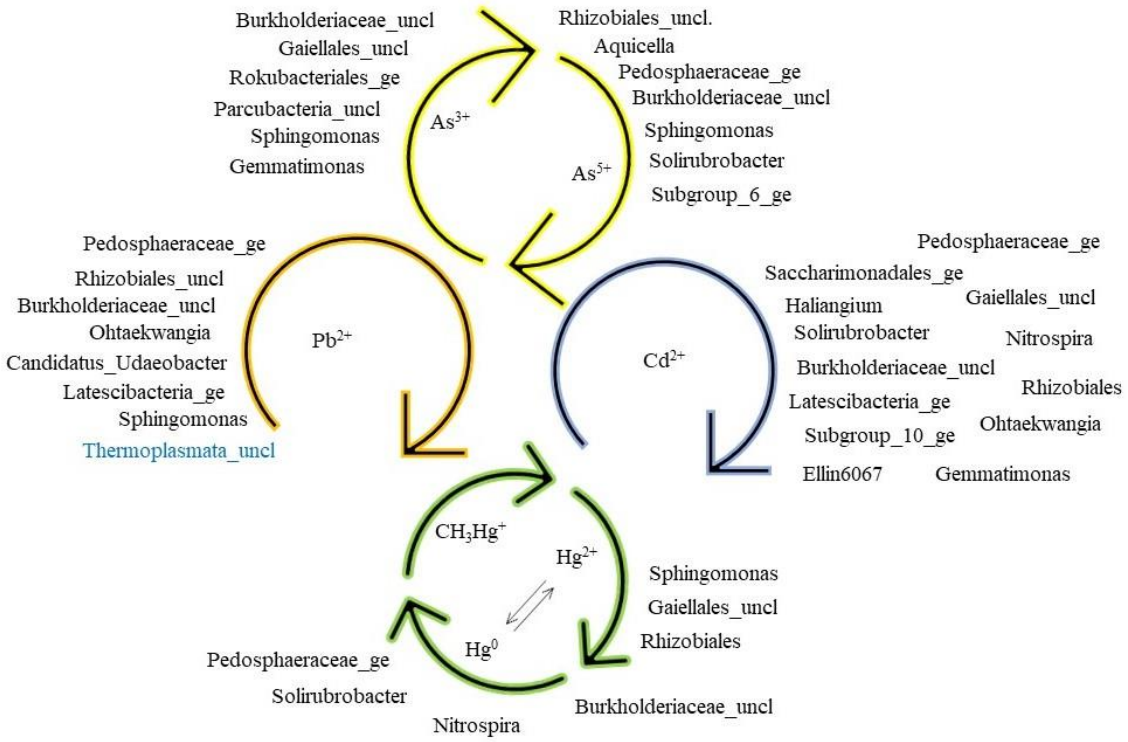

Figure 28. The role of abundant genera originating from the different samples, identified by NGS analysis in Salgótarján and Ózd soil samples, in the biogeochemical cycle of As, Pb, Hg, and Cd. The arrows represent the transformation between oxidation states (a result of oxidation/reduction reactions). The positions of the genera in cycles were identified either by the metal(loid) resistance genes in their genome and/or by published literature.

One of the most studied efflux systems that provide resistance against Cd, Zn, and Co is regulated by czc operon and consists of three structural genes, CzcA (chemiosmotic antiporter), CzcB (membrane fusion protein), and CzcC (outer membrane protein). Resistance to Pb^{2+} regulated by *pbrABCD* operon, where *pbrA* encodes P-type ATPase efflux pumps, *pbrB* manages the transport of metals in periplasmic space, *pbrC* -signal peptidase and *pbrD* emerges as intracellular metal binding protein (Hynninen et al., 2009; Naik & Dubey, 2013). The number of additional genes, including *pbrTR*, *cadCA*, etc., encode various Pb and Cd efflux mechanisms as well, however, efflux mechanisms used against other divalent metals can

participate in Pb and Cd resistance (Silver & Phung, 2005).Metallothioneins are considered cation binding proteins that play a significant role in decreasing free metal cations in cells and thus reducing the toxicity of Pb^{2+}, Cd^{2+} in the cytoplasm. Previous studies reported intracellular and extracellular precipitation and binding of Pb and Cd for different *Staphylococcus, Pseudomonas, Cupriavidus*, and *Bacillus* sp. (Abbas et al., 2018; Naik & Dubey, 2013; Ron et al., 1992; Rozycki & Nies, 2009). Furthermore, literature data show that most of the abundant genera identified in this study, such as *Sphingomonas, Ohtaekwangia, Haliangium, Gemmatimonas, Rhizobiales, Nitrospira*, etc. (Figure 14; Figure 28), carry Pb and Cd resistant genes and play a significant role in the biogeochemical cycle of these elements.

5.3. Metal(loid) tolerant/resistant bacterial strains isolated from soil samples

Due to the high level of metal(loid) contamination in the soil environment in both cities, the number of metal(loid) tolerant bacteria was significantly high (Figure 19). However, only 22 strains were able to grow in elevated metal(loid) concentrations, and especially members of *Cupriavidus*, *Bacillus,* and *Pseudomonas* genera were noticeable (Table 10), as was also reported by other studies (Gupta et al., 2012; Mihdhir & Assaeedi, 2016; Monsieurs et al., 2011). Some of the strains showed limited growth in As test, whereas most of them were capable of tolerating high Pb, Cd, and Hg concentrations. The fact that isolated strains from the high metal(loid) contaminated sites may be the cause of their great tolerance to metal(loid)s (Abou-Shanab et al., 2007). In natural conditions, soil bacteria are exposed to metal(loid)s in solution or adsorbed on soil colloids, which leads to the selection of tolerant bacteria in the population. On the other hand, due to adaptation, microorganisms isolated from metal(loid)-contaminated habitats frequently show tolerance to multiple contaminants (Abou-Shanab et al., 2007). Among the isolated strains, *Cupriavidus* sp. illustrated comparatively high resistance to PTE, particularly Cd and was selected for further identification of resistance mechanisms through genomic analysis.

5.3.1. Metal(loid) resistance and its mechanisms in *Cupriavidus campinensis*

5.3.1.1. Genome characteristics

Since the first isolation of *C. campinensis* (Goris et al., 2001), most of the metabolic pathways and characteristics were still unknown due to the lack of whole-genome information on the species. For the first time, the genome of *C. campinensis* S14E4C was analysed (Figure 20) and the genome sequence revealed that the strain has additional capabilities over metal(loid)

resistance, degradation of aromatic compounds, antibiotic resistance, etc. that enhance its potential for use in biotechnological applications (Table 10 and Table 11). Several annotation and alignment tools (PATRIC, RAST, DFAST) were employed to detect genes with high accuracy and predict open reading frames.

It is indicated that *C. campinensis* S14E4C adapts and resists the effect of environmental stresses by functional genes and genes related to plasmid partitioning. The plasmid initiating protein (*RepA*) is solid evidence for plasmid existence that perform heavy metal and antibiotic resistance. Through a combination of sequencing and comparative genomics, our study has provided a comprehensive genomic description of the species *Cupriavidus campinensis* (Figure 20 and Figure 21).

Previous studies depicted that known members of the *Cupriavidus* genus contain 2 large replicons (generally a chromosome) and several plasmids (Amadou et al., 2008; Cuadrado et al., 2010; Hong et al., 2012; Janssen et al., 2010; Moriuchi et al., 2019; Poehlein et al., 2011; Wang et al., 2015). By using SPAdes software, we were able to identify two existing plasmids (Table 12). The alignments of the genomes clarified that the identical genes in Plasmid1 of the S14E4C exist in both plasmids of the *C. metallidurans* CH34, whereas only a few positions are similar among plasmid 2 and CH34 plasmids. After the annotation of the plasmid sequences, it is assumed that in the strain S14E4C, the main replicon carried most of the essential housekeeping genes, including those for translation, production of ribosomes, DNA replication, DNA repair, cell components, and resistance. The existence of the rRNA operon (*rrn*) on plasmids and chromids was earlier reported on *Bacillus* and *Paracoccus* species (Anda et al., 2015) as well, due to its functional importance.

5.3.1.2. Metabolic pathways

The pathways of sulfur oxidation require five *sox* genes which encode three key periplasmic protein complexes: *soxYZ*, a sulfur carrier protein, *soxXA*, a c-type cytochrome complex, and *soxB*, a sulfate thiol hydrolase (Janssen et al., 2010). It turned out that the metabolism of ketogluconates (which can serve as the sole carbon and energy source for various bacteria) in *Cupriavidus campinensis* S14E4C differs from previously identified *Cupriavidus* species. In *C. campinensis* strain S14E4C, the process proceeds via conversion to 6-phosphogluconate that is further metabolized through the Entner-Doudoroff (EDP) and/or Pentose Phosphate pathways (PPP) (Abbaszade et al., 2020). The process is encoded by *pglDH* gene, whereas there are no genes for 6-phosphogluconate dehydrogenase (6-PGDH) in any earlier sequenced,

phylogenetically related *Cupriavidus* species (e.g. *C. metallidurans, C gilardii, C. necator*, etc.; Figure 23, Figure 24) (Janssen et al., 2010).

In the S14E4C strain, D-cysteine is decomposed into pyruvate, H_2S, and NH_3 by D-cysteine desulfohydrase. Decomposition of D-cysteine by the desulfohydrase (*dcyD* gene) produces H_2S, which the bacterium can use as a sulfur source. The desulfhydrase appears in a cluster with two proteins (CAP, CPP*)*, probably involved in transport processes, and a gene encoding a periplasmic cystine-binding protein (CBP) (Berthoumieux et al., 2013).

5.3.1.3. Genes/gene clusters of heavy metal(loid) resistance (HMR)

Compared to the metal(loid) resistant bacterium *Cupriavidus metallidurans* CH34, strain S14E4C carries many typical metal resistance clusters, such as *czcABC*, *copCBA*, etc. (Janssen et al., 2010). However, metal resistance capacity for various metal tolerant strains (Table 10 and Table 11) and mechanisms can differ slightly. For instance, alternate cation-specific mechanisms of Zn^{2+}, $Cd^{2+,}$ and Co^{2+} resistance and transport are encoded by the same genes (*czcRDABC*) (Chizzola & Mitteregger, 2005). However, Hg^{2+} and As^{3+} resistance mechanisms differ from Cd^{2+}, Pb^{2+}, and Zn^{2+} resistance. Unlike the CH34, *pbr* operon is absent in S14E4C, but previous researches indicate that heavy metal-(Cd, Co, Pb, Zn)-translocating P-type ATPase genes can perform Pb^{2+} resistance as well (Naik & Dubey, 2013).

Mercuric ions are toxic to bacteria as they bind to sulfhydryl groups and prevent the synthesis of macromolecules and the activity of enzymes. Genes encoding the resistance to Hg are a well-known property of both Gram-positive and Gram-negative bacteria that are generally located in plasmids (Gupta et al., 1999; Nascimento & Chartone-Souza, 2003).
The *merC*, *merT*, *merE,* and *merP* genes function as a membrane or periplasmic transport of organic and inorganic Hg^{2+} (Table 13 and Figure 22). The *merA* and *merB* genes are responsible for the demethylation of organic mercury compounds by the cleavage C-Hg bonds, encoding mercuric reductase and the enzyme organomercurial lyase, directly followed by genes encoding transport and transcriptional regulators. The other gene encoding organomercury resistance, *merD*, a secondary regulatory protein, also binds to the same region as *merR*, which is involved in transcriptional regulation (Figure 22) (Brown et al., 2003; Naguib et al., 2018).

In the existing operon of arsenic (*arsRBC;* Table 13), the *arsC*, arsenate reductase can transform the arsenate to arsenite, and the rest of the process is encoded by *arsB*, an integral membrane protein, to prohibit arsenic accumulation by expelling out of the cytoplasm (Yang

et al., 2012; Zhu et al., 2014). Meanwhile, the metalloregulatory protein ArsR (encoded by *arsR*) enables the transcription of the operon by attaching the promoter region (Busenlehner et al., 2003; Fekih et al., 2018). The strain can oxidize methyl arsenate compounds (by *arsH* gene) that contribute to the global biotransformation of arsenic (Yang & Rosen, 2016). Among the bacterial species, the *arsH* is widely distributed in Proteobacteria (not present in Gram-positive) and similarly to other *ars* genes located mainly in the chromosome (Fekih et al., 2018; Páez-Espino et al., 2015).

It can be concluded that metal(loid) detoxification in *C. campinensis* S14E4C primarily occurs by efflux system(s): RND (Resistance, Nodulation, cell Division) family of permeases, the CDF (Cation Diffusion Facilitator) family of heavy metal(loid) transporters and the P-type ATPase family of ion pumps may operate on a variety of ions (Hu & Zhao, 2006), including Cd^{2+}, Pb^{2+}, Hg^{2+}, and others (e.g., Zn^{2+}, Ni^{2+}, etc. Table 13). Thus, after a comprehensive genomic analysis, due to its identified metal(loid) resistance mechanisms, *Cupriavidus campinensis* S14E4C was considered a potential candidate for bioremediation (Abbaszade et al., 2020). However, further research is required to apply the strain in metal(loid) contaminated soils.

5.4. Human health risk assessment - health effects

The health risk estimation based on the total concentration of Pb represents a long-term threat and can overrate the authentic health risk (Liu et al., 2016). In Salgótarján and Ózd, the total concentration of the studied PTE in the urban soils alerted six sampling sites (Salgótarján: STN24 - playground, and STN30 - roadside, Ózd: OZD13 - kindergarten, OZD38 - former industrial site, OZD42 - playground, and OZD54 - recent industrial site; Figure 7), which were considered as highly contaminated areas. At these sites, the PTE contents exceed the maximum threshold value (Table 4) for the acceptable concentration of PTEs in soils (Figure 9) assigned by the European Commission (CSTEE, 2000) and the Hungarian government (HUGD, 2009). The determined values represent the effect of the soil PTE concentration, through different pathways, on the permitted blood lead level (max. 50 µg/L As, 100 µg/L Pb, 20 µg/L Hg, 5 µg/L Cd: CDC, 2012). Therefore, an additional assessment of human health risk was performed according to US EPA models (RAIS, 2017; US EPA, 1989a, 1989b) on total PTE content to reveal the risk possibility of high PTE-contaminated sites in Salgótarján and Ózd. Chronic and carcinogenic health risk assessment analysis (Table 14) showed that the average non-carcinogenic risk assessment values are similar in Salgótarján and Ózd, indicating the hazard

quotient (HQ) of PTE for adults and children is below the safe value (HQ<1) in ingestion, inhalation, and dermal exposure (Figure 25). However, in two sampling sites of Salgótarján (STN24 - playground and STN30 - roadside) and four sampling sites of Ózd (OZD13 - kindergarten, OZD38 - former industrial site, OZD42 - playground, and OZD54 - recent industrial site; Figure 26) combined effect of PTE are higher than safe level and could carry possible risk to adults and children's health (HI>1). High values suggested that PTE pollution could represent a significant non-carcinogenic health risk at the contaminated sites, which pose a high non-carcinogenic health risk for children compared to adults, as was similarly reported by previous studies (Gržetić et al. 2008; Tepanosyan et al. 2017). The findings also show that the ingestion pathway contributes the most to non-carcinogenic risk in both adults and children, followed by the dermal pathway. Inhalation is the least dangerous pathway for PTE exposure (Figure 25 and Figure 26).

In terms of carcinogenic risk, both cities pose a low carcinogenic risk and thus are considered safe (Table 14; Figure 27). Cao et al. (2014) reported a potential cancer risk after long-term exposure even to a low amount of toxic elements. However, the severity and exposure level depend on the interaction degree with contaminants and the ingestion rate of As and Pb (RAIS, 2017). Arsenic is known as a carcinogen in the lung, liver, skin, and other internal organs, which is strongly associated with chronic exposure in earlier childhood (Naujokas et al., 2013; Ramsey, 2015). Therefore, the sampling sites with high PTE contamination causing chronic risk (Figure 26) might also result in further carcinogenic health issues.

Several factors (e.g., lifestyle, healthcare system, environmental influences, or genetic factors) influence the general health state, the mortality rate, etc. of a country. The general health state and mortality risk of the Hungarian population (male and females) was analysed by EFOT project at the National Centre for Public Health Analysis Information System (NEKIR), which conducted extensive surveys between 2013-2018 for male and females. Based on the results, Northern Hungary has a higher-level general mortality rate than other parts of the country (Figure 29 and Figure 30). The general mortality rates in Salgótarján and Ózd districts compared to Hungarian average values (BNO-10.:A00-Y98) for a female and male population are shown in Figure S2.1 - 4, respectively, where the mortality rate in Ózd is higher than Salgótarján. Particularly, in Salgótarján, the mortality rate of females are slightly lower than that of males. In Ózd, however, the mortality rate of females is significantly higher than males. It cannot be assumed that only the PTE contamination of the studied cities is responsible for the above-mentioned values for the general mortality rates of males and females. However,

PTE contaminations should be taken seriously since it contributes to the worse health state in the studied cities.

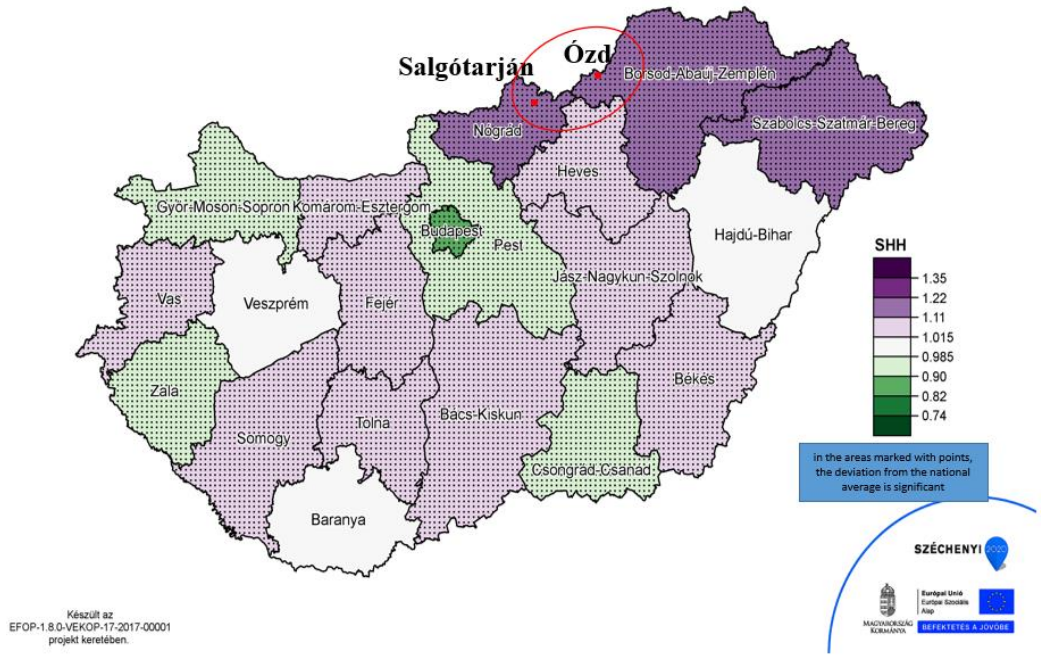

Figure 29. Deaths due to all death types of the **female** population of Hungary (BNO-10.:A00-Y98) at the county level between 2014-2018 (based on: https://efop180.antsz.hu/nekinf-terkep)

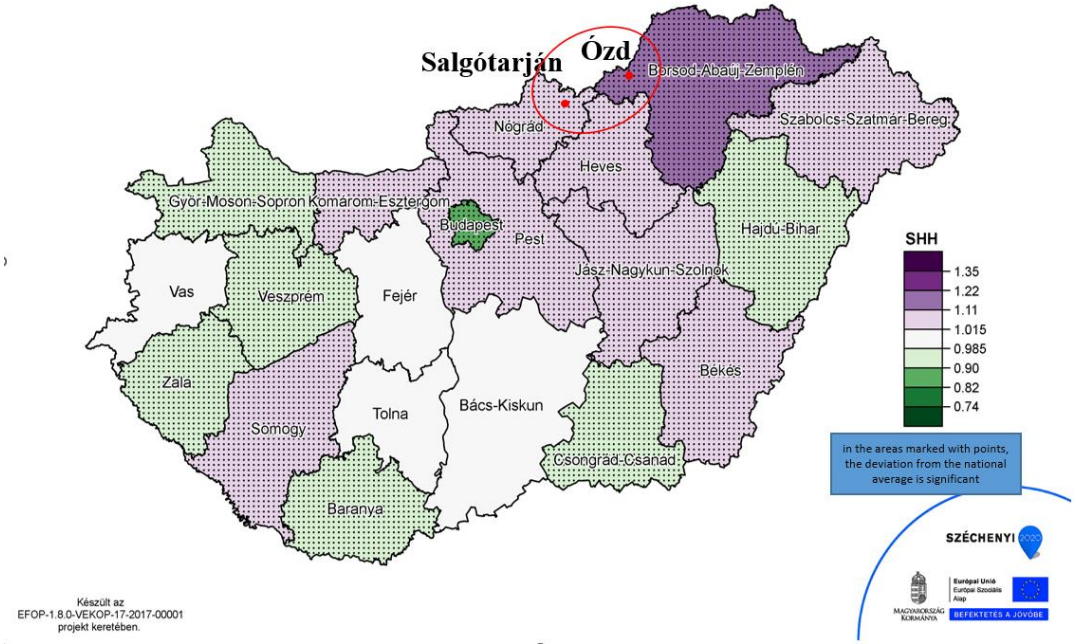

Figure 30. Deaths due to all death types of the **male** population of Hungary (BNO-10.:A00-Y98) at the county level between 2014-2018

Chapter 6: CONCLUSIONS

In my PhD research, the potentially toxic element contamination, and its impact on the urban soil microbial community in two former industrial cities of Hungary was studied. Using comprehensive geochemical and microbiological analytical techniques, as well as statistical analysis, it is concluded that there is a significant metal(loid) contamination in Salgótarján and Ózd cities, which changed the proportion of soil fractions and organic content. Furthermore, it was observed that the metal(loid) contamination caused significant toxicity to the soil microbial community and thus changed the structure of abundant and rare taxa. The sampling sites with high concentrations of PTE can cause a potential chronic health risk for children, however, during these experiments, a bacterial strain was isolated, which is a prospective candidate for bioremediation to remove toxic compounds from the soil environment.

THESIS POINTS

1. Industrial activities caused significant potentially toxic elements (PTE) contamination in Salgótarján and Ózd urban soils. In both cities, there is a heterogenous distribution of As, Pb, Hg, and Cd, and the concentrations were all higher than their correspondent geochemical background values. Except for Hg in Salgótarján, all PTE in both cities exceeded the maximum permissible soil values. It was concluded that in Salgótarján urban soils, organic content plays a significant role on Pb, Hg, Cd, and Fe on As mobility, whereas, in Ózd urban soils, Fe and Mn most likely constraints PTE mobility, thus bioavailability on the surface environment.

2. Compared to local geochemical background (control) samples, there is a minimal enrichment of studied PTE (< 2) in Salgótarján soils, whereas, in Ózd soils, the enrichment is significantly high (2< x <16) and primarily found around industrial sites. Analysis of local contamination sources indicated that in both cities, PTE concentration results from various contamination sources, whereas local coal ash in Salgótarján and smelter slag in Ózd are the predominant pollution sources. This suggests that anthropogenic input from industrial operations was substantial enough to cause significant alterations in soils.

3. Proteobacteria, Acidobacteria, Planctomycetes, Actinobacteria, and Bacteroidetes are dominant phyla in selected Salgótarján and Ózd urban soils, however, concentration differences of contaminants and other soil parameters (organic matter, soil fractions, pH) affected soil community and structure in various ways. It was found that the low soil PTE and high organic content enhanced the diversity, on the other hand, high PTE contamination depleted soil organic matter and resulted in a diversity decrease. A shift in community composition was observed particularly in rare taxa, where high PTE contamination killed the sensitive members of the communities and increased the number of PTE-resistant genera.

4. A high number of metal(loid) resistant isolates indicate selective pressure of contaminants formed resistant bacterial communities, and these communities developed various resistance mechanisms. The comprehensive examination of the most metal(loid) resistant bacterial strain, *Cupriavidus campinensis* S14E4C, revealed that the strain can grow in high metal(loid) exposed environments and carry a significant number of metal(loid) resistant genes encoding various resistance mechanisms. Thus, the strain is effective and suitable for bioremediation, which can transfer toxic compounds to less or non-toxic compounds.

5. Arsenic, lead, mercury, and cadmium contaminants can cause significant health issues and endanger local resident's life. The non-carcinogenic health risk assessment, performed especially on kindergarten, playgrounds, and parks, suggested both cities as safe areas for adults, but it can be hazardous to children's health. Thus, high PTE contaminated sites are not suggested for cultivation and playground purposes; however, further investigations are required.

Acknowledgements

First of all, I am grateful to my supervisors, **Erika Tóth, Dr.** and **Csaba Szabó, Dr.**, for their patience, guidance, and invaluable advice throughout this work since I have become a member of their team. I am also thankful to all my colleagues, particularly Dava, Nelson, Tani, Thomas, Laszlo, Abel, Marwene, Sára, Rózsa, etc., who helped and motivated me during the scientific work. Moreover, I am also thankful to several present and former students/scientists of LRG and the Department for Microbiology, who instructed me and increased the quality of my research (Peter, Dóra, Balázs, Attila). Also, I am grateful to Zsuzsanna Szabó-Krausz, Dr. and Márialigeti Károly, Dr. for thesis revision, their valuable suggestions.

Last but not least, I am grateful to my Family and Friends for their continuous support that kept me going.

This work was financially supported by the Stipendium Hungaricum, ELTE Doctoral School of Environmental Sciences, ELTE Talent Support, and the ELTE Thematic Excellence Program 2020, Supported by the National Research - Development and Innovation Office - TKP2020-IKA-05.

REFERENCES:

Abbas, S. Z., Rafatullah, M., Hossain, K., Ismail, N., Tajarudin, H. A., & Abdul Khalil, H. P. S. (2018). A review on mechanism and future perspectives of cadmium-resistant bacteria. *International Journal of Environmental Science and Technology*, *15*(1), 243–262. https://doi.org/10.1007/s13762-017-1400-5

Abbaszade, G., Szabó, A., Vajna, B., Farkas, R., Szabó, C., & Tóth, E. (2020). Whole genome sequence analysis of Cupriavidus campinensis S14E4C, a heavy metal resistant bacterium. *Molecular Biology Reports*, *47*(5), 3973–3985. https://doi.org/10.1007/s11033-020-05490-8

Abbaszade, G., Tserendorj, D., Salazar, N., Zacháry, D., Völgyesi, P., Tóth, E., & Szabó, C. (2022). Lead and stable lead isotopes as tracers of soil pollution and human health risk assessment in former industrial cities of Hungary. *Applied Geochemistry*, 105397. https://doi.org/https://doi.org/10.1016/j.apgeochem.2022.105397

Abdulkarim, M., Grema, H. M., Adamu, I. H., Mueller, D., Schulz, M., Ulbrich, M., Miocic, J. M., & Preusser, F. (2021). Effect of using different chemical dispersing agents in grain size analyses of fluvial sediments via laser diffraction spectrometry. *Methods and Protocols*, *4*(3), 1–13. https://doi.org/10.3390/mps4030044

Abou-Shanab, R. A. I., van Berkum, P., & Angle, J. S. (2007). Heavy metal resistance and genotypic analysis of metal resistance genes in gram-positive and gram-negative bacteria present in Ni-rich serpentine soil and in the rhizosphere of Alyssum murale. *Chemosphere*, *68*(2), 360–367. https://doi.org/10.1016/j.chemosphere.2006.12.051

Achilleos, G. A. (2011). The Inverse Distance Weighted interpolation method and error propagation mechanism - creating a DEM from an analogue topographical map. *Journal of Spatial Science*, *56*(2), 283–304. https://doi.org/10.1080/14498596.2011.623348

Akinola, S. A., Ayangbenro, A. S., & Babalola, O. O. (2021). The diverse functional genes of maize rhizosphere microbiota assessed using shotgun metagenomics. *Journal of the Science of Food and Agriculture*, *101*(8), 3193–3201. https://doi.org/10.1002/jsfa.10948

Alfred R. Conkinlin, J. (2014). Introduction to Soil Chemistry. In *Introduction to Soil Chemistry*. https://doi.org/10.1002/9781118773383

Ali, H., Khan, E., & Ilahi, I. (2019). Environmental chemistry and ecotoxicology of hazardous heavy metals: Environmental persistence, toxicity, and bioaccumulation. *Journal of Chemistry*, *2019*(Cd). https://doi.org/10.1155/2019/6730305

Alloway, B. J. (2013). Heavy metals in soils. In *Handbook on the Toxicology of Metals: Fifth Edition*.

https://doi.org/10.1016/s0165-9936(96)90032-1

Amadou, C., Mangenot, S., Glew, M., Bontemps, C., Capela, D., Dossat, C., Marchetti, M., Servin, B., Saad, M., Schenowitz, C., Batut, J., & Masson-boivin, C. (2008). Genome sequence of the □-rhizobium. *Genome Research*, 1472–1483. https://doi.org/10.1101/gr.076448.108.7

Anda, M., Ohtsubo, Y., Okubo, T., Sugawara, M., Nagata, Y., Tsuda, M., Minamisawa, K., & Mitsui, H. (2015). Bacterial clade with the ribosomal RNA operon on a small plasmid rather than the chromosome. *Proceedings of the National Academy of Sciences of the United States of America*, *112*(46), 14343–14347. https://doi.org/10.1073/pnas.1514326112

Anderson, M. J. (2001). *Austral Ecology - 2001 - Anderson - A new method for non-parametric multivariate analysis of variance.pdf*.

Anne, C. (1984). Nonparametric Estimation of the Number of Classes in a Population. *Scandinavian Journal of Statistics*, *11*(4), 265.

Antipov, D., Hartwick, N., Shen, M., Raiko, M., & Pevzner, P. A. (2016). *plasmidSPAdes : Assembling Plasmids from Whole Genome Sequencing Data*. *April*, 1–7.

Argyraki, A., Kelepertzis, E., Botsou, F., Paraskevopoulou, V., Katsikis, I., & Trigoni, M. (2018). Environmental availability of trace elements (Pb, Cd, Zn, Cu) in soil from urban, suburban, rural and mining areas of Attica, Hellas. *Journal of Geochemical Exploration*, *187*(January), 201–213. https://doi.org/10.1016/j.gexplo.2017.09.004

Arsham, H., & Lovric, M. (2011). *Bartlett's Test BT - International Encyclopedia of Statistical Science* (M. Lovric (Ed.); pp. 87–88). Springer Berlin Heidelberg. https://doi.org/10.1007/978-3-642-04898-2_132

Ayala-Muñoz, D., Burgos, W. D., Sánchez-España, J., Couradeau, E., Falagán, C., & Macalady, J. L. (2020). Metagenomic and metatranscriptomic study of microbial metal resistance in an acidic pit lake. *Microorganisms*, *8*(9), 1–271350. https://doi.org/10.3390/microorganisms8091350

Baba, H., Tsuneyama, K., Yazaki, M., Nagata, K., Minamisaka, T., Tsuda, T., Nomoto, K., Hayashi, S., Miwa, S., Nakajima, T., Nakanishi, Y., Aoshima, K., & Imura, J. (2013). The liver in itai-itai disease (chronic cadmium poisoning): Pathological features and metallothionein expression. *Modern Pathology*, *26*(9), 1228–1234. https://doi.org/10.1038/modpathol.2013.62

Bankevich, A., Nurk, S., Antipov, D., Gurevich, A. A., Dvorkin, M., Kulikov, A. S., Lesin, V. M., Nikolenko, S. I., Pham, S., Prjibelski, A. D., Pyshkin, A. V., Sirotkin, A. V., Vyahhi, N., Tesler, G., Alekseyev, M. A., & Pevzner, P. A. (2012). SPAdes: A new genome assembly algorithm and

its applications to single-cell sequencing. *Journal of Computational Biology*, *19*(5), 455–477. https://doi.org/10.1089/cmb.2012.0021

Battaglia-Brunet, F., Dictor, M.-C., Garrido, F., Crouzet, C., Morin, D., Dekeyser, K., Clarens, M., & Baranger, P. (2002). *An arsenic III -oxidizing bacterial population: selection, characterization, and performance in reactors* (p. Journal of Applied Microbiology, 93, 656-667).

Berthoumieux, S., De Jong, H., Baptist, G., Pinel, C., Ranquet, C., Ropers, D., & Geiselmann, J. (2013). Shared control of gene expression in bacteria by transcription factors and global physiology of the cell. *Molecular Systems Biology*, *9*(634), 1–11. https://doi.org/10.1038/msb.2012.70

Bhanarkar, A. D., Gavane, A. G., Tajne, D. S., Tamhane, S. M., & Nema, P. (2008). Composition and size distribution of particules emissions from a coal-fired power plant in India. *Fuel*, *87*(10–11), 2095–2101. https://doi.org/10.1016/j.fuel.2007.11.001

Bini, E. (2010). Archaeal transformation of metals in the environment. *FEMS Microbiology Ecology*, *73*(1), 1–16. https://doi.org/10.1111/j.1574-6941.2010.00876.x

Birke, M., Rauch, U., & Stummeyer, J. (2011). Urban Geochemistry of Berlin, Germany. *Mapping the Chemical Environment of Urban Areas*, 245–268. https://doi.org/10.1002/9780470670071.ch17

Bollhöfer, a., Rosman, K. J. R. J. R., Boilhiifer, A., Rosman, K. J. R. J. R., Bollhöfer, a., & Rosman, K. J. R. J. R. (2001). Lead isotopic ratios in European atmospheric aerosols. *Physics and Chemistry of the Earth, Part B: Hydrology, Oceans and Atmosphere*, *26*(10), 835–838. https://doi.org/10.1016/S1464-1909(01)00094-6

Bouskill, N. J., Barker-Finkel, J., Galloway, T. S., Handy, R. D., & Ford, T. E. (2010). Temporal bacterial diversity associated with metal-contaminated river sediments. *Ecotoxicology*, *19*(2), 317–328. https://doi.org/10.1007/s10646-009-0414-2

Brettin, T., Davis, J. J., Disz, T., Edwards, R. A., Gerdes, S., Olsen, G. J., Olson, R., Overbeek, R., Parrello, B., Pusch, G. D., Shukla, M., Thomason, J. A., Stevens, R., Vonstein, V., Wattam, A. R., & Xia, F. (2015). RASTtk: A modular and extensible implementation of the RAST algorithm for building custom annotation pipelines and annotating batches of genomes. *Scientific Reports*, *5*. https://doi.org/10.1038/srep08365

Brochier-Armanet, C., Boussau, B., Gribaldo, S., & Forterre, P. (2008). Mesophilic crenarchaeota: proposal for a third archaeal phylum, the Thaumarchaeota. *Nature Reviews Microbiology*, *6*(3), 245–252. https://doi.org/10.1038/nrmicro1852

Brown, N. L., Stoyanov, J. V., Kidd, S. P., & Hobman, J. L. (2003). The MerR family of transcriptional

regulators. *FEMS Microbiology Reviews*, *27*(2–3), 145–163. https://doi.org/10.1016/S0168-6445(03)00051-2

Bureau Veritas. (2021). *https://miningtheabitibi.virtex.ca/files/brochures/163/Bureau%20Veritas%20-%20USD%20Fee%20Schedule%202021.pdf*.

Busenlehner, L. S., Pennella, M. A., & Giedroc, D. P. (2003). The SmtB/ArsR family of metalloregulatory transcriptional repressors: Structural insights into prokaryotic metal resistance. *FEMS Microbiology Reviews*, *27*(2–3), 131–143. https://doi.org/10.1016/S0168-6445(03)00054-8

Cao, S., Duan, X., Zhao, X., Ma, J., Dong, T., Huang, N., Sun, C., He, B., & Wei, F. (2014). Health risks from the exposure of children to As, Se, Pb and other heavy metals near the largest coking plant in China. *Science of the Total Environment*, *472*, 1001–1009. https://doi.org/10.1016/j.scitotenv.2013.11.124

Caporale, A. G., & Violante, A. (2016). Chemical Processes Affecting the Mobility of Heavy Metals and Metalloids in Soil Environments. *Current Pollution Reports*, *2*(1), 15–27. https://doi.org/10.1007/s40726-015-0024-y

CDC. (2012). Response to Advisory Committee on Childhood Lead Poisoning Prevention Recommendations in "Low Level Lead Exposure Harms Children: A Renewed Call of Primary Prevention." *Morbidity Mortality Weekly*, *61*(20), 383.

CDC. (2019). *Centers for Diseas Control and Prevention, Agency for Toxic Substances and Disease Registry. Substance priority List. https://www.atsdr.cdc.gov/SPL/#2019spl*.

CDC. (2021). *Centers for Diseas Control and Prevention, Agency for Toxic Substances and Disease Registry. https://www.atsdr.cdc.gov*.

Chen, J., Tan, M., Li, Y., Zhang, Y., Lu, W., Tong, Y., Zhang, G., & Li, Y. (2005). A lead isotope record of shanghai atmospheric lead emissions in total suspended particles during the period of phasing out of leaded gasoline. *Atmospheric Environment*, *39*(7), 1245–1253. https://doi.org/10.1016/j.atmosenv.2004.10.041

Cheng-Shiuan Lee* and Nicholas S. Fisher. (2020). Microbial generation of elemental mercury from dissolved methylmercury in seawater. *Physiology & Behavior*, *176*(5), 139–148. https://doi.org/10.1002/lno.11068.Microbial

Chizzola, R., & Mitteregger, U. S. (2005). Cadmium and zinc interactions in trace element accumulation in chamomile. *Journal of Plant Nutrition*, *28*(8), 1383–1396.

https://doi.org/10.1081/PLN-200067470

Chodak, M., Gołebiewski, M., Morawska-Płoskonka, J., Kuduk, K., & Niklińska, M. (2013). Diversity of microorganisms from forest soils differently polluted with heavy metals. *Applied Soil Ecology*, *64*, 7–14. https://doi.org/10.1016/j.apsoil.2012.11.004

Colombo, M. J., Ha, J., Reinfelder, J. R., Barkay, T., & Yee, N. (2014). Oxidation of Hg(0) to Hg(II) by diverse anaerobic bacteria. *Chemical Geology*, *363*, 334–340. https://doi.org/10.1016/j.chemgeo.2013.11.020

Csorba, S., Üveges, J., & Makó, A. (2014). Relationship between soil properties and potentially toxic element content based on the dataset of the Soil Information and Monitoring System in Hungary. *Central European Geology*, *57*(3), 253–263. https://doi.org/10.1556/CEuGeol.57.2014.3.2

CSTEE. (2000). *Commission, European. 2000. "Brussels, B2/JCD/Csteeop/ PbDK50500 /D(00) SCIENTIFIC COMMITTEE ON TOXICITY, ECOTOXICITY AND THE ENVIRONMENT (CSTEE)." (1):1–31.*

Cuadrado, V., Gomila, M., Merini, L., Giulietti, A. M., & Moore, E. R. B. (2010). Cupriavidus pampae sp. nov., a novel herbicide-degrading bacterium isolated from agricultural soil. *International Journal of Systematic and Evolutionary Microbiology*, *60*(11), 2606–2612. https://doi.org/10.1099/ijs.0.018341-0

Cui, B., Zhu, M., Jiang, Y., Jiang, Y., & Cao, H. (2014). Identification of the sources of metals and arsenic in river sediments by multivariate analysis and geochemical approaches. *Journal of Soils and Sediments*, *14*(8), 1456–1468. https://doi.org/10.1007/s11368-014-0930-4

Darling, A. C. E., Mau, B., Blattner, F. R., & Perna, N. T. (2004). Mauve: Multiple alignment of conserved genomic sequence with rearrangements. *Genome Research*, *14*(7), 1394–1403. https://doi.org/10.1101/gr.2289704

Dash, H. R., & Das, S. (2012). Bioremediation of mercury and the importance of bacterial mer genes. *International Biodeterioration and Biodegradation*, *75*, 207–213. https://doi.org/10.1016/j.ibiod.2012.07.023

Dash, H. R., Mangwani, N., Chakraborty, J., Kumari, S., & Das, S. (2013). Marine bacteria: Potential candidates for enhanced bioremediation. *Applied Microbiology and Biotechnology*, *97*(2), 561–571. https://doi.org/10.1007/s00253-012-4584-0

Davis, J. J., Gerdes, S., Olsen, G. J., Olson, R., Pusch, G. D., Shukla, M., Vonstein, V., Wattam, A. R., & Yoo, H. (2016). PATtyFams: Protein families for the microbial genomes in the PATRIC

database. *Frontiers in Microbiology*, *7*(FEB), 1–12. https://doi.org/10.3389/fmicb.2016.00118

Demetriades, A., & Birke, M. (2015). *Urban Geochemical Mapping Manual: Sampling, Sample preparation, Laboratory analysis, Quality control check, Statistical processing and Map plotting*.

Dragović, S., Mihailović, N., & Gajić, B. (2008). Heavy metals in soils: Distribution, relationship with soil characteristics and radionuclides and multivariate assessment of contamination sources. *Chemosphere*, *72*(3), 491–495. https://doi.org/10.1016/j.chemosphere.2008.02.063

Duan, R., Lin, Y., Zhang, J., Huang, M., Du, Y., Yang, L., Bai, J., Xiang, G., Wang, Z., & Zhang, Y. (2021). Changes in diversity and composition of rhizosphere bacterial community during natural restoration stages in antimony mine. *PeerJ*, *9*, 1–22. https://doi.org/10.7717/peerj.12302

Edgar, R. C. (2004). MUSCLE: Multiple sequence alignment with high accuracy and high throughput. *Nucleic Acids Research*, *32*(5), 1792–1797. https://doi.org/10.1093/nar/gkh340

EEA. (2007). Progress in management of contaminated sites (CSI 015/LSI 003). *European Environmental Agency*. https://doi.org/http://www.eea.europa.eu/data-and-maps/indicators

EIA. (2016). *U.S. Energy Information Administration 2016 https://www.eia.gov/coal/annual/pdf/acr.pdf*.

Epp Schmidt, D. J., Kotze, D. J., Hornung, E., Setälä, H., Yesilonis, I., Szlavecz, K., Dombos, M., Pouyat, R., Cilliers, S., Tóth, Z., & Yarwood, S. (2019). Metagenomics Reveals Bacterial and Archaeal Adaptation to Urban Land-Use: N Catabolism, Methanogenesis, and Nutrient Acquisition. *Frontiers in Microbiology*, *10*(October), 1–17. https://doi.org/10.3389/fmicb.2019.02330

Ettler, V. (2015). Soil contamination near non-ferrous metal smelters: A review. *Applied Geochemistry*, *64*, 56–74. https://doi.org/10.1016/j.apgeochem.2015.09.020

Evangelou, V. P. (2008). *Environmental Soil and Water Chemistry: Principles and Applications. European journal of soil Sciences, https://doi.org/10.1046/j.1365-2389.2000.00334-4.x*.

Fashola, M. O., Ngole-Jeme, V. M., & Babalola, O. O. (2016). Heavy metal pollution from gold mines: Environmental effects and bacterial strategies for resistance. *International Journal of Environmental Research and Public Health*, *13*(11). https://doi.org/10.3390/ijerph13111047

Fekih, I. Ben, Zhang, C., Li, Y. P., Zhao, Y., Alwathnani, H. A., Saquib, Q., Rensing, C., & Cervantes, C. (2018). Distribution of arsenic resistance genes in prokaryotes. *Frontiers in Microbiology*, *9*(OCT), 1–11. https://doi.org/10.3389/fmicb.2018.02473

Flament, P., Bertho, M. L., Deboudt, K., Véron, A., & Puskaric, E. (2002). European isotopic signatures for lead in atmospheric aerosols: A source apportionment based upon 206Pb/207Pb ratios. *Science of the Total Environment*, *296*(1–3), 35–57. https://doi.org/10.1016/S0048-9697(02)00021-9

Flora, G., Gupta, D., & Tiwari, A. (2012). Toxicity of lead: A review with recent updates. *Interdisciplinary Toxicology*, *5*(2), 47–58. https://doi.org/10.2478/v10102-012-0009-2

Friedlová, M. (2010). The influence of heavy metals on soil biological and chemical properties. *Soil and Water Research*, *5*(1), 21–27. https://doi.org/10.17221/11/2009-swr

Gaberšek, M., & Gosar, M. (2018). Geochemistry of urban soil in the industrial town of Maribor, Slovenia. *Journal of Geochemical Exploration*, *187*(June 2017), 141–154. https://doi.org/10.1016/j.gexplo.2017.06.001

Gadd, G. M., & Pan, X. (2016). Biomineralization, bioremediation and biorecovery of toxic metals and radionuclides. *Geomicrobiology Journal*, *33*(3–4), 175–178. https://doi.org/10.1080/01490451.2015.1087603

Galušková, I., Mihaljevič, M., Borůvka, L., Drábek, O., Frühauf, M., & Němeček, K. (2014). Lead isotope composition and risk elements distribution in urban soils of historically different cities Ostrava and Prague, the Czech Republic. *Journal of Geochemical Exploration*, *147*(PB), 215–221. https://doi.org/10.1016/j.gexplo.2014.02.022

Garcia-Guinea, J., Virgilio, C., Recio-Vazquez, L., Crespo-Feo, E., Gonzalez-Martin, R., & Laura, T. (2010). Influence of accumulation of heaps of steel slag on the environment: Determination of heavy metals content in the soils. *Anais Da Academia Brasileira de Ciencias*, *82*(2), 267–277. https://doi.org/10.1590/s0001-37652010000200003

Gąsiorek, M., Kowalska, J., Mazurek, R., & Pająk, M. (2017). Comprehensive assessment of heavy metal pollution in topsoil of historical urban park on an example of the Planty Park in Krakow (Poland). *Chemosphere*, *179*(March), 148–158. https://doi.org/10.1016/j.chemosphere.2017.03.106

Gaur, N., Flora, G., Yadav, M., & Tiwari, A. (2014). A review with recent advancements on bioremediation-based abolition of heavy metals. *Environmental Sciences: Processes and Impacts*, *16*(2), 180–193. https://doi.org/10.1039/c3em00491k

Gbogbo, F., Arthur-Yartel, A., Bondzie, J. A., Dorleku, W. P., Dadzie, S., Kwansa-Bentum, B., Ewool, J., Billah, M. K., & Lamptey, A. M. (2018). Risk of heavy metal ingestion from the consumption of two commercially valuable species of fish from the fresh and coastal waters of Ghana. *PLoS ONE*, *13*(3), 1–17. https://doi.org/10.1371/journal.pone.0194682

Genchi, G., Sinicropi, M. S., Lauria, G., Carocci, A., & Catalano, A. (2020). The effects of cadmium toxicity. *International Journal of Environmental Research and Public Health*, *17*(11), 1–24. https://doi.org/10.3390/ijerph17113782

Ghorbani, N. R., Salehrastin, N., & Moeini, A. (2002). Heavy metals affect the microbial populations and their activities. *Symposium, Paper no.*(54), 1–11.

Ghosh, A. K., Bhattacharyya, P., & Pal, R. (2004). Effect of arsenic contamination on microbial biomass and its activities in arsenic contaminated soils of Gangetic West Bengal, India. *Environment International*, *30*(4), 491–499. https://doi.org/10.1016/j.envint.2003.10.002

Gomathy, M., & Sabarinathan, K. G. (2015). Microbial Mechanisms of Heavy Metal Tolerance- a Review. *Agricultural Reviews*, *31*(2), 133–138.

Goris, J., De Vos, P., Coenye, T., Hoste, B., Jansses, D., Brim, H., Diels, L., Mergeay, M., Kersters, K., & Vandamme, P. (2001). Classification of metal-resistant bacteria from industrial biotopes as Ralstonia campinensis sp. nov., Ralstonia metallidurans sp. nov. and Ralstonia basilensis Steinle et al. 1998 emend. *International Journal of Systematic and Evolutionary Microbiology*, *51*(5), 1773–1782. https://doi.org/10.1099/00207713-51-5-1773

Goyer, R. A. (1993). Lead toxicity: Current concerns. *Environmental Health Perspectives*, *100*, 177–187. https://doi.org/10.1289/ehp.93100177

Gržetić, I., & Ahmed Ghariani, R. H. (2008). Potential health risk assessment for soil heavy metal contamination in the central zone of Belgrade (Serbia). *Journal of the Serbian Chemical Society*, *73*(8–9), 923–934. https://doi.org/10.2298/JSC0809923G

Gupta, A., Phung, L. T., Chakravarty, L., & Silver, S. (1999). Mercury resistance in Bacillus cereus RC607: Transcriptional organization and two new open reading frames. *Journal of Bacteriology*, *181*(22), 7080–7086.

Gupta, K., Chatterjee, C., & Gupta, B. (2012). Isolation and characterization of heavy metal tolerant Gram-positive bacteria with bioremedial properties from municipal waste rich soil of Kestopur canal (Kolkata), West Bengal, India. *Biologia*, *67*(5), 827–836. https://doi.org/10.2478/s11756-012-0099-5

Gurevich, A., Saveliev, V., Vyahhi, N., & Tesler, G. (2013). QUAST: Quality assessment tool for genome assemblies. *Bioinformatics*, *29*(8), 1072–1075. https://doi.org/10.1093/bioinformatics/btt086

Hall, J. P. J., Harrison, E., Pärnänen, K., Virta, M., & Brockhurst, M. A. (2020). The Impact of Mercury

Selection and Conjugative Genetic Elements on Community Structure and Resistance Gene Transfer. *Frontiers in Microbiology*, *11*(August), 1–14. https://doi.org/10.3389/fmicb.2020.01846

Hallenbeck, W. H., Health, P., Box, P. O., & Illinois, C. (1984). *H u m a n health effects of exposure to cadmium*. *50*(1978), 136–142.

Hiller, E., Lachká, L., Jurkovič, Ľ., Ďurža, O., Fajčíková, K., & Vozár, J. (2016). Occurrence and distribution of selected potentially toxic elements in soils of playing sites: a case study from Bratislava, the capital of Slovakia. *Environmental Earth Sciences*, *75*(20). https://doi.org/10.1007/s12665-016-6210-4

Hiller, E., Mihaljevič, M., Filová, L., Lachká, L., Jurkovič, Ľ., Kulikova, T., Fajčíková, K., Šimurková, M., & Tatarková, V. (2017). Occurrence of selected trace metals and their oral bioaccessibility in urban soils of kindergartens and parks in Bratislava (Slovak Republic) as evaluated by simple in vitro digestion procedure. *Ecotoxicology and Environmental Safety*, *144*(December 2016), 611–621. https://doi.org/10.1016/j.ecoenv.2017.06.040

Hong, K. W., Thinagaran, D., Gan, H. M., Yin, W. F., & Chan, K. G. (2012). Whole-genome sequence of cupriavidus sp. Strain BIS7, A heavy-metal-resistant bacterium. *Journal of Bacteriology*, *194*(22), 6324. https://doi.org/10.1128/JB.01608-12

Hong, Y. S., Kim, Y. M., & Lee, K. E. (2012). Methylmercury exposure and health effects. *Journal of Preventive Medicine and Public Health*, *45*(6), 353–363. https://doi.org/10.3961/jpmph.2012.45.6.353

Hong, Y. S., Song, K. H., & Chung, J. Y. (2014). Health effects of chronic arsenic exposure. *Journal of Preventive Medicine and Public Health*, *47*(5), 245–252. https://doi.org/10.3961/jpmph.14.035

Horvart, M., Kotnik, J., & Estellano, V. (2019). Technical information report on Hg monitoring in soil. *UN Environment Programme (UNEP)*, *September*.

Hu, N., & Zhao, B. (2006). *Key genes involved in heavy-metal resistance in Pseudomonas*. 1–6. https://doi.org/10.1111/j.1574-6968.2006.00505.x

Huang, C. C., Liang, C. M., Yang, T. I., Chen, J. L., & Wang, W. K. (2021). Shift of bacterial communities in heavy metal-contaminated agricultural land during a remediation process. *PLoS ONE*, *16*(7 July), 1–17. https://doi.org/10.1371/journal.pone.0255137

HUGD. (2009). *Government Decree No 6/2009. Joint Government Decree on the environmental standards for Earth materials, B pollution threshold. <http://www.complex.hu/jr/gen/hjegy_doc.cgi?docid=A0900006.KVV>*.

Hughes, J. B., Hellmann, J. J., Ricketts, T. H., Bohannan, B. J. M., Sinclair, L., Osman, O. A., Bertilsson, S., Eiler, A., Sala, V., De Faveri, E., Li, C., Lim, K. M. K., Chng, K. R., Nagarajan, N., Nishida, S., Ono, Y., Sekimizu, K., Hanning, I., Diaz-Sanchez, S., … Michaelakis, A. (2016). Counting the Uncountable : Statistical Approaches to Estimating Microbial Diversity MINIREVIEW Counting the Uncountable : Statistical Approaches to Estimating Microbial Diversity. *Applied and Environmental Microbiology*, *10*(1), 4399–4406. https://doi.org/10.1128/AEM.67.10.4399

Huseen, H. M., & Mohammed, A. J. (2019). Heavy Metals Causing Toxicity in Fishes. *Journal of Physics: Conference Series*, *1294*(6). https://doi.org/10.1088/1742-6596/1294/6/062028

Hynninen, A., Touzé, T., Pitkänen, L., Mengin-Lecreulx, D., & Virta, M. (2009). An efflux transporter PbrA and a phosphatase PbrB cooperate in a lead-resistance mechanism in bacteria. *Molecular Microbiology*, *74*(2), 384–394. https://doi.org/10.1111/j.1365-2958.2009.06868.x

Ibanez, J. G., Hernandez-Esparza, M., Doria-Serrano, C., Fregoso-Infante, A., & Singh, M. M. (2007). Effects of Pollutants on the Chemistry of the Atmosphere, Hydrosphere, and Lithosphere. *Environmental Chemistry*, 167–197. https://doi.org/10.1007/978-0-387-31435-8_8

Ilacqua, V., Freeman, N. C. J., Fagliano, J., & Lioy, P. J. (2003). The historical record of air pollution as defined by attic dust. *Atmospheric Environment*, *37*(17), 2379–2389. https://doi.org/10.1016/S1352-2310(03)00126-2

Imperato, M., Adamo, P., Naimo, D., Arienzo, M., Stanzione, D., & Violante, P. (2003). Spatial distribution of heavy metals in urban soils of Naples city (Italy). *Environmental Pollution*, *124*(2), 247–256. https://doi.org/10.1016/S0269-7491(02)00478-5

Jain, C., Rodriguez-R, L. M., Phillippy, A. M., Konstantinidis, K. T., & Aluru, S. (2018). High throughput ANI analysis of 90K prokaryotic genomes reveals clear species boundaries. *Nature Communications*, *9*(1), 1–8. https://doi.org/10.1038/s41467-018-07641-9

Jaishankar, M., Tseten, T., Anbalagan, N., Mathew, B. B., & Beeregowda, K. N. (2014). Toxicity, mechanism and health effects of some heavy metals. *Interdisciplinary Toxicology*, *7*(2), 60–72. https://doi.org/10.2478/intox-2014-0009

Janssen, P. H. (2006). Identifying the dominant soil bacterial taxa in libraries of 16S rRNA and 16S rRNA genes. *Applied and Environmental Microbiology*, *72*(3), 1719–1728. https://doi.org/10.1128/AEM.72.3.1719-1728.2006

Janssen, P. J., van Houdt, R., Moors, H., Monsieurs, P., Morin, N., Michaux, A., Benotmane, M. A., Leys, N., Vallaeys, T., Lapidus, A., Monchy, S., Médigue, C., Taghavi, S., McCorkle, S., Dunn,

J., van der Lelie, D., & Mergeay, M. (2010). The complete genome sequence of Cupriavidus metallidurans strain CH34, a master survivalist in harsh and anthropogenic environments. *PLoS ONE*, *5*(5). https://doi.org/10.1371/journal.pone.0010433

Jarosławiecka, A., & Piotrowska-Seget, Z. (2014). Lead resistance in micro-organisms. *Microbiology (United Kingdom)*, *160*(PART 1), 12–25. https://doi.org/10.1099/mic.0.070284-0

Jones, R., Robeson, M., Lauber, C., Hamady, M., Knight, R., & Fierer, N. (2008). A comprehensive survey of soil acidobacterial diversity using pyrosequencing and clone library analyses. *Bone*, *23*(1), 1–7. https://doi.org/10.1038/ismej.2008.127.A

Kaiser, H. F. (1974). (1974). An index of factorial simplicity. *Psychometrika*, *39*, 31–36.

Kamunda, C., Mathuthu, M., & Madhuku, M. (2016). Health risk assessment of heavy metals in soils from witwatersrand gold mining basin, South Africa. *International Journal of Environmental Research and Public Health*, *13*(7). https://doi.org/10.3390/ijerph13070663

Kandeler, F., Kampichler, C., & Horak, O. (1996). Influence of heavy metals on the functional diversity of soil microbial communities. *Biology and Fertility of Soils*, *23*(3), 299–306. https://doi.org/10.1007/BF00335958

Keegan, T. J., Farago, M. E., Thornton, I., Hong, B., Colvile, R. N., Pesch, B., Jakubis, P., & Nieuwenhuijsen, M. J. (2006). Dispersion of As and selected heavy metals around a coal-burning power station in central Slovakia. *Science of the Total Environment*, *358*(1–3), 61–71. https://doi.org/10.1016/j.scitotenv.2005.03.020

Kelepertzis, E., Komárek, M., Argyraki, A., & Šillerová, H. (2016). Metal(loid) distribution and Pb isotopic signatures in the urban environment of Athens, Greece. *Environmental Pollution*, *213*, 420–431. https://doi.org/10.1016/j.envpol.2016.02.049

Ketris, M. P., & Yudovich, Y. E. (2009). Estimations of Clarkes for Carbonaceous biolithes: World averages for trace element contents in black shales and coals. *International Journal of Coal Geology*, *78*(2), 135–148. https://doi.org/10.1016/j.coal.2009.01.002

Khademi, H., Gabarrón, M., Abbaspour, A., Martínez-Martínez, S., Faz, A., & Acosta, J. A. (2019). Environmental impact assessment of industrial activities on heavy metals distribution in street dust and soil. In *Chemosphere* (Vol. 217). Elsevier Ltd. https://doi.org/10.1016/j.chemosphere.2018.11.045

Kierczak, J., Potysz, A., Pietranik, A., Tyszka, R., Modelska, M., Néel, C., Ettler, V., & Mihaljevič, M. (2013). Environmental impact of the historical Cu smelting in the Rudawy Janowickie Mountains

(south-western Poland). *Journal of Geochemical Exploration*, *124*, 183–194. https://doi.org/10.1016/j.gexplo.2012.09.008

Kim, R. Y., Yoon, J. K., Kim, T. S., Yang, J. E., Owens, G., & Kim, K. R. (2015). Bioavailability of heavy metals in soils: definitions and practical implementation—a critical review. *Environmental Geochemistry and Health*, *37*(6), 1041–1061. https://doi.org/10.1007/s10653-015-9695-y

Komárek, M., Ettler, V., Chrastný, V., & Mihaljevič, M. (2008). Lead isotopes in environmental sciences: A review. *Environment International*, *34*(4), 562–577. https://doi.org/10.1016/j.envint.2007.10.005

Konert, M., & Vandenberghe, J. (1997). Comparison of laser grain size analysis with pipette and sieve analysis: A solution for the underestimation of the clay fraction. *Sedimentology*, *44*(3), 523–535. https://doi.org/10.1046/j.1365-3091.1997.d01-38.x

Kozich, J. J., Westcott, S. L., Baxter, N. T., Highlander, S. K., & Schloss, P. D. (2013). Development of a dual-index sequencing strategy and curation pipeline for analyzing amplicon sequence data on the miseq illumina sequencing platform. *Applied and Environmental Microbiology*, *79*(17), 5112–5120. https://doi.org/10.1128/AEM.01043-13

Laidlaw, M. A. S., & Taylor, M. P. (2011). Potential for childhood lead poisoning in the inner cities of Australia due to exposure to lead in soil dust. *Environmental Pollution*, *159*(1), 1–9. https://doi.org/10.1016/j.envpol.2010.08.020

Lee, I. S., Kim, O. K., Chang, Y. Y., Bae, B., Kim, H. H., & Baek, K. H. (2002). Heavy metal concentrations and enzyme activities in soil from a contaminated Korean shooting range. *Journal of Bioscience and Bioengineering*, *94*(5), 406–411. https://doi.org/10.1016/S1389-1723(02)80217-1

Lee, P. K., Choi, B. Y., & Kang, M. J. (2015). Assessment of mobility and bio-availability of heavy metals in dry depositions of Asian dust and implications for environmental risk. *Chemosphere*, *119*, 1411–1421. https://doi.org/10.1016/j.chemosphere.2014.10.028

Leiva-Presa, À., Capdevila, M., & Gonàles-Duarte, P. (2004). Mercury(II) binding to metallothioneins: Variables governing the formation and structural features of the mammalian Hg-MT species. In *European Journal of Biochemistry* (Vol. 271, Issues 23–24, pp. 4872–4880). Eur. J. Biochem. https://doi.org/10.1111/j.1432-1033.2004.04456.x

Li, J., Wen, Y., & Yang, X. (2021). Understanding the responses of soil bacterial communities to long-term fertilization regimes using DNA and RNA sequencing. *Agronomy*, *11*(12). https://doi.org/10.3390/agronomy11122425

Li, X., Meng, D., Li, J., Yin, H., Liu, H., Liu, X., Cheng, C., Xiao, Y., Liu, Z., & Yan, M. (2017). Response of soil microbial communities and microbial interactions to long-term heavy metal contamination. *Environmental Pollution*, *231*, 908–917. https://doi.org/10.1016/j.envpol.2017.08.057

Li, X., Wu, T., Bao, H., Liu, X., Xu, C., Zhao, Y., Liu, D., & Yu, H. (2017). Potential toxic trace element (PTE) contamination in Baoji urban soil (NW China): spatial distribution, mobility behavior, and health risk. *Environmental Science and Pollution Research*, *24*(24), 19749–19766. https://doi.org/10.1007/s11356-017-9526-z

Li, X., Zhang, L., & Wang, G. (2014). Genomic evidence reveals the extreme diversity and wide distribution of the arsenic-related genes in Burkholderiales. *PLoS ONE*, *9*(3), 1–11. https://doi.org/10.1371/journal.pone.0092236

Liang, Y., Xiao, X., Nuccio, E. E., Yuan, M., Zhang, N., Xue, K., Cohan, F. M., Zhou, J., & Sun, B. (2020). Differentiation strategies of soil rare and abundant microbial taxa in response to changing climatic regimes. *Environmental Microbiology*, *22*(4), 1327–1340. https://doi.org/10.1111/1462-2920.14945

Liao, X., Zhang, C., Sun, G., Li, Z., Shang, L., Fu, Y., He, Y., & Yang, Y. (2018). Assessment of metalloid and metal contamination in soils from hainan, china. *International Journal of Environmental Research and Public Health*, *15*(3). https://doi.org/10.3390/ijerph15030454

Lin, H., Ascher, D. B., Myung, Y., Lamborg, C. H., Hallam, S. J., Gionfriddo, C. M., Holt, K. E., & Moreau, J. W. (2021). Mercury methylation by metabolically versatile and cosmopolitan marine bacteria. *ISME Journal*, *15*(6), 1810–1825. https://doi.org/10.1038/s41396-020-00889-4

Liu, C., Lu, L., Huang, T., Huang, Y., Ding, L., & Zhao, W. (2016). The distribution and health risk assessment of metals in soils in the vicinity of industrial sites in Dongguan, China. *International Journal of Environmental Research and Public Health*, *13*(8). https://doi.org/10.3390/ijerph13080832

Liu, Y., Gao, T., Wang, X., Fu, J., Zuo, M., Yang, Y., Yin, Z., Wang, Z., Tai, X., & Chang, G. (2022). Effects of heavy metals on bacterial community surrounding Bijiashan mining area located in northwest China. *Open Life Sciences*, *17*(1), 40–54. https://doi.org/10.1515/biol-2022-0008

Ljung, K., Selinus, O., & Otabbong, E. (2006). Metals in soils of children's urban environments in the small northern European city of Uppsala. *Science of the Total Environment*, *366*(2–3), 749–759. https://doi.org/10.1016/j.scitotenv.2005.09.073

Löfgren, Å., & Hammar, H. (2000). The phase-out of leaded gasoline in the EU: A successful failure?

Transportation Research Part D: Transport and Environment, *5*(6), 419–431. https://doi.org/10.1016/S1361-9209(00)00009-2

Lottermoser, B. G. (2002). Mobilization of heavy metals from historical smelting slag dumps, north Queensland, Australia. *Mineralogical Magazine*, *66*(4), 475–490. https://doi.org/10.1180/0026461026640043

Löv, Å., Cornelis, G., Larsbo, M., Persson, I., Sjöstedt, C., Gustafsson, J. P., Boye, K., & Kleja, D. B. (2018). Particle- and colloid-facilitated Pb transport in four historically contaminated soils - Speciation and effect of irrigation intensity. *Applied Geochemistry*, *96*(March), 327–338. https://doi.org/10.1016/j.apgeochem.2018.07.012

Lu, L., Liu, G., Wang, J., & Wu, Y. (2017). Bioavailability and mobility of heavy metals in soil in vicinity of a coal mine from Huaibei, China. *Human and Ecological Risk Assessment*, *23*(5), 1164–1177. https://doi.org/10.1080/10807039.2017.1308816

Luo, X. S., Xue, Y., Wang, Y. L., Cang, L., Xu, B., & Ding, J. (2015). Source identification and apportionment of heavy metals in urban soil profiles. *Chemosphere*, *127*, 152–157. https://doi.org/10.1016/j.chemosphere.2015.01.048

Luo, Z., Ma, J., Chen, F., Li, X., & Zhang, S. (2018). Effects of Pb smelting on the soil bacterial community near a secondary lead plant. *International Journal of Environmental Research and Public Health*, *15*(5). https://doi.org/10.3390/ijerph15051030

Luo, Z., Ma, J., Chen, F., Li, X., Zhang, S., Luo, Z., Ma, J., Chen, F., Li, X., Zhang, S., Smelting, P., Luo, Z., & Ma, J. (2019). *Effects of Pb Smelting on the Soil Bacterial Community near a Secondary Lead Plant To cite this version : HAL Id : hal-02179316 Effects of Pb Smelting on the Soil Bacterial Community near a Secondary Lead Plant*. 0–16. https://doi.org/10.3390/ijerph15051030

Lyon, D. Y., & Vogel, T. M. (2011). Bioaugmentation as a Strategy for the Treatment of Persistent Pollutants. In *Comprehensive Biotechnology, Second Edition* (Second Edi, Vol. 6, Issue May 2009). Elsevier B.V. https://doi.org/10.1016/B978-0-08-088504-9.00366-4

Mahbub, K. R., Subashchandrabose, S. R., Krishnan, K., Naidu, R., & Megharaj, M. (2017). Mercury alters the bacterial community structure and diversity in soil even at concentrations lower than the guideline values. *Applied Microbiology and Biotechnology*, *101*(5), 2163–2175. https://doi.org/10.1007/s00253-016-7965-y

Maity, J. P., Chen, G. S., Huang, Y. H., Sun, A. C., & Chen, C. Y. (2019). Ecofriendly Heavy Metal Stabilization: Microbial Induced Mineral Precipitation (MIMP) and Biomineralization for Heavy

Metals within the Contaminated Soil by Indigenous Bacteria. *Geomicrobiology Journal*, *36*(7), 612–623. https://doi.org/10.1080/01490451.2019.1597216

Malik, A., & Jaiswal, R. (2000). Metal resistance in Pseudomonas strains isolated from soil treated with industrial wastewater. *World Journal of Microbiology and Biotechnology*, *16*(2), 177–182. https://doi.org/10.1023/A:1008905902282

Matta, G., & Gjyli, L. (2016). Mercury, lead and arsenic: Impact on environment and human health. *Journal of Chemical and Pharmaceutical Sciences*, *9*(2), 718–725.

McIlwaine, R., Doherty, R., Cox, S. F., & Cave, M. (2017). The relationship between historical development and potentially toxic element concentrations in urban soils. *Environmental Pollution*, *220*, 1036–1049. https://doi.org/10.1016/j.envpol.2016.11.040

Meier-Kolthoff, J. P., & Göker, M. (2019). TYGS is an automated high-throughput platform for state-of-the-art genome-based taxonomy. *Nature Communications*, *10*(1). https://doi.org/10.1038/s41467-019-10210-3

Mhete, M., Eze, P. N., Rahube, T. O., & Akinyemi, F. O. (2020). Soil properties influence bacterial abundance and diversity under different land-use regimes in semi-arid environments. *Scientific African*, *7*. https://doi.org/10.1016/j.sciaf.2019.e00246

Mihailović, A., Budinski-Petković, L., Popov, S., Ninkov, J., Vasin, J., Ralević, N. M., & Vučinić Vasić, M. (2015). Spatial distribution of metals in urban soil of Novi Sad, Serbia: GIS based approach. *Journal of Geochemical Exploration*, *150*, 104–114. https://doi.org/10.1016/j.gexplo.2014.12.017

Mihdhir, A. A., & Assaeedi, A. S. (2016). Detection, Identification and Characterization of Some Heavy Metals Tolerant Bacteria. *Journal of Microbial & Biochemical Technology*, *8*(3), 226–230. https://doi.org/10.4172/1948-5948.1000290

Minamata UN convention. (2017). *https://www.mercuryconvention.org/sites/default/files/2021-06/Minamata-Convention-booklet-Sep2019-EN.pdf*.

Mohammad Ali, M., Hossain, D., Al-Imran, Suzan Khan, M., Begum, M., & Hasan Osman, M. (2021). Environmental Pollution with Heavy Metals: A Public Health Concern. *Heavy Metals - Their Environmental Impacts and Mitigation*, 2021. https://doi.org/10.5772/intechopen.96805

Molnár, S., Barna, G., Draskovits, E., Földényi, R., Hernádi, H., Bakacsi, Z., & Makó, A. (2019). Analysis of correlations between BET-specific surface area, humus materials and other soil properties on typical Hungarian soil types. *Agrokemia Es Talajtan*, *68*(1), 57–77.

https://doi.org/10.1556/0088.2019.00039

Monchy, S., Vallaeys, T., Bossus, A., & Mergeay, M. (2006). Metal transport ATPase genes from Cupriavidus metallidurans CH34: A transcriptomic approach. *International Journal of Environmental Analytical Chemistry*, *86*(9), 677–692. https://doi.org/10.1080/03067310600583824

Monsieurs, P., Moors, H., Van Houdt, R., Janssen, P. J., Janssen, A., Coninx, I., Mergeay, M., & Leys, N. (2011). Heavy metal resistance in Cupriavidus metallidurans CH34 is governed by an intricate transcriptional network. *BioMetals*, *24*(6), 1133–1151. https://doi.org/10.1007/s10534-011-9473-y

Moriuchi, R., Dohra, H., Kanesaki, Y., & Ogawa, N. (2019). Complete genome sequence of 3-chlorobenzoate-degrading bacterium Cupriavidus necator NH9 and reclassification of the strains of the genera cupriavidus and ralstonia based on phylogenetic and whole-genome sequence analyses. *Frontiers in Microbiology*, *10*(FEB), 1–21. https://doi.org/10.3389/fmicb.2019.00133

Mugwar, A. J. (2015). *Bioprecipitation of Heavy Metals and Radionuclides with Calcium Carbonate in Aqueous Solutions and Particulate Media*. *December*, 242.

Naguib, M. M., El-Gendy, A. O., & Khairalla, A. S. (2018). Microbial Diversity of Mer Operon Genes and Their Potential Rules in Mercury Bioremediation and Resistance. *The Open Biotechnology Journal*, *12*(1), 56–77. https://doi.org/10.2174/1874070701812010056

Naik, M. M., & Dubey, S. K. (2013). Lead resistant bacteria: Lead resistance mechanisms, their applications in lead bioremediation and biomonitoring. In *Ecotoxicology and Environmental Safety* (Vol. 98, pp. 1–7). Elsevier. https://doi.org/10.1016/j.ecoenv.2013.09.039

Nakatsu, C. H., Carmosini, N., Baldwin, B., Beasley, F., Kourtev, P., & Konopka, A. (2005). Soil microbial community responses to additions of organic carbon substrates and heavy metals (Pb and Cr). *Applied and Environmental Microbiology*, *71*(12), 7679–7689. https://doi.org/10.1128/AEM.71.12.7679-7689.2005

Nascimento, A. M. A., & Chartone-Souza, E. (2003). Operon mer: Bacterial resistance to mercury and potential for bioremediation of contaminated environments. *Genetics and Molecular Research*, *2*(1), 92–101.

Naujokas, M. F., Anderson, B., Ahsan, H., Vasken Aposhian, H., Graziano, J. H., Thompson, C., & Suk, W. A. (2013). The broad scope of health effects from chronic arsenic exposure: Update on a worldwide public health problem. *Environmental Health Perspectives*, *121*(3), 295–302. https://doi.org/10.1289/ehp.1205875

Neethu, C. S., Rahiman, K. M. M., Saramma, A. V., & Hatha, A. A. M. (2015). Heavy-metal resistance in gram-negative bacteria isolated from kongsfjord, Arctic. *Canadian Journal of Microbiology*, *61*(6), 429–435. https://doi.org/10.1139/cjm-2014-0803

Neuhäuser, M. (2011). *Wilcoxon–Mann–Whitney Test BT - International Encyclopedia of Statistical Science* (M. Lovric (Ed.); pp. 1656–1658). Springer Berlin Heidelberg. https://doi.org/10.1007/978-3-642-04898-2_615

Nicholls, D. G., & Ferguson, S. J. (2013). Transporters: Structure and mechanism. In *Bioenergetics*. https://doi.org/10.1016/b978-0-12-388425-1.00008-7

Nies, D. H. (1999). Microbial heavy-metal resistance. *Applied Microbiology and Biotechnology*, *51*(6), 730–750. https://doi.org/10.1007/s002530051457

Niu, X., Zhou, J., Wang, X., Su, X., Du, S., Zhu, Y., Yang, J., & Huang, D. (2020). Indigenous Bacteria Have High Potential for Promoting Salix integra Thunb. Remediation of Lead-Contaminated Soil by Adjusting Soil Properties. *Frontiers in Microbiology*, *11*(May), 1–13. https://doi.org/10.3389/fmicb.2020.00924

Noll, M. R. (2003). Trace Elements in Terrestrial Environments. In *Journal of Environmental Quality* (Vol. 32, Issue 1). https://doi.org/10.2134/jeq2002.3740

Nriagu, J. O. (1990). *THE RISE AND FALL OF LEADED GASOLINE JEROME*. *92*, 13–28.

Okoro, H. K., & Fatoki, O. S. (2012). A Review of Sequential Extraction Procedures for Heavy Metals Speciation in Soil and Sediments. *Journal of Environmental & Analytical Toxicology*, *01*(S1). https://doi.org/10.4172/scientificreports.181

Oksanen, J., Blanchet, F. G., Friendly, M., Kindt, R., Legendre, P., Mcglinn, D., Minchin, P. R., O'hara, R. B., Simpson, G. L., Solymos, P., Henry, M., Stevens, H., Szoecs, E., & Maintainer, H. W. (2019). Package "vegan" Title Community Ecology Package. *Community Ecology Package*, *2*(9), 1–297.

Omokhagbor Adams, G., Tawari Fufeyin, P., Eruke Okoro, S., & Ehinomen, I. (2020). Bioremediation, Biostimulation and Bioaugmention: A Review. *International Journal of Environmental Bioremediation & Biodegradation*, *3*(1), 28–39. https://doi.org/10.12691/ijebb-3-1-5

Ondov, B. D., Treangen, T. J., Melsted, P., Mallonee, A. B., Bergman, N. H., Koren, S., & Phillippy, A. M. (2016). Mash: Fast genome and metagenome distance estimation using MinHash. *Genome Biology*, *17*(1), 1–14. https://doi.org/10.1186/s13059-016-0997-x

OSHA. (1991). *US Occupational Safety and Health Administration standard 1910.1025 App B.*

(Updated in 1991) https://www.osha.gov/laws-regs/regulations/standardnumber/1910/1910.1025AppB.

Pacyna, E. G., Pacyna, J. M., Fudala, J., Strzelecka-Jastrzab, E., Hlawiczka, S., Panasiuk, D., Nitter, S., Pregger, T., Pfeiffer, H., & Friedrich, R. (2007). Current and future emissions of selected heavy metals to the atmosphere from anthropogenic sources in Europe. *Atmospheric Environment*, *41*(38), 8557–8566. https://doi.org/10.1016/j.atmosenv.2007.07.040

Páez-Espino, A. D., Durante-Rodríguez, G., & de Lorenzo, V. (2015). Functional coexistence of twin arsenic resistance systems in Pseudomonas putida KT2440. *Environmental Microbiology*, *17*(1), 229–238. https://doi.org/10.1111/1462-2920.12464

Palansooriya, K. N., Shaheen, S. M., Chen, S. S., Tsang, D. C. W., Hashimoto, Y., Hou, D., Bolan, N. S., Rinklebe, J., & Ok, Y. S. (2020). Soil amendments for immobilization of potentially toxic elements in contaminated soils: A critical review. *Environment International*, *134*(November 2019), 105046. https://doi.org/10.1016/j.envint.2019.105046

Pandey, G. (2014). Heavy metals causing toxicity in humans, animals and environment. *Journal of Chemical and Pharmaceutical Science*, *3*(December), 172–174.

Park, J. D., & Zheng, W. (2012). Human exposure and health effects of inorganic and elemental mercury. *Journal of Preventive Medicine and Public Health*, *45*(6), 344–352. https://doi.org/10.3961/jpmph.2012.45.6.344

Parzentny, H. R., & Róg, L. (2021). Distribution and mode of occurrence of Co, Ni, Cu, Zn, As, Ag, Cd, Sb, Pb in the feed coal, fly ash, slag, in the topsoil and in the roots of trees and undergrowth downwind of three power stations in poland. *Minerals*, *11*(2), 1–33. https://doi.org/10.3390/min11020133

Patrício, A. R., Herbst, L. H., Duarte, A., Vélez-Zuazo, X., Loureiro, N. S., Pereira, N., Tavares, L., & Toranzos, G. A. (2012). Global phylogeography and evolution of chelonid fibropapilloma-associated herpesvirus. *Journal of General Virology*, *93*(5), 1035–1045. https://doi.org/10.1099/vir.0.038950-0

Peter S. Hooda. (2010). *Trace elements in Soils*. Wiley, p 618.

Petrus, A. K., Rutner, C., Liu, S., Wang, Y., & Wiatrowski, H. A. (2015). Mercury reduction and methyl mercury degradation by the soil bacterium Xanthobacter autotrophicus Py2. *Applied and Environmental Microbiology*, *81*(22), 7833–7838. https://doi.org/10.1128/AEM.01982-15

Petruzzelli, G., Pedron, F., & Rosellini, I. (2020). Bioavailability and bioaccessibility in soil: A short

review and a case study. *AIMS Environmental Science*, *7*(2), 208–224. https://doi.org/10.3934/environsci.2020013

Pirrone, N., Cinnirella, S., Feng, X., Finkelman, R. B., Friedli, H. R., Leaner, J., Mason, R., Mukherjee, A. B., Stracher, G. B., Streets, D. G., & Telmer, K. (2010). Global mercury emissions to the atmosphere from anthropogenic and natural sources. *Atmospheric Chemistry and Physics*, *10*(13), 5951–5964. https://doi.org/10.5194/acp-10-5951-2010

Poehlein, A., Kusian, B., Friedrich, B., Daniel, R., & Bowien, B. (2011). Complete genome sequence of the type strain Cupriavidus necator N-1. *Journal of Bacteriology*, *193*(18), 5017. https://doi.org/10.1128/JB.05660-11

Pudasainee, D., Kurian, V., & Gupta, R. (2020). Coal: Past, present, and future sustainable use. In *Future Energy: Improved, Sustainable and Clean Options for Our Planet*. Elsevier Ltd. https://doi.org/10.1016/B978-0-08-102886-5.00002-5

R Core Team. (2020). *R Core Team. R: A Language and Environment for Statistical Computing; R Foundation for Statistical Computing: Vienna, Austria,*.

Radomirović, M., Ćirović, Ž., Maksin, D., Bakić, T., Lukić, J., Stanković, S., & Onjia, A. (2020). Ecological Risk Assessment of Heavy Metals in the Soil at a Former Painting Industry Facility. *Frontiers in Environmental Science*, *8*(September), 1–15. https://doi.org/10.3389/fenvs.2020.560415

RAIS. (2017). *Risk Exposure Models for Chemicals User's Guide. Risk Assess (2017) Inf. Syst [WWW Document] https://rais.ornl.gov/tools/rais_chemical_risk_guide.html, Accessed 1st Jan 2017*.

Raj, D., Kumar, A., & Maiti, S. K. (2019). Evaluation of toxic metal(loid)s concentration in soils around an open-cast coal mine (Eastern India). *Environmental Earth Sciences*, *78*(22). https://doi.org/10.1007/s12665-019-8657-6

Ramsey, K. (2015). *13 - Arsenic and Respiratory Disease* (S. J. S. B. T.-H. of A. T. Flora (Ed.); pp. 335–347). Academic Press. https://doi.org/https://doi.org/10.1016/B978-0-12-418688-0.00013-7

Reimann, C., Demetriades, A., Eggen, O. A., & Filzmoser, P. (2009). *EuroGeoSurveys Geochemistry Expert Group The EuroGeoSurveys Geochemical Map- ping of Agricultural and Grazing Land Soils Project (GEMAS) e Evaluation of Quality Control Results of Aqua Regia Extraction Analysis 049, 92 Norges Geologiske Undersøkelse Repor*.

Rene, E.R., Sahinkaya, E., Lewis, A., Lens, P. (2017). *Environmental Chemistry for a Sustainable World Sustainable Heavy Metal Remediation Volume 1: Principles and Processes* (Vol. 1).

http://www.springer.com/series/8380

Ron, E. Z., Minz, D., Finkelstein, N. P., & Rosenberg, E. (1992). Interactions of bacteria with cadmium. *Biodegradation*, *3*(2–3), 161–170. https://doi.org/10.1007/BF00129081

Ronquist, F., Teslenko, M., Van Der Mark, P., Ayres, D. L., Darling, A., Höhna, S., Larget, B., Liu, L., Suchard, M. A., & Huelsenbeck, J. P. (2012). Mrbayes 3.2: Efficient bayesian phylogenetic inference and model choice across a large model space. *Systematic Biology*, *61*(3), 539–542. https://doi.org/10.1093/sysbio/sys029

Ruby, M. V., Schoof, R., Brattin, W., Goldade, M., Post, G., Harnois, M., MOsby, E., Casteel, S. W., Berti, W., Carpenter, M., Edwards, D., Cragin, D., & Chappell, W. (1999). Advances in evaluating the oral bioavailability of inorganics in soil for use in human health risk assessment. *Environmental Science and Technology*, *33*(21), 3697–3705. https://doi.org/10.1021/es990479z

Šajn, R. (2002). Influence of mining and metallurgy on chemical composition of soil and attic dust in Meža valley, Slovenia. *Geologija*, *45*(2), 547–552. https://doi.org/10.5474/geologija.2002.063

Salma, I., Maenhaut, W., Dubtsov, S., Zemplén-Papp, É., & Záray, G. (2000). Impact of phase out of leaded gasoline on the air quality in Budapest. *Microchemical Journal*, *67*(1–3), 127–133. https://doi.org/10.1016/S0026-265X(00)00108-9

Salminen, R., Batista, M. ., Bidovec, M., Demetriades, A., De Vivo, B., De Vos, W., Duris, M., Gilucis, A., Gregorauskiene, V., Halamic, J., Heitzmann, P., Lima, A., Jordan, G., Klaver, G., Klein, P., Lis, J., Locutura, J., Marsina, K., Mazreku, A., O'Connor, P. ., … Tarvainen, T. (2005). FOREGS Geochemical Atlas of Europe , Part 1 : Background Information , Geochemical Atlas of Europe Part 2 Interpretation of Geochemical Maps , Additional Tables ,. *EuroGeoSurveys*, *July 2014*, 525.

Sandaa, R. A., Torsvik, V., & Enger. (2001). Influence of long-term heavy-metal contamination on microbial communities in soil. *Soil Biology and Biochemistry*, *33*(3), 287–295. https://doi.org/10.1016/S0038-0717(00)00139-5

Sankarammal, M., Thatheyus, A., & Ramya, D. (2014). Bioremoval Of Cadmium Using Pseudomonas fluorescens. *Open Journal of Water Pollution and Treatment*, *2014*(2), 92–100. https://doi.org/10.15764/wpt.2014.02010

Schoeters, G., Den Hond, E., Zuurbier, M., Naginiene, R., Van Den Hazel, P., Stilianakis, N., Ronchetti, R., & Koppe, J. G. (2006). Cadmium and children: Exposure and health effects. *Acta Paediatrica, International Journal of Paediatrics*, *95*(SUPPL. 453), 50–54. https://doi.org/10.1080/08035320600886232

Schöler, A., Jacquiod, S., Vestergaard, G., Schulz, S., & Schloter, M. (2017). Analysis of soil microbial communities based on amplicon sequencing of marker genes. *Biology and Fertility of Soils*, *53*(5), 485–489. https://doi.org/10.1007/s00374-017-1205-1

Seddaiu, G., Porcu, G., Ledda, L., Roggero, P. P., Agnelli, A., & Corti, G. (2013). Soil organic matter content and composition as influenced by soil management in a semi-arid Mediterranean agro-silvo-pastoral system. *Agriculture, Ecosystems and Environment*, *167*, 1–11. https://doi.org/10.1016/j.agee.2013.01.002

Shade, A., Jones, S. E., Gregory Caporaso, J., Handelsman, J., Knight, R., Fierer, N., & Gilbert, J. A. (2014). Conditionally rare taxa disproportionately contribute to temporal changes in microbial diversity. *MBio*, *5*(4). https://doi.org/10.1128/mBio.01371-14

Shahid, M. (2017). *Biogeochemical Behaviour of Heavy Metals in Soil-Plant System*. www.hec.gov.pk

Shannon, C. E. (1948). A mathematical theory of communication. *The Bell System Technical Journal*, *27*(3), 379–423. https://doi.org/10.1002/j.1538-7305.1948.tb01338.x

Shapiro, S. S., & Wilk, M. B. (1965). An Analysis of Variance Test for Normality (Complete Samples). *Biometrika*, *52*(3/4), 591. https://doi.org/10.2307/2333709

Sheik, C. S., Mitchell, T. W., Rizvi, F. Z., Rehman, Y., Faisal, M., Hasnain, S., McInerney, M. J., & Krumholz, L. R. (2012). Exposure of soil microbial communities to chromium and arsenic alters their diversity and structure. *PLoS ONE*, *7*(6). https://doi.org/10.1371/journal.pone.0040059

Shi, K., Wang, Q., & Wang, G. (2020). *Microbial Oxidation of Arsenite : Regulation , Chemotaxis , Phosphate Metabolism and Energy Generation*. *11*(September), 1–10. https://doi.org/10.3389/fmicb.2020.569282

Shotyk, W., & Le Roux, G. (2005). Biogeochemistry and cycling of lead. *Metal Ions in Biological Systems*, *43*, 239–275. https://doi.org/10.1201/9780824751999.ch10

Silver, S., & Phung, L. T. (1996). Bacterial heavy metal resistance: New surprises. *Annual Review of Microbiology*, *50*, 753–789. https://doi.org/10.1146/annurev.micro.50.1.753

Silver, S., & Phung, L. T. (2005). A bacterial view of the periodic table: Genes and proteins for toxic inorganic ions. *Journal of Industrial Microbiology and Biotechnology*, *32*(11–12), 587–605. https://doi.org/10.1007/s10295-005-0019-6

Simpson, E. H. (1949). Measurement of diversity [16]. In *Nature* (Vol. 163, Issue 4148, p. 688). https://doi.org/10.1038/163688a0

Sipos, P., Németh, T., & Kis, V. (2013). Lead isotope composition and host phases in airborne particulate matter from Budapest, Hungary. *Central European Geology*, *56*(1), 39–57. https://doi.org/10.1556/CEuGeol.56.2013.1.4

Smith, D. R., & Flegal, A. R. (1995). Lead in the biosphere: Recent trends. *Ambio*, *24*(1), 21–23.

Sobolev, D., & Begonia, M. F. T. (2008). Effects of heavy metal contamination upon soil microbes: Lead-induced changes in general and denitrifying microbial communities as evidenced by molecular markers. *International Journal of Environmental Research and Public Health*, *5*(5), 450–456. https://doi.org/10.3390/ijerph5050450

Spearman, C. (1904). The Proof and Measurement of Association between Two Things. *The American Journal of Psychology*, *15*(1), 72–101. https://doi.org/10.2307/1412159

Srinivasan, S., Hoffman, N. G., Morgan, M. T., Matsen, F. A., Fiedler, T. L., Hall, R. W., Ross, F. J., McCoy, C. O., Bumgarner, R., Marrazzo, J. M., & Fredricks, D. N. (2012). Bacterial communities in women with bacterial vaginosis: High resolution phylogenetic analyses reveal relationships of microbiota to clinical criteria. *PLoS ONE*, *7*(6). https://doi.org/10.1371/journal.pone.0037818

Srivastava, P., & Kowshik, M. (2013). Mechanisms of metal resistance and homeostasis in Haloarchaea. *Archaea*, *2013*. https://doi.org/10.1155/2013/732864

Stamatakis, A. (2014). RAxML version 8: A tool for phylogenetic analysis and post-analysis of large phylogenies. *Bioinformatics*, *30*(9), 1312–1313. https://doi.org/10.1093/bioinformatics/btu033

Stamatakis, A., Hoover, P., & Rougemont, J. (2008). A rapid bootstrap algorithm for the RAxML web servers. *Systematic Biology*, *57*(5), 758–771. https://doi.org/10.1080/10635150802429642

Statista. (2022). *Yearly cadmium production. https://www.statista.com/statistics/264983/production-of-cadmium/#:~:text=In%202021%2C%20the%20global%20refinery,of%20cadmium%20that%20same%20year*.

Sun, H., Shao, C., Jin, Q., Li, M., Zhang, Z., Liang, H., Lei, H., Qian, J., & Zhang, Y. (2022). Effects of cadmium contamination on bacterial and fungal communities in Panax ginseng-growing soil. *BMC Microbiology*, *22*(1), 1–14. https://doi.org/10.1186/s12866-022-02488-z

Sun, R., & Chen, L. (2016). Assessment of heavy metal pollution in topsoil around Beijing metropolis. *PLoS ONE*, *11*(5), 1–13. https://doi.org/10.1371/journal.pone.0155350

Takáč, P., Szabová, T., Kozáková, L., Benková, M., & Takáč, P. (2009). Heavy metals and their bioavailability from soils in the long-term polluted Central Spiš region of SR. *Plant, Soil and Environment*, *55*(4), 167–172. https://doi.org/10.17221/21/2009-pse

Tamayo-Figueroa, D. P., Castillo, E., & Brandão, P. F. B. (2019). Metal and metalloid immobilization by microbiologically induced carbonates precipitation. *World Journal of Microbiology and Biotechnology*, *35*(4), 1–10. https://doi.org/10.1007/s11274-019-2626-9

Tanizawa, Y., Fujisawa, T., & Nakamura, Y. (2018). DFAST: A flexible prokaryotic genome annotation pipeline for faster genome publication. *Bioinformatics*, *34*(6), 1037–1039. https://doi.org/10.1093/bioinformatics/btx713

Tawfik, D. S., & Viola, R. E. (2012). Arsenate replacing phosphate - alternative life chemistries and ion promiscuity. *National Institute of Health*, *50*(7), 1128–1134. https://doi.org/10.1021/bi200002a.Arsenate

Tchounwou, P. B., Yedjou, C. G., Patlolla, A. K., & Sutton, D. J. (2013). Molecular, clinical and environmental toxicology: v.2: Clinical toxicology. *Choice Reviews Online*, *47*(10), 47-5683-47–5683. https://doi.org/10.5860/choice.47-5683

Teixeira, F. B., de Oliveira, A. C. A., Leão, L. K. R., Fagundes, N. C. F., Fernandes, R. M., Fernandes, L. M. P., da Silva, M. C. F., Amado, L. L., Sagica, F. E. S., de Oliveira, E. H. C., Crespo-Lopez, M. E., Maia, C. S. F., & Lima, R. R. (2018). Exposure to inorganic mercury causes oxidative stress, cell death, and functional deficits in the motor cortex. *Frontiers in Molecular Neuroscience*, *11*(May), 1–11. https://doi.org/10.3389/fnmol.2018.00125

Tepanosyan, G., Maghakyan, N., Sahakyan, L., & Saghatelyan, A. (2017). Heavy metals pollution levels and children health risk assessment of Yerevan kindergartens soils. *Ecotoxicology and Environmental Safety*, *142*(April), 257–265. https://doi.org/10.1016/j.ecoenv.2017.04.013

Tepanosyan, G., Sahakyan, L., Belyaeva, O., Maghakyan, N., & Saghatelyan, A. (2017). Human health risk assessment and riskiest heavy metal origin identification in urban soils of Yerevan, Armenia. *Chemosphere*, *184*, 1230–1240. https://doi.org/10.1016/j.chemosphere.2017.06.108

Ullrich, S. M., Ramsey, M. H., & Helios-Rybicka, E. (1999). Total and exchangeable concentrations of heavy metals in soils near Bytom, an area of Pb/Zn mining and smelting in Upper Silesia, Poland. *Applied Geochemistry*, *14*(2), 187–196. https://doi.org/10.1016/S0883-2927(98)00042-0

US EPA. (1989a). *Risk Assessment Guidance for Superfund (RAGS), Volume I: Human Health Evaluation Manual (HHEM). Part A. Baseline Risk Assessment (1989) EPA/540/1e89/002*.

US EPA. (1989b). *Risk Assessment Guidance for Superfund Volume I Human Health Evaluation Manual (Part A) Interim Final Risk Assessment Guidance for Superfund Human Health Evaluation Manual (Part A) Interim Final (1989)*.

US EPA. (1991). *U.S. Environmental Protection Agency. Human Health Evaluation Manual, Supplemental Guidance: Standard Default Exposure Factors; USEPA:Washington, DC, USA, 1991*.

US EPA. (2011). *U.S. Environmental Protection Agency. 2011. Recommended Use of BW3/4 as the Default Method in Derivation of the Oral Reference Dose. Available online: https://nepis.epa.gov/Exe/ZyPURL.cgi?Dockey=P100W7T2.txt.*

US EPA. (2014). *United States Environmental Protection Agency (US EPA), 2014. Cleaning up the Nation's Hazardous Wastes Sites, http://www.epa.gov/superfund/*.

US EPA. (2016). *US Environmental Protection Agency 2016. Drinking Water Regulations and Contaminants. https://www.epa.gov/sites/default/files/2016-06/documents/npwdr_complete_table.pdf.*

USGS. (2020). *United States Geological Survey 2020. https://pubs.usgs.gov/periodicals/mcs2020/mcs2020-cadmium.pdf*.

Vicentin, R. P., DOS Santos, J. V., Labory, C. R. G., DA Costa, A. M., Moreira, F. M. de S., & Alves, E. (2018). Tolerance to and accumulation of cadmium, copper, and zinc by Cupriavidus necator. *Revista Brasileira de Ciencia Do Solo*, *42*, 1–12. https://doi.org/10.1590/18069657rbcs20170080

von Rozycki, T., & Nies, D. H. (2009). Cupriavidus metallidurans: Evolution of a metal-resistant bacterium. *Antonie van Leeuwenhoek, International Journal of General and Molecular Microbiology*, *96*(2 SPEC. ISS.), 115–139. https://doi.org/10.1007/s10482-008-9284-5

Wang, C., Zhou, X., Guo, D., Zhao, J. hua, Yan, L., Feng, G. zhong, Gao, Q., Yu, H., & Zhao, L. po. (2019). Soil pH is the primary factor driving the distribution and function of microorganisms in farmland soils in northeastern China. *Annals of Microbiology*, *69*(13), 1461–1473. https://doi.org/10.1007/s13213-019-01529-9

Wang, J., Su, J., Li, Z., Liu, B., Cheng, G., Jiang, Y., Li, Y., Zhou, S., & Yuan, W. (2019). Source apportionment of heavy metal and their health risks in soil-dustfall-plant system nearby a typical non-ferrous metal mining area of Tongling, Eastern China. *Environmental Pollution*, *254*, 113089. https://doi.org/10.1016/j.envpol.2019.113089

Wang, W.-X. (2016). Bioaccumulation and Biomonitoring. In *Marine Ecotoxicology*. Elsevier Inc. https://doi.org/10.1016/b978-0-12-803371-5.00004-7

Wang, X., Chen, M., Xiao, J., Hao, L., Crowley, D. E., Zhang, Z., Yu, J., Huang, N., Huo, M., & Wu, J. (2015). Genome sequence analysis of the naphthenic acid degrading and metal resistant

bacterium cupriavidus gilardii CR3. *PLoS ONE*, *10*(8), 1–21. https://doi.org/10.1371/journal.pone.0132881

Wang, X., Ya, T., Zhang, M., Liu, L., Hou, P., & Lu, S. (2019). Cadmium (II) alters the microbial community structure and molecular ecological network in activated sludge system. *Environmental Pollution*, *255*, 113225. https://doi.org/10.1016/j.envpol.2019.113225

Wang, Z., Watanabe, I., Ozaki, H., & Zhang, J. (2018). Enrichment and Bioavailability of Trace Elements in Soil in Vicinity of Railways in Japan. *Archives of Environmental Contamination and Toxicology*, *74*(1), 16–31. https://doi.org/10.1007/s00244-017-0471-0

Wattam, A. R., Davis, J. J., Assaf, R., Boisvert, S., Brettin, T., Bun, C., Conrad, N., Dietrich, E. M., Disz, T., Gabbard, J. L., Gerdes, S., Henry, C. S., Kenyon, R. W., Machi, D., Mao, C., Nordberg, E. K., Olsen, G. J., Murphy-Olson, D. E., Olson, R., … Stevens, R. L. (2017). Improvements to PATRIC, the all-bacterial bioinformatics database and analysis resource center. *Nucleic Acids Research*, *45*(D1), D535–D542. https://doi.org/10.1093/nar/gkw1017

Wei, Z., Wang, D., Zhou, H., & Qi, Z. (2011). Assessment of soil heavy metal pollution with Principal component analysis and Geoaccumulation index. *Procedia Environmental Sciences*, *10*(PART C), 1946–1952. https://doi.org/10.1016/j.proenv.2011.09.305

White, W. M. (2018). Encyclopedia of geochemistry: A Comprehensive Reference Source on the Chemistry of the Earth. In *Springer International Publishing*.

Wickham, H. (2010). ggplot2: Elegant Graphics for Data Analysis - Bookreview. *Journal of Statistical Software*, *35*(July), 1–3. https://doi.org/10.1007/978-0-387-98141-3

Wong, C. S. C., Li, X., & Thornton, I. (2006). Urban environmental geochemistry of trace metals. *Environmental Pollution*, *142*(1), 1–16. https://doi.org/10.1016/j.envpol.2005.09.004

Wu, B., Wu, X., Shi, X., Zhang, X., Qiao, S., Hu, L., Liu, J., Liu, S., Zhang, J., Zhang, H., & Zhu, A. (2021). Lead isotopes in the Central Yellow Sea Mud: Evidence of atmospheric deposition and its implication for regional energy consumption shift. *Environmental Pollution*, *268*, 115702. https://doi.org/10.1016/j.envpol.2020.115702

Wuana, R. A., & Okieimen, F. E. (2011). Heavy Metals in Contaminated Soils: A Review of Sources, Chemistry, Risks and Best Available Strategies for Remediation. *ISRN Ecology*, *2011*, 1–20. https://doi.org/10.5402/2011/402647

Xie, F., Ma, H., Quan, S., Liu, D., Chen, G., Chao, Y., & Qian, S. (2014). Pseudomonas kunmingensis sp. nov., an exopolysaccharide-producing bacterium isolated from a phosphate mine.

International Journal of Systematic and Evolutionary Microbiology, *64*(PART 2), 559–564. https://doi.org/10.1099/ijs.0.055632-0

Xu, M., Huang, Q., Xiong, Z., Liao, H., Lv, Z., Chen, W., Luo, X., & Haoa, X. (2021). Distinct Responses of Rare and Abundant Microbial Taxa to In Situ Chemical Stabilization of Cadmium-Contaminated Soil. *American Society for Miccrobiology*.

Yang, H. C., Fu, H. L., Lin, Y. F., & Rosen, B. P. (2012). Pathways of Arsenic Uptake and Efflux. In *Current Topics in Membranes* (Vol. 69). Elsevier. https://doi.org/10.1016/B978-0-12-394390-3.00012-4

Yang, H. C., & Rosen, B. P. (2016). New mechanisms of bacterial arsenic resistance. *Biomedical Journal*, *39*(1), 5–13. https://doi.org/10.1016/j.bj.2015.08.003

Yang, J., Wang, S., Guo, Z., Deng, Y., Xu, M., Zhang, S., Yin, H., Liang, Y., Liu, H., Miao, B., Meng, D., Liu, X., & Jiang, L. (2020). Spatial distribution of toxic metal(Loid)s and microbial community analysis in soil vertical profile at an abandoned nonferrous metal smelting site. *International Journal of Environmental Research and Public Health*, *17*(19), 1–17. https://doi.org/10.3390/ijerph17197101

Yao, X., Zhang, J., Tian, L., & Guo, J. (2016). The effect of heavy metal contamination on the bacterial community structure at Jiaozhou Bay ,. *Brazilian Journal of Microbiology*, *48*(1), 71–78. https://doi.org/10.1016/j.bjm.2016.09.007

Yavitt, J. B., Pipes, G. T., Olmos, E. C., Zhang, J., & Shapleigh, J. P. (2021). Soil Organic Matter, Soil Structure, and Bacterial Community Structure in a Post-Agricultural Landscape. *Frontiers in Earth Science*, *9*(February), 1–15. https://doi.org/10.3389/feart.2021.590103

Yilmaz, P., Parfrey, L. W., Yarza, P., Gerken, J., Pruesse, E., Quast, C., Schweer, T., Peplies, J., Ludwig, W., & Glöckner, F. O. (2014). The SILVA and "all-species Living Tree Project (LTP)" taxonomic frameworks. *Nucleic Acids Research*, *42*(D1), 643–648. https://doi.org/10.1093/nar/gkt1209

Yoon, S. H., Ha, S. M., Kwon, S., Lim, J., Kim, Y., Seo, H., & Chun, J. (2017). Introducing EzBioCloud: A taxonomically united database of 16S rRNA gene sequences and whole-genome assemblies. *International Journal of Systematic and Evolutionary Microbiology*, *67*(5), 1613–1617. https://doi.org/10.1099/ijsem.0.001755

Yoon, S. H., Ha, S. min, Lim, J., Kwon, S., & Chun, J. (2017). A large-scale evaluation of algorithms to calculate average nucleotide identity. *Antonie van Leeuwenhoek, International Journal of General and Molecular Microbiology*, *110*(10), 1281–1286. https://doi.org/10.1007/s10482-017-

0844-4

Yu, K., & Rinklebe, J. (2015). Soil redox potential and pH controllers. *Methods in Biogeochemistry of Wetlands*, *10*, 107–116. https://doi.org/10.2136/sssabookser10.c7

Yu, M. F., Shu, B., Li, Z., Liu, G., Liu, W., Yang, Y., & Ma, L. (2022). Co-selective Pressure of Cadmium and Doxycycline on the Antibiotic and Heavy Metal Resistance Genes in Ditch Wetlands. *Frontiers in Microbiology*, *13*(February), 1–12. https://doi.org/10.3389/fmicb.2022.820920

Yu, X., Zhao, J. T., Liu, X., Sun, L. X., Tian, J., & Wu, N. (2021). Cadmium Pollution Impact on the Bacterial Community Structure of Arable Soil and the Isolation of the Cadmium Resistant Bacteria. *Frontiers in Microbiology*, *12*(July), 1–11. https://doi.org/10.3389/fmicb.2021.698834

Yun, Y., Wang, H., Man, B., Xiang, X., Zhou, J., Qiu, X., Duan, Y., & Engel, A. S. (2016). The relationship between pH and bacterial communities in a single karst ecosystem and its implication for soil acidification. *Frontiers in Microbiology*, *7*(DEC), 23–32. https://doi.org/10.3389/fmicb.2016.01955

Zacháry, D., Jordan, G., Völgyesi, P., Bartha, A., & Szabó, C. (2015). Urban geochemical mapping for spatial risk assessment of multisource potentially toxic elements - A case study in the city of Ajka, Hungary. *Journal of Geochemical Exploration*, *158*, 186–200. https://doi.org/10.1016/j.gexplo.2015.07.015

Zhang, M.-K., & Wang, L.-P. (2007). [Impact of heavy metals pollution on soil organic matter accumulation]. *The journal of applied ecology*, *18*(7), 1479–1483.

Zhang, M. K., Liu, Z. Y., & Wang, H. (2010). Use of single extraction methods to predict bioavailability of heavy metals in polluted soils to rice. *Communications in Soil Science and Plant Analysis*, *41*(7), 820–831. https://doi.org/10.1080/00103621003592341

Zhang, Y., Wang, M., Huang, B., Akhtar, M. S., Hu, W., & Xie, E. (2018). Soil mercury accumulation, spatial distribution and its source identification in an industrial area of the Yangtze Delta, China. *Ecotoxicology and Environmental Safety*, *163*(July), 230–237. https://doi.org/10.1016/j.ecoenv.2018.07.055

Zhu, L., Tang, J., Lee, B., Zhang, Y., & Zhang, F. (2010). Lead concentrations and isotopes in aerosols from Xiamen, China. *Marine Pollution Bulletin*, *60*(11), 1946–1955. https://doi.org/10.1016/j.marpolbul.2010.07.035

Zhu, Y.-G., Yoshinaga, M., Zhao, F.-J., & Rosen, B. P. (2014). Earth Abides Arsenic

Biotransformations. *Annual Review of Earth and Planetary Sciences*, *42*(1), 443–467. https://doi.org/10.1146/annurev-earth-060313-054942

Zou, L., Lu, Y., Dai, Y., Khan, M. I., & Gustave, W. (2021). *Spatial Variation in Microbial Community in Response to As and Pb Contamination in Paddy Soils Near a Pb-Zn Mining Site*. *9*(April), 1–11. https://doi.org/10.3389/fenvs.2021.630668

Appendix

Table S1. The concentration of PTEs in Salgótarján soils. The samples are ordered based on their categories

Sample	Categories	As	Pb	Hg	Cd
STN 001 US	kindergarten	9.55	20.45	0.089	0.195
STN 002 US	kindergarten	6.3	25.56	0.066	0.32
STN 003 US	kindergarten	7.4	19.54	0.063	0.39
STN 004 US	kindergarten	5.5	23.66	0.045	0.33
STN 005 US	kindergarten	4	12.14	0.042	0.15
STN 006 US	kindergarten	4.9	21.52	0.029	0.17
STN 007 US	kindergarten	6.8	16.13	0.047	0.14
STN 012 US	kindergarten	3.7	14.89	0.045	0.13
STN 013 US	kindergarten	6.7	19.4	0.034	0.16
STN 008 US	Playground	5.4	18.41	0.068	0.2
STN 010 US	Playground	4.7	8.51	0.028	0.11
STN 014 US	Playground	26.1	31.51	0.132	0.56
STN 015 US	Playground	4.6	11.84	0.043	0.1
STN 016 US	Playground	11.8	20.48	0.057	0.17
STN 017 US	Playground	4.9	12.15	0.042	0.22
STN 020 US	Playground	6.8	41.16	0.086	0.37
STN 023 US	Playground	6.4	12.45	0.451	0.15
STN 024 US	Playground	15.7	1692	0.1405	1.405
STN 025 US	Playground	12.8	19.45	0.049	0.18
STN 028 US	Playground	6.5	24.83	0.07	0.26
STN 009 US	Park	73.6	80.77	0.396	0.66
STN 011 US	Park	4.4	15.94	0.047	0.23
STN 019 US	Park	17.4	25.93	0.076	0.64
STN 027 US	Park	7.5	17.21	0.048	0.19

STN 029 US	Park	22.3	29.79	0.126	0.29
STN 032 US	Park	15.4	26.07	0.08	0.24
STN 018 US	Others- Cemetery	17.7	33.95	0.215	0.4
STN 021 US	Others- Roadside	13	31.82	0.098	0.78
STN 022 US	Others- Roadside	6.9	17.22	0.316	0.17
STN 026 US	Others- Roadside	6.3	36.71	0.064	0.18
STN 030 US	Others- Roadside	8.5	433	0.306	1.59
STN 031 US	Others- Garden	4.5	17.1	0.03	0.14
STN 033 US	Others- Roadside	8.4	24.19	0.067	0.23
STN 034 US	Others- Roadside	12.4	60.98	0.082	0.77
STN 035 US	Others- Roadside	14	19.64	0.098	0.21
STN 036 US	Others- Cemetery	6	15.78	0.036	0.37
STN 037 US	Forest background/control	6.8	16.65	0.054	0.18

Table S2. The concentration of PTEs in Ózd soils. The samples are ordered based on their categories

Sample	Categories	As	Pb	Hg	Cd
OZD 005 US	Kindergarten	6.6	39.99	0.2	0.5
OZD 006 US	Kindergarten	7.2	31.37	0.084	0.33
OZD 007 US	Kindergarten	6	34.71	0.084	0.48
OZD 008 US	Kindergarten	8.5	61.46	0.414	0.81
OZD 009 US	Kindergarten	6.2	52.3	0.07	0.49
OZD 010 US	Kindergarten	6.2	21.86	0.051	0.26
OZD 012 US	Kindergarten	5.6	26.87	0.062	0.38
OZD 013 US	Kindergarten	16.8	173.13	0.341	2.91
OZD 014 US	Kindergarten	5.3	20.31	0.039	0.29
OZD 015 US	Kindergarten	4.9	21.7	0.125	0.29
OZD 018 US	Kindergarten	7.4	49.68	0.116	0.67
OZD 019 US	Kindergarten	10	45.95	0.249	0.95
OZD 023 US	Kindergarten	5	28.78	0.059	0.3
OZD 045 US	Kindergarten	6	41.9	0.12	0.55
OZD 046 US	Kindergarten	13.8	40.51	0.138	0.51
OZD 001 US	Playground	4.3	18.66	0.059	0.3
OZD 002 US	Playground	4	14.82	0.035	0.14
OZD 003 US	Playground	8.3	29.48	0.078	0.47
OZD 004 US	Playground	4.7	17.57	0.045	0.31
OZD 011 US	Playground	5.5	22.83	0.062	0.26
OZD 021 US	Playground	8.1	29.7	0.085	0.57
OZD 025 US	Playground	7.7	36.26	0.524	0.38
OZD 026 US	Playground	7.1	42.37	0.11	0.55
OZD 027 US	Playground	6.4	28.62	0.05	0.36
OZD 028 US	Playground	7.4	48.15	0.097	0.65
OZD 029 US	Playground	7.9	18.9	0.036	0.25

OZD 030 US	Playground	4.4	18.81	0.033	0.33
OZD 039 US	playground	10.3	23.49	0.082	0.36
OZD 041 US	playground	5.4	24.83	0.061	0.26
OZD 042 US	playground	23.8	250.91	0.894	3.03
OZD 047 US	Playground	6.4	30.49	0.134	0.47
OZD 060 US	playground	10.6	42.37	0.132	0.39
OZD 024 US	Park	5.2	26.56	0.063	0.36
OZD 031 US	Park	13.7	62.81	0.204	0.87
OZD 040 US	Park	20.3	62.78	0.388	0.51
OZD 051 US	Park	6.7	20.51	0.058	0.31
OZD 032 US	Others	4.4	15.43	0.038	0.18
OZD 033 US	Others	5	17.3	0.043	0.16
OZD 034 US	Others	5	19.3	0.049	0.2
OZD 035 US	Others	4.4	19.81	0.041	0.22
OZD 036 US	Others	2.7	6.55	0.015	0.11
OZD 037 US	Others	11.8	124.72	0.315	1.4
OZD 038 US	Others - old industry	27.1	596.43	0.652	5.17
OZD 043 US	Others	4.1	22	0.042	0.22
OZD 048 US	Others	11.6	43.16	0.101	1.65
OZD 049 US	Others	7.7	27.55	0.089	0.42
OZD 050 US	Others	6.8	31.05	0.09	0.38
OZD 052 US	Others	4.3	14.05	0.027	0.21
OZD 053 US	Others	6.3	33.96	0.085	0.46
OZD 054 US	Others - new industry	35.9	1673.5	4.893	62.89
OZD 055 US	Others	6.5	60.71	0.126	0.81
OZD 056 US	Others	4.7	29.76	0.217	0.54
OZD 057 US	Others	7.8	46.61	0.106	0.67
OZD 058 US	Others	5.4	31.73	0.076	0.36
OZD 059 US	Others	5.3	23.13	0.043	0.32
OZD 000 US	Background sample/control	6	17.49	0.079	0.13

Table S3. The results of Enrichment factor calculations for Salgótarján and Ózd. Enrichment levels are as following: deficiency to minimal enrichment (EF≤2), moderate enrichment (2<EF≤5), significant enrichment (5<EF≤20), very high enrichment (20<EF≤40), and extremely high enrichment (EF>40)

Sample	As	Pb	Hg	Cd	Sample	As	Pb	Hg	Cd
STN 001 US	0.57	0.50	0.67	0.44	OZD 001 US	1.31	1.95	1.37	4.23
STN 002 US	0.32	0.52	0.42	0.61	OZD 002 US	1.14	1.45	0.76	1.84
STN 003 US	0.44	0.47	0.47	0.87	OZD 003 US	1.38	1.68	0.98	3.60
STN 004 US	0.35	0.61	0.36	0.79	OZD 004 US	1.26	1.62	0.92	3.84
STN 005 US	0.21	0.26	0.28	0.30	OZD 005 US	1.77	3.68	4.07	6.19
STN 006 US	0.27	0.48	0.20	0.35	OZD 006 US	1.69	2.53	1.50	3.58
STN 007 US	0.28	0.27	0.24	0.22	OZD 007 US	1.50	2.98	1.60	5.55
STN 008 US	0.30	0.42	0.48	0.43	OZD 008 US	2.00	4.96	7.40	8.80
STN 009 US	3.19	1.43	2.16	1.08	OZD 009 US	1.62	4.69	1.39	5.91
STN 010 US	0.33	0.24	0.25	0.29	OZD 010 US	1.86	2.24	1.16	3.59
STN 011 US	0.21	0.31	0.28	0.41	OZD 011 US	1.32	1.89	1.13	2.89
STN 012 US	0.22	0.37	0.34	0.30	OZD 012 US	1.40	2.31	1.18	4.40
STN 013 US	0.22	0.26	0.14	0.20	OZD 013 US	4.84	17.11	7.46	38.70
STN 014 US	1.12	0.55	0.72	0.91	OZD 014 US	1.03	1.36	0.58	2.61
STN 015 US	0.29	0.30	0.34	0.24	OZD 015 US	1.10	1.68	2.14	3.01
STN 016 US	0.59	0.42	0.36	0.32	OZD 018 US	2.09	4.82	2.49	8.75
STN 017 US	0.28	0.28	0.30	0.48	OZD 019 US	2.55	4.02	4.82	11.17
STN 018 US	0.79	0.62	1.20	0.67	OZD 021 US	1.08	1.35	0.86	3.50
STN 019 US	0.74	0.45	0.41	1.03	OZD 023 US	1.64	3.24	1.47	4.54
STN 020 US	0.25	0.62	0.40	0.52	OZD 024 US	1.48	2.60	1.37	4.74
STN 021 US	0.67	0.67	0.64	1.52	OZD 025 US	1.85	3.00	9.59	4.22
STN 022 US	0.32	0.32	1.83	0.30	OZD 026 US	1.94	3.97	2.28	6.93
STN 023 US	0.42	0.33	3.69	0.37	OZD 027 US	1.41	2.16	0.84	3.66
STN 024 US	0.80	35.42	0.91	2.72	OZD 028 US	2.02	4.51	2.01	8.19
STN 025 US	0.73	0.46	0.35	0.39	OZD 029 US	2.06	1.69	0.71	3.01

STN 026 US	0.30	0.70	0.38	0.32		OZD 030 US	1.44	2.12	0.82	5.00
STN 027 US	0.38	0.35	0.30	0.36		OZD 031 US	2.95	4.65	3.34	8.66
STN 028 US	0.29	0.46	0.40	0.44		OZD 032 US	1.02	1.23	0.67	1.93
STN 029 US	0.75	0.41	0.53	0.37		OZD 033 US	1.36	1.62	0.89	2.01
STN 030 US	0.51	10.68	2.33	3.63		OZD 034 US	1.20	1.58	0.89	2.21
STN 031 US	0.27	0.42	0.23	0.32		OZD 035 US	1.32	2.03	0.93	3.04
STN 032 US	0.78	0.54	0.51	0.46		OZD 036 US	0.96	0.80	0.40	1.80
STN 033 US	0.38	0.45	0.39	0.40		OZD 037 US	2.98	10.81	6.05	16.33
STN 034 US	0.65	1.30	0.54	1.51		OZD 038 US	6.19	46.73	11.31	54.50
STN 035 US	0.67	0.38	0.59	0.38		OZD 039 US	3.05	2.39	1.85	4.93
STN 036 US	0.21	0.23	0.16	0.50		OZD 040 US	6.39	6.78	9.27	7.41
						OZD 041 US	1.31	2.07	1.12	2.91
						OZD 042 US	4.37	15.80	12.46	25.67
						OZD 043 US	1.10	2.02	0.86	2.72
						OZD 045 US	1.49	3.57	2.27	6.31
						OZD 046 US	3.73	3.76	2.83	6.37
						OZD 047 US	1.62	2.64	2.57	5.48
						OZD 048 US	2.91	3.71	1.92	19.09
						OZD 049 US	2.53	3.10	2.22	6.36
						OZD 050 US	1.76	2.76	1.77	4.54
						OZD 051 US	1.47	1.54	0.96	3.13
						OZD 052 US	1.19	1.34	0.57	2.69
						OZD 053 US	1.67	3.10	1.72	5.64
						OZD 054 US	6.33	101.15	65.48	511.41
						OZD 055 US	1.50	4.79	2.20	8.60
						OZD 056 US	1.38	3.00	4.84	7.32
						OZD 057 US	2.29	4.70	2.36	9.08
						OZD 058 US	1.28	2.58	1.37	3.94
						OZD 059 US	1.35	2.02	0.83	3.76
						OZD 060 US	2.79	3.83	2.64	4.74

Table S4. Environmental Parameters and FE, Mn content in Salgótarján and Ózd soils

	TN	NH_4^+	NO_3^-	TOC	$CaCO_3$	pH	Eh (mV)	clay	silt	sand	Fe	Mn
	mg/kg	mg/kg	mg/kg	wt%	wt%			V%	V%	V%	wt%	mg/kg
STN 01 US	0.13	3.42	30.33	1.39	2.89	7.54	-28.40	20.16	58.56	21.28	2.20	396
STN 02 US	0.23	6.21	21.20	1.89	0.66	7.13	-6.70	17.99	68.59	13.42	1.95	439
STN03 US	0.19	5.03	17.60	1.76	1.03	7.62	-32.00	19.16	57.10	23.74	1.68	396
STN 04 US	0.07	3.62	11.89	0.72	0.95	7.60	-30.80	17.09	35.53	47.38	1.71	339
STN 05 US	0.16	4.89	13.21	1.33	2.44	7.52	-27.30	22.88	58.53	18.59	1.96	281
STN 06 US	0.08	3.42	13.21	0.63	0.21	7.35	-18.40	15.41	44.05	40.54	1.78	352
STN 07 US	0.10	3.62	9.65	0.87	0.29	7.40	-20.40	32.41	50.56	17.03	2.10	272
STN 08 US	0.19	4.52	10.05	1.61	0.54	7.31	-15.70	28.68	53.27	18.05	1.83	321
STN 09 US	0.21	3.32	4.43	1.66	1.77	5.86	59.00	16.47	52.87	30.66	2.65	355
STN 10 US	0.14	4.02	19.61	1.24	3.72	7.62	-31.70	10.13	39.99	49.88	1.54	245
STN 11 US	0.25	5.53	21.11	1.82	0.95	7.46	-23.60	15.18	52.46	32.35	2.06	330
STN 12 US	0.21	6.21	42.92	1.64	1.53	7.25	-13.60	14.15	58.79	27.06	1.61	324
STN 13 US	0.14	5.03	4.52	1.19	0.37	7.50	-25.60	40.56	52.23	7.21	2.16	537
STN 14 US	0.21	2.12	5.29	1.69	0.08	6.61	20.10	13.35	45.90	40.75	2.50	509
STN 15 US	0.13	3.42	25.92	1.15	1.07	7.51	-26.50				1.59	280
STN 16 US	0.09	3.25	18.56	0.78	0.33	7.55	-28.50	19.64	57.78	22.58	2.10	287
STN 17 US	0.12	3.91	11.74	0.95	0.62	7.51	-26.50	62.22	11.31	26.48	1.67	266
STN 18 US	0.38	8.27	46.54	4.38	0.70	7.18	-9.80	8.37	57.23	34.40	2.09	349
STN 19 US	0.27	11.18	21.29	2.67	0.00	5.88	57.90	16.08	72.12	11.81	2.01	344
STN 20 US	0.41	12.84	21.60	3.12	0.00	5.14	96.10			1.46	2.12	784
STN 21 US	0.23	7.14	32.86	2.28	3.30	7.52	-26.80	4.04	38.64	57.32	1.67	388
STN 22 US	0.20	7.34	20.06	1.58	0.25	7.34	-17.30	10.70	50.92	38.38	2.25	380
STN 23 US	0.05	1.86	7.89	0.55	1.94	7.56	-28.80	9.74	45.63	44.63	1.62	251
STN 24 US	0.37	1.64	4.91	1.92	0.64	7.56	-29.40	12.40	41.43	46.18	2.44	566
STN 25 US	0.17	4.18	12.99	1.54	1.24	7.34	-17.50	16.27	45.61	38.12	2.07	366
STN 26 US	0.24	5.88	13.57	1.83	0.08	7.01	0.20	11.54	69.62	18.84	1.96	350

STN 27 US	0.07	3.25	12.53	0.62	7.60	7.81	-41.30	25.23	39.81	34.96	2.62	267
STN 28 US	0.34	11.71	14.37	3.02	0.00	5.96	53.90	25.04	54.17	20.79	1.66	599
STN 29 US	0.21	10.76	17.61	2.55	1.49	7.30	-15.60	20.66	50.42	28.92	2.33	323
STN 30 US	0.30	2.77	10.53	4.00	0.60	7.44	-22.60	7.08	59.16	33.75	1.96	354
STN 31 US	0.13	5.43	14.48	0.96	1.49	7.45	-23.20	12.73	37.01	50.26	1.88	329
STN 32 US	0.14	3.71	18.56	1.47	0.66	7.43	-22.00	14.58	49.45	35.97	2.29	367
STN 33 US	0.15	5.24	11.43	1.64	0.33	7.58	-29.80	11.43	52.08	36.49	1.98	433
STN 34 US	0.17	6.33	11.76	1.68	1.07	7.64	-32.50	11.28	47.06	41.66	2.36	465
STN 35 US	0.19	8.35	4.64	1.96	0.29	7.31	-16.10	11.03	56.22	32.75	2.10	376
STN 36 US	0.13	3.81	1.91	1.06	0.00	6.37	33.20	20.83	59.58	19.60	2.27	431

	TN	NH_4^+	NO_3^-	TOC	$CaCO_3$	pH	Eh (mV)	clay	silt	sand	Fe	Mn
	mg/kg	mg/kg	mg/kg	wt%	wt%			V%	V%	V%	wt%	mg/kg
OZD 01 US	0.38	23.42	31.94	2.93	14.04	7.83	-56.8	5.2	59.226	35.574	1.57	544
OZD 02 US	0.16	7.76	20.68	1.28	0.53	7.61	-41.2	9.8	46.159	44.041	2.01	452
OZD 03 US	0.34	6.42	31.53	2.51	5.16	7.7	-44.4	17.7	68.472	13.828	2.66	714
OZD 04 US	0.15	6.21	9.31	1.08	12.63	7.76	-49	15.6	52.457	31.943	2.14	402
OZD 05 US	0.16	6.85	10.76	1.14	3.59	7.77	-44.9	14.1	59.736	26.164	2.42	394
OZD 06 US	0.21	10.05	13.57	1.77	1.16	7.45	-36.4	17.6	46.767	35.633	2.36	534
OZD 07 US	0.10	4.52	7.24	0.74	1.53	7.71	-45.6	7.6	48.644	43.756	3.11	481
OZD 08 US	0.14	5.72	14.29	1.06	4.05	7.65	-50.9	18	57.796	24.204	2.9	815
OZD 09 US	0.28	7.98	23.42	1.96	2.23	7.7	-42.9	13.4	57.038	29.562	2.25	390
OZD 10 US	0.29	9.87	26.33	2.21	0.21	7.54	-37.8	11.2	62.542	26.258	1.68	425
OZD 11 US	0.29	7.01	15.76	1.97	0.70	7.55	-35.5	19.4	59.312	21.288	1.85	353
OZD 12 US	0.16	4.02	34.69	1.21	3.51	7.76	-49.8	21.08	50.719	28.201	2.38	498
OZD 13 US	0.19	7.04	21.62	1.49	2.56	7.64	-39.4	9.5	51.032	39.468	4.27	950
OZD 14 US	0.18	7.92	34.50	1.31	0.21	7.47	-30.8	22.8	58.535	18.665	2.35	440
OZD 15 US	0.09	3.52	3.02	0.74	2.65	7.72	-46.5	15.1	47.034	37.866	2.33	441
OZD 18 US	0.25	8.79	13.96	2.18	7.29	7.83	-58.1	4.03	41.199	54.771	2.38	652

OZD 19 US	0.16	7.14	12.86	1.35	1.37	7.33	-35.3	9.7	49.849	40.451	2.83	845
OZD 20 US	0.50	13.23	27.84	3.47	4.02	7.59	-36.8	24.8	67.245	7.955	2.81	459
OZD 21 US	0.22	5.57	28.31	1.93	1.04	6.95	-25.5	7.1	49.703	43.197	1.88	342
OZD 23 US	0.27	12.93	11.89	2.27	0.08	7.3	-16.5	18	55.273	26.727	2.24	561
OZD 24 US	0.13	5.17	7.24	1.16	4.23	7.58	-36.4	14	52.54	33.46	2.34	390
OZD 25 US	0.28	9.58	38.33	2.34	5.80	7.86	-41.7	10.3	50.814	38.886	2.5	528
OZD 27 US	0.28	8.52	34.07	2.35	0.41	7.56	-36.9	15.4	61.445	23.155	2.17	597
OZD 28 US	0.17	8.10	21.43	1.69	4.35	8.05	-61.3	6.13	48.902	44.968	2.63	971
OZD 29 US	0.24	11.38	19.13	2.21	0.00	6.9	-7.5	10.7	47.096	42.204	2.2	409
OZD 30 US	0.22	11.38	7.24	1.60	10.35	7.53	-42.7	11.2	43.734	45.066	1.98	361
OZD 31 US	0.39	11.46	9.65	2.97	4.10	7.52	-37.4	6.5	43.032	50.468	2.95	565
OZD 32 US	0.18	10.34	3.62	1.47	0.00	7.01	-9.4	21.8	55.512	22.688	2.14	481
OZD 33 US	0.19	8.80	1.47	1.54	0.00	7.13	-10.9				1.93	475
OZD 34 US	0.19	10.76	1.96	1.63	0.00	7.08	-5.6	19.3	55.642	25.058	1.92	442
OZD 35 US	0.23	7.34	3.91	1.68	0.00	6.93	0.4	12.05	56.22	31.73	1.72	452
OZD 36 US	0.09	5.10	2.78	0.70	20.71	7.63	-48.9	12.66	45.09	42.25	1.47	195
OZD 37 US	0.19	5.38	3.42	1.93	5.30	7.81	-52	6.9	48.396	44.704	4.19	1305
OZD 38 US	0.14	3.62	2.07	1.85	16.44	7.9	-55.2	6.6	33.59	59.81	9.93	3590
OZD 39 US	0.32	10.42	7.68	2.87	0.41	7.51	-32.8	11.2	45.808	42.992	2.22	409
OZD 40 US	0.35	9.55	3.52	5.36	0.00	6.96	-7.9	8.7	33.808	57.492	2.23	420
OZD 41 US	0.25	13.07	2.51	1.94	0.00	6.9	-3.4	12.9	56.589	30.511	2.01	451
OZD 42 US	0.17	5.86	4.26	1.44	9.21	7.66	-44.7	11	39.721	49.279	4.44	3612
OZD 43 US	0.10	3.81	1.43	0.72	1.70	7.44	-32.3	21.8	51.624	26.576	2.04	315
OZD 45 US	0.09	2.66	2.66	0.86	1.82	7.68	-48	23	41.012	35.988	2.72	522
OZD 46 US	0.39	11.91	6.19	5.43	1.28	7.35	-25.5	10	41.852	48.148	2.76	630
OZD 47 US	0.22	8.17	5.84	1.71	4.47	7.61	-42	12.1	59.017	28.883	2.29	465
OZD 48 US	0.25	9.34	4.67	2.48	4.97	7.32	-30.8	16	56.254	27.746	2.47	369
OZD 49 US	0.36	10.75	14.71	3.96	1.86	7.53	-36.1	2.7	33.5	63.8	2.82	503
OZD 50 US	0.22	10.42	10.42	2.07	4.89	7.72	-44.8	17.5	51.298	31.202	2.24	709
OZD 51 US	0.39	13.03	7.24	2.61	4.97	7.6	38.5	15	63.003	21.997	2.24	440

OZD 52 US	0.22	8.17	4.09	1.62	8.61	7.55	-40.5	13.5	54.443	32.057	1.71	253
OZD 53 US	0.14	7.24	3.62	1.32	1.49	7.64	-44.7	14.32	60.079	25.601	2.48	683
OZD 54 US	0.05	1.96	0.49	0.93	8.06	8.26	-77.5	4.74	23.012	72.248	11.63	2946
OZD 55 US	0.49	10.99	4.52	3.90	5.18	7.53	-4.2	7.8	58.131	34.069	2.24	750
OZD 56 US	0.11	4.52	3.96	0.77	7.79	7.6	-39	17.1	49.192	33.708	1.88	325
OZD 57 US	0.38	10.05	4.02	3.27	8.86	7.82	-51.5	13	60.707	26.293	2.04	950
OZD 58 US	0.28	7.76	1.94	2.42	0.00	7.24	-14.3	18.2	59.817	21.983	2.05	428
OZD 59 US	0.17	5.17	2.59	1.21	0.21	7.56	-36.6	29.8	54.327	15.873	2.07	514
OZD 60 US	0.51	12.82	4.52	6.90	0.00	7.3	-15.7	17.4	59.767	22.833	2.37	614

Table S5. Bacteria OTU (class level) in Salgótarján and Ózd soils. Only most abundant 50 classes were represented in the table

taxon	STN09	STN14	STN24	STN30	STN37	OZD02	OZD25	OZD38	OZD39	OZD42	OZD54
Bacteroidia	256	189	231	238	134	153	132	279	173	148	138
Gammaproteobacteria	167	167	171	192	124	219	202	256	193	200	152
Alphaproteobacteria	98	133	136	151	105	139	155	225	113	153	214
Deltaproteobacteria	152	190	169	155	126	188	114	143	156	161	99
Verrucomicrobiae	189	140	151	103	70	98	96	114	146	81	65
Planctomycetacia	139	140	185	133	101	168	111	153	108	142	131
Subgroup_6	99	103	118	83	120	167	121	138	162	160	54
Parcubacteria	80	125	102	100	62	24	55	97	37	48	89
Thermoleophilia	108	66	70	58	47	60	51	31	63	60	41
Actinobacteria	72	61	100	65	49	85	65	82	82	73	70
Phycisphaerae	87	74	61	45	57	53	53	79	71	83	51
Saccharimonadia	41	41	67	86	26	12	36	41	14	16	81
Gemmatimonadetes	44	65	61	66	53	37	50	76	30	62	33
Blastocatellia_(Subgroup_4)	53	65	57	45	45	21	51	27	21	28	39
Acidimicrobiia	58	60	58	61	55	64	51	42	53	58	49
Anaerolineae	16	50	36	60	22	22	20	12	8	16	32

OM190	12	30	22	12	23	47	19	12	34	31	5
Chloroflexia	23	19	29	32	16	15	14	15	7	14	42
Acidobacteriia	38	23	16	25	25	17	18	25	15	12	26
Proteobacteria_unclassified	9	15	15	20	5	19	27	26	36	14	14
Holophagae	10	21	11	24	12	12	20	27	5	9	13
Latescibacteria_cl	7	22	5	11	26	21	16	5	15	11	0
Actinobacteria_unclassified	12	7	5	8	7	15	12	11	23	8	10
KD4-96	14	18	22	17	8	17	15	10	9	9	15
Longimicrobia	0	5	1	5	2	2	0	12	2	7	21
Gracilibacteria	19	21	15	11	10	4	18	6	4	8	16
Microgenomatia	7	19	15	21	16	0	3	4	3	2	12
NC10	7	11	7	8	16	20	9	3	8	9	3
Subgroup_17	6	19	17	15	3	14	11	7	8	11	1
Chlamydiae	16	18	19	17	5	6	10	8	4	6	13
Thermoanaerobaculia	2	18	7	10	8	10	4	6	1	15	3
ABY1	3	18	7	7	5	2	10	1	2	3	3
MB-A2-108	12	14	9	13	8	15	17	3	9	7	4
Bacilli	5	11	5	17	9	4	5	1	7	3	9
Dehalococcoidia	3	14	8	15	13	14	9	8	5	15	9
Lineage_IIa	15	9	11	6	10	4	2	7	7	2	1
Subgroup_5	9	14	8	2	8	6	5	3	8	5	2
Clostridia	11	4	1	14	5	0	2	0	1	0	0
Acidobacteria_unclassified	4	3	4	4	3	13	4	8	9	3	1
TK10	13	8	10	10	10	5	11	8	9	8	8
Babeliae	3	12	9	5	3	1	3	3	3	2	5
Subgroup_22	6	9	2	3	9	11	5	1	6	4	1
Lineage_IIb	11	6	6	3	5	5	1	3	3	6	4
S0134_terrestrial_group	1	7	4	11	7	2	4	11	0	7	9
Nitrospira	3	10	6	6	5	7	11	5	4	5	5
Fimbriimonadia	2	5	10	5	2	4	3	3	1	1	7

FBP_cl	2	0	3	5	2	3	1	4	3	0	10
Pla4_lineage	2	10	5	3	5	10	5	4	5	9	2
Chloroflexi_unclassified	1	3	6	6	4	4	3	4	1	2	9
Bacteria_unclassified	89	83	143	151	120	204	197	175	240	187	104

Table S6. Archaea OTU (class level) in Salgótarján and Ózd soils

taxon	STN09	STN14	STN24	STN30	STN37	OZD02	OZD25	OZD38	OZD39	OZD42	OZD54
Altiarchaeia	0	0	0	0	0	0	0	1	0	0	0
Bathyarchaeia	0	0	0	2	0	0	0	0	0	0	0
Iainarchaeia	0	2	1	1	1	0	1	0	0	1	0
Methanobacteria	0	0	0	2	1	0	1	0	0	0	0
Methanomicrobia	0	0	0	2	0	0	0	0	0	0	0
Thermoplasmata	3	6	4	10	4	6	21	4	2	9	5
Woesearchaeia	11	31	19	23	31	5	24	1	9	17	7
Group_1.1c	1	0	0	0	0	0	0	0	0	0	0
Nitrososphaeria	17	13	13	10	10	15	39	9	20	21	5
Archaea_unclassified	0	0	1	0	4	0	4	0	1	3	1
Euryarchaeota_unclassified	0	0	0	0	0	1	1	0	0	1	0
Nanoarchaeaeota_unclassified	1	0	1	0	0	0	0	0	0	0	0

Table S7. Colony forming Unit analysis- The number of metal resistant bacteria in Salgótarján and Ózd soils (*10^4). In all cases the concentration of metal(loid)s were 200 mg/L.

Sample	STN09	STN14	STN24	STN30	STN37	OZD02	OZD25	OZD38	OZD39	OZD42	OZD54
Pb	14.56	2.25	23.33	16.16	3.44	3.70	3.40	3.20	11.70	5.40	0.52
Cd	1.17	0.08	0.59	1.53	0.07	0.00	0.01	1.30	0.00	0.00	0.00
Hg	0.00	0.00	0.02	0.02	0.00	0.00	0.00	0.00	0.00	0.00	0.00
As	0.00	0.00	0.00	0.00	0.00	0.00	0.00	0.00	0.00	0.00	0.00

Table S8. Results of Health risk assessment for Salgótarján (STN) and Ózd (OZD). CR-Carcinogenic risk. Ing-ingestion, inh-inhalation, dems-dermal pathways

	Chronic risk					
STN	Adults			Children		
	HQ_ing	HQ_inh	HQ_dems	HQ_ing	HQ_inh	HQ_dems
As	5.06E-02	7.78E-06	1.25E-02	4.72E-01	1.82E-05	6.05E-02
Pb	3.12E-02	-	-	2.91E-01	-	-
Hg	4.71E-04	2.53E-07	1.17E-04	4.39E-03	5.90E-07	5.63E-04
Cd	9.74E-04	1.31E-06	2.41E-04	9.09E-03	3.07E-06	1.16E-03
OZD	Adults			Children		
	HQ_ing	HQ_inh	HQ_dems	HQ_ing	HQ_inh	HQ_dems
As	3.81E-02	5.86E-06	9.43E-03	3.56E-01	1.37E-05	4.55E-02
Pb	3.13E-02	-	-	2.92E-01	-	-
Hg	1.05E-03	5.62E-07	2.60E-04	9.78E-03	1.31E-06	1.25E-03
Cd	4.83E-03	6.52E-06	1.20E-03	4.51E-02	1.52E-05	5.77E-03

	Carcinogenic risk					
STN	CR	Adults		CR	Children	
	ADI-ing	ADI-inh	ADI-dems	ADI-ing	ADI-inh	ADI-dems
As	9.76E-06	1.50E-08	2.42E-06	9.11E-06	2.25E-07	2.26E-06
Pb	4.09E-07	3.11E-10	-	3.82E-07	1.31E-11	-
Hg	-	-	-	-	-	-
Cd	-	2.02E-10	-	-	1.89E-10	-
OZD	CR	Adults		CR	Children	
	ADI-ing	ADI-inh	ADI-dems	ADI-ing	ADI-inh	ADI-dems
As	7.35E-06	1.13E-08	1.82E-06	6.86E-06	1.70E-07	1.70E-06
Pb	4.10E-07	3.12E-10	-	3.83E-07	1.31E-11	-
Hg	-	-	-	-	-	-
Cd	-	1.00E-09	-	-	9.36E-10	-

Figure S1. Some examples of observed slag material below the surface (Sample STN09-left, OZD42- right)

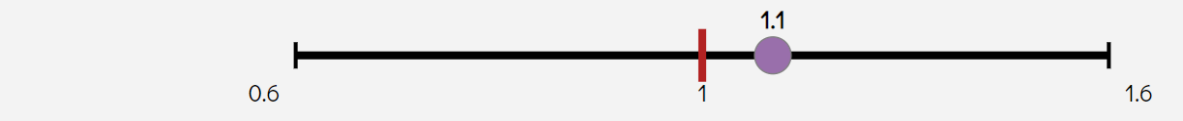

Figure S2.1. General mortality among the **female** population (BNO-10.:A00-Y98) in Salgótarján district (2013-2018) (source: https://efop180.antsz.hu/nekinf-diagram). Purple colour shows if the mortality risk was significantly higher than the national average mortality risk.

Figure S2.2. General mortality among the **female** population (BNO-10.:A00-Y98) in Ózd district (2013-2018) (source: https://efop180.antsz.hu/nekinf-diagram)

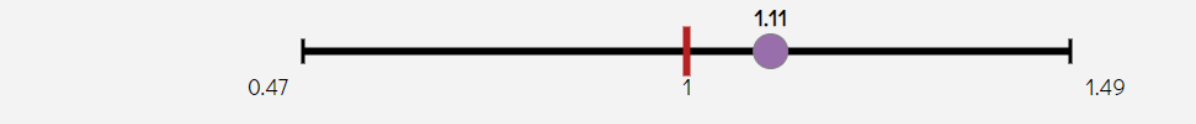

Figure S2.3. General mortality among the **male** population (BNO-10.:A00-Y98) in Salgótarján district (2013-2018) (source: https://efop180.antsz.hu/nekinf-diagram)

Figure S2.4. General mortality among the **male** population (BNO-10.:A00-Y98) in Ózd district (2013-2018) (source: https://efop180.antsz.hu/nekinf-diagram)

EÖTVÖS LORÁND UNIVERSITY
DECLARATION FORM
for disclosure of a doctoral dissertation

I. The data of the doctoral dissertation:
Name of the author: **Gorkhmaz Abbaszade**
MTMT-identifier: **10078596**
Title and subtitle of the doctoral dissertation: **Environmental contamination of potentially toxic elements (PTE) and its effect on soil microbial communities in former industrial cities of Northern Hungary (Salgótarján and Ózd)**

Keywords: **1. Soil metal(loid) contamination; 2. Enrichment factor; 3. Mobility of toxic elements; 4. Metal(loid) resistant bacteria; 5. Health risk assessment**

DOI-identifier[72]: 10.15476/ELTE.2022.179

Name of the doctoral school: **Environmental sciences**
Name of the doctoral programme: **Environmental Biology and Environmental Earth Sciences**
Name and scientific degree of the supervisor: **Erika Tóth, Dr., Csaba Szabó, Dr.**
Workplace of the supervisor: **Eötvös Loránd University**

II. Declarations
1. As the author of the doctoral dissertation,[73]
a) I agree to public disclosure of my doctoral dissertation after obtaining a doctoral degree in the storage of ELTE Digital Institutional Repository. I authorize the administrator of the Department of Doctoral, Habilitational and International Affairs of the Dean's Office of the Faculty of Science to upload the dissertation and the abstract to ELTE Digital Institutional Repository, and I authorize the administrator to fill all the declarations that are required in this procedure.
b) I request to defer public disclosure to the University Library and the ELTE Digital Institutional Repository until the date of announcement of the patent or protection. For details, see the attached application form;[74]
c) I request in case the doctoral dissertation contains qualified data pertaining to national security, to disclose the doctoral dissertation publicly to the University Library and the ELTE Digital Institutional Repository ensuing the lapse of the period of the qualification process.;[75]
d) I request to defer public disclosure to the University Library and the ELTE Digital Institutional Repository, in case there is a publishing contract concluded during the doctoral procedure or up until the award of the degree. However, the bibliographical data of the work shall be accessible to the public. If the publication of the doctoral dissertation will not be carried out within a year from the award of the degree subject to the publishing contract, I agree to the public disclosure of the doctoral dissertation and abstract to the University Library and the ELTE Digital Institutional Repository.[76]
2. As the author of the doctoral dissertation, I declare that
a) the doctoral dissertation and abstract uploaded to the ELTE Digital Institutional Repository are entirely the result of my own intellectual work and as far as I know, I did not infringe anyone's intellectual property rights.;
b) the printed version of the doctoral dissertation and the abstract are identical with the doctoral dissertation files (texts and diagrams) submitted on electronic device.
3. As the author of the doctoral dissertation, I agree to the inspection of the dissertation and the abstract by uploading them to a plagiarism checker software.

Budapest, 25.08.2022

……

Signature of dissertation author

72 Filled by the administrator of the faculty offices.
73 The relevant part shall be underlined.
74 Submitting the doctoral dissertation to the Disciplinary Doctoral Council, the patent or protection application form and the request for deferment of public disclosure shall also be attached.
75 Submitting the doctoral dissertation, the notarial deed pertaining to the qualified data shall also be attached.
76 Submitting the doctoral dissertation, the publishing contract shall also be attached.